

# Swirl String Theory (SST) Canon v0.5.12: Core Axioms, Postulates, Constants, Master Equations, and Lagrangian Framework

Omar Iskandarani

Independent Researcher, Groningen, The Netherlands\*

(Dated: December 2, 2025)

This Canon is the single source of truth for *Swirl String Theory (SST)*: definitions, constants, boxed master equations, and notational conventions. It unifies the core hydrodynamic, electromagnetic, and gauge principles of the theory. **This version canonizes the following principles:**

- I** The foundational hydrodynamic laws, including the Chronos–Kelvin Invariant and Swirl Coulomb constant  $\Lambda$
- II** The Swirl–Electromagnetic Bridge, linking swirl dynamics directly to Maxwell’s equations.
- III** The emergence of the  $SU(3) \times SU(2) \times U(1)$  gauge sector and a first-principles derivation of the weak mixing angle  $\theta_W$ .
- IV** A parameter-free prediction for the Electroweak Symmetry Breaking (EWSB) scale.
- V** A formal dynamical rule for quantum measurement via  $R \leftrightarrow T$  phase transitions.

## Core Axioms (SST)

- 1. Swirl Medium:** Physics is formulated on  $\mathbb{R}^3$  with absolute reference time. Dynamics occur in a frictionless, incompressible *swirl condensate*, which serves as a universal substrate.

- 2. Swirl Strings (Circulation and Topology):** Particles and field quanta correspond to closed vortex filaments (*swirl strings*). The circulation of the swirl velocity around any closed loop is quantized:

$$\Gamma = \oint \mathbf{v}_O \cdot d\ell = n \Gamma_0, \quad n \in \mathbb{Z}, \quad \Gamma_0 = 2\pi r_c \|\mathbf{v}_O\|.$$

Discrete quantum numbers (mass, charge, spin) track to the topological invariants of the swirl string.

- 3. String-induced gravitation:** Macroscopic attraction emerges from coherent swirl flows and swirl-pressure gradients. The effective gravitational coupling  $G_{\text{swirl}}$  is fixed by canonical constants.

- 4. Swirl Clocks:** Local proper-time rate depends on tangential swirl speed  $v$ , ticking slower by the factor  $S_t = \sqrt{1 - v^2/c^2}$  relative to an observer at rest in the medium.

- 5. Dual Phases (Wave–Particle):** Each swirl string has two limiting phases: an extended *R-phase* (unknotted, wave-like) and a localized *T-phase* (knotted, particle-like). Measurement is a dynamical transition between these phases.

- 6. Taxonomy:** Unknotted excitations correspond to bosonic modes, with photons realized as *pulsed torsional R-phase excitations* (rotational wave packets of the swirl director field). Torus knots correspond to leptons (e.g. electron =  $3_1$ ), and chiral hyperbolic knots to quarks (proton =  $5_2 + 5_2 + 6_1$  composite). Linked knots describe nuclei and bound states.

## Preface: Reader Pathways

This document formalizes SST in a self-contained manner, but it is structured to accommodate different levels of reader expertise.

**Beginner-level readers** are encouraged to focus on the physical descriptions and boxed highlights in the main text, skipping the more technical derivations (which are relegated to the appendices and side notes).

**Expert readers** can delve into the detailed derivations and dimensional analyses in the appendices to verify consistency and connect SST formulas to classical limits.

**Active researchers** should consult the formal axiomatic system section and appendices for the rigorous foundation, as well as the traceability tables and glossary that link each canonical statement to established physics or experimental context. Throughout the text, important equations, axioms, and theorems are presented in numbered, boxed form for quick reference. Pedagogical sidebars can be expanded in future versions to provide intuitive explanations, historical notes, or illustrative diagrams without interrupting the flow of the formal development.

---

\* ORCID: 0009-0006-1686-3961, DOI: 10.5281/zenodo.17789611

<b>I Foundations</b>	<b>4</b>
I Sevenfold Genesis of the Swirling Cosmos . . . . .	4
II Canon Governance and Status Taxonomy . . . . .	6
III Core Axioms (SST) . . . . .	7
<b>II Geometry, Fields, and Lagrangian</b>	<b>9</b>
IV Formal Structure and Canonical Framework . . . . .	9
V Self-Similarity and Stability of Swirl Structures . . . . .	9
VI Golden Principle for Discrete Layering . . . . .	10
VII Symmetry and Dark-Knot Classification . . . . .	12
VIII Calibrations & Protocols (Empirical) . . . . .	12
IX Historical Context . . . . .	14
X Classical Invariants: Chronos–Kelvin and Clock–Radius Transport . . . . .	14
XI Classical Invariants and Swirl Quantization . . . . .	14
XII Canonical Constants and Effective Densities . . . . .	15
XIII Effective Medium: Coarse-Graining Derivation of $\rho_f$ . . . . .	18
XIV Genus-2 Foliation and Topological Compactification . . . . .	18
XV Knot Taxonomy . . . . .	19
XVI The Swirl–Electromagnetic Bridge . . . . .	19
XVII Swirl–EM Emergence . . . . .	20
XVIII Engineered Bulk Signaling Channel (BASC) . . . . .	21
XIX Unified SST Lagrangian . . . . .	21
XX Master Equations and Canonical Relations . . . . .	22
XXI Master Equations: Hydrogen Soft-Core + Bohr Recovery . . . . .	24
XXII Emergent Gauge Fields and Topology . . . . .	25
XXIII Coherence Conductivity and Chirality in 1D (Patch) . . . . .	26
XXIV Swirl Pressure Law (Euler Corollary) . . . . .	29
XXV Canonical Closure for the Gamma Coil (S40, +11, -9): Helicity and Lift Routes . . . . .	29
XXVI Gauge/EWSB Sector: Empirical-First Box + Theory . . . . .	29
<b>III Gravity, Hydrogen, and Cosmology</b>	<b>30</b>
XXVII Swirl Gravitation and the Hydrogen-Gravity Mechanism . . . . .	30
XXVIII Quantum Measurement: Kernel Law + Near-Field Corollary + Bounds . . . . .	31
XXIX Quantum Computing Sector (Preview) . . . . .	31
XXX Hydrogen-Gravity Construction . . . . .	32
XXXI Wave-Particle Duality and Quantum Measurement . . . . .	32
XXXII Swirl-Tensor Correspondence and External Vortex Field Theories . . . . .	33
XXXIII Corollary: Coherence-Modulated Duality Ellipse (SST) . . . . .	34
XXXIV Exact SST Definition of the Cosmological Term . . . . .	35
XXXV Three-Swirl Circulation Law and Emergent Cosmological Term . . . . .	36
XXXVI Derivations and Numerical Benchmarks . . . . .	37
XXXVII Systematic Dimensional & Recovery Checks . . . . .	38
XXXVIII Invariant Mass from the Canonical Lagrangian . . . . .	39
XXXIX Canonical Status and Outlook . . . . .	41
<b>IV Modules and Applications</b>	<b>42</b>
A Derivation of Chronos–Kelvin Invariant (Axiom 1) . . . . .	42
B Swirl Coulomb Potential Derivation . . . . .	43
C Effective Density $\rho_f$ Derivation . . . . .	45
D Electromagnetic Emergence via $\mathbf{a}(x, t)$ . . . . .	46
E Traceability and Consistency Table . . . . .	46
F Glossary of Notation and Knot Taxonomy . . . . .	46
G $2 \times 2$ near-degenerate solution (sketch) . . . . .	49
H Coinductive Stability and the Golden Filter . . . . .	49
I Swirl Hamiltonian Density . . . . .	51
J Dimensional Analyses & Recovery Limits . . . . .	51
K Hydrogen Soft-Core Numerics . . . . .	52
L Photon/Unknot Sector . . . . .	52
M Swirl Pressure Law—Galaxy-Scale Integrals . . . . .	52
N Calibration Protocol Notes . . . . .	52
O Experimental Status & Bounds . . . . .	52
P Notation, Ontology, Glossary . . . . .	53
Q Derivation of the Swirl→Bulk Coupling $\mathcal{G}_{\text{loop}}$ . . . . .	54
R Conversation-Derived Insights . . . . .	54
S Knot Stability and Protection . . . . .	56
XX Multipoles, Photon Note, $G_{\text{swirl}}$ Identity, Taxonomy . . . . .	59
XXI Computing Hyperbolic Volume of Knot Complements (VAM pipeline) . . . . .	60
XXII Rosetta→Code Consistency Rule (Invariant-Mass Sector) . . . . .	61
XXIII Swirl–EM Transduction Echo Model (Deswal-type Cavities) . . . . .	62
XXIV SST Unruh Scaling and Superradiant Delay . . . . .	63
XXV Two-Vacuum Structure and Dual-Burst Unruh Superradiance . . . . .	64
XXVI TOPOLOGICAL ORIGIN OF THE ELECTRON ANOMALOUS MAGNETIC MOMENT . . . . .	70
References . . . . .	71

## SST Canon v0.5.12 Glossary

TABLE I. Primitive and Derived Canonical Constants (see Section [XII](#))

Symbol	Definition	Canonical Value / Relation
$\Gamma_0$	Primitive Circulation Quantum	$6.4 \times 10^3 \text{ m}^2 \text{s}^{-1}$ (Table <a href="#">V</a> )
$r_c$	Swirl String Core Radius	$1.40897017 \times 10^{-15} \text{ m}$ (Table <a href="#">V</a> )
$\rho_f$	Effective Fluid Density	$7.0 \times 10^{-7} \text{ kg m}^{-3}$ (Table <a href="#">V</a> )
$v_{\mathcal{O}}$	Canonical Swirl Speed ( $  v_{\mathcal{G}}  $ )	$1.09384563 \times 10^6 \text{ m s}^{-1}$ (Table <a href="#">V</a> )
$\rho_m$	Mass-Equivalent Density	$\rho_E / c^2 \approx 3.89 \times 10^{18} \text{ kg m}^{-3}$ (Table <a href="#">V</a> )
$\Lambda$	Swirl Coulomb Constant	$4\pi\rho_m v_{\mathcal{O}} r_c^3$ (Eq. <a href="#">XXA</a> )
$G_{swirl}$	Gravitational Coupling	$\frac{v_{\mathcal{O}} c^5 t_p^2}{2 F_{\max} r_c^2} \approx G_N$ (Eq. <a href="#">XXE</a> )

TABLE II. Core Ontology and Hydrodynamic Mechanics (see Section [III](#))

Concept	Canonical Definition
Swirl Medium	Frictionless, incompressible swirl condensate on $\mathbb{R}^3$ with absolute time $t$ (Axiom <a href="#">1</a> ).
Swirl String	Closed vortex filament where circulation is quantized ( $\Gamma = n\Gamma_0$ ) and particles are topological knots (Axiom <a href="#">2</a> ).
Chronos-Kelvin Invariant	Conservation law generalizing Kelvin's theorem to include time dilation: $\frac{D}{Dt}(R^2\omega) = 0$ (Section <a href="#">X</a> ).
Swirl Clock ( $S_t$ )	Local proper-time rate factor dependent on tangential swirl speed: $S_t = \sqrt{1 - v^2/c^2}$ (Axiom <a href="#">4</a> ).
Zero-Parameter Principle	Axiom stating all dimensional constants are determined by the triplet $(\Gamma_0, \rho_f, r_c)$ and topology (Section <a href="#">XII</a> ).
Swirl Pressure Law	Radial pressure gradient sustaining centripetal force: $\frac{dp_{swirl}}{dr} = \rho_f \frac{v_\theta^2}{r}$ (Eq. <a href="#">XXB</a> ).

TABLE III. Topological Phase and Particle Taxonomy (see Section [XV](#))

Entity	Topological Class	Physical Realization
R-Phase	Unknotted (0 <sub>1</sub> )	Radiative, wave-like, massless (Bosons) (Axiom <a href="#">5</a> ).
T-Phase	Knotted	Tangible, particle-like, massive (Fermions) (Axiom <a href="#">5</a> ).
Photon	Torsional Pulse	Rotating oscillation of the director field (helicity $\pm 1$ ) (Axiom <a href="#">6</a> ).
Electron ( $e^-$ )	Torus Knot (3 <sub>1</sub> )	Trefoil knot; simplest lepton (Axiom <a href="#">6</a> ).
Up Quark ( $u$ )	Twist Knot (5 <sub>2</sub> )	Chiral hyperbolic knot (Axiom <a href="#">6</a> ).
Down Quark ( $d$ )	Twist Knot (6 <sub>1</sub> )	Chiral hyperbolic knot (Axiom <a href="#">6</a> ).
Proton	Composite Linkage	5 <sub>2</sub> + 5 <sub>2</sub> + 6 <sub>1</sub> (uud) configuration (Axiom <a href="#">6</a> ).

TABLE IV. Advanced Gauge, Logic, and Field Concepts (see Sections [VI](#), [VIIIA](#))

Symbol	Term	Definition
$\phi$	Golden Principle	Scaling factor $\phi \approx 1.618$ controlling mass/energy layers: $E_n = E_0 \phi^{2n}$ (Eq. <a href="#">1</a> ).
$\mathcal{K}$	Kairos Event	Topological bifurcation or phase jump in $S_t$ (reconnection event) (Section <a href="#">VIIA</a> ).
$\varrho$	Swirl Areal Density	Density of vortex cores per unit area; sources emergent EM fields via $\nabla \times \mathbf{E}$ (Definition <a href="#">XVI</a> ).
$\theta_W$	Weak Mixing Angle	Ratio of director stiffness constants for $U(1)$ and $SU(2)$ sectors (Theorem <a href="#">XXII</a> ).
BASC	Bulk Signaling Channel	Engineered region allowing scalar bulk field $p(x, t)$ transduction (Section <a href="#">XVIII</a> ).
$\omega$	Vorticity Magnitude	Local vorticity $  \nabla \times \mathbf{v}  $ ; defines the wave proxy in duality relations (Section <a href="#">XXXIII</a> ).

# Part I

## Foundations

### I. SEVENFOLD GENESIS OF THE SWIRLING COSMOS

**Canonical Cosmogony (SST + STC Mapped)** This section compresses the sixteen stages of *The Simplicity Codex* [51] into seven logically complete emergence stages, consistent with the SST Canon **v0.5.12** and the Lagrangian EFT [55]. Each stage represents a parameter-free imprint of physical law onto the condensate.

#### Stage 1: Logical Substrate (Pre-Swirl Potential)

A Haar-neutral, scale-free potential field encodes possible circulation states. No time or space exist yet — only relational templates. Global  $\mathbb{Z}_2$  (chirality) and  $\mathbb{Z}_3$  (triadic closure) symmetries are imprinted as pre-physical rules:

$$\Gamma \mapsto -\Gamma, \quad \Gamma_1 + \Gamma_2 + \Gamma_3 = 0 \pmod{2\pi}$$

laying the groundwork for matter/antimatter duality and baryon triplet stability.

(STC Stages 1–3)

#### Stage 2: Big Condensation (First Manifestation)

When the information complexity  $\mathcal{I}_{\text{swirl}}$  exceeds the Guardian threshold, the swirl condensate forms as an incompressible, inviscid medium on  $\mathbb{R}^3$  with absolute time  $t$ . Primary constants lock in by resonance:

$$\Gamma_0 = 2\pi r_c \|\mathbf{v}_{\mathcal{O}}\|, \quad \tau_{\text{beat}} = \frac{2\pi r_c}{\|\mathbf{v}_{\mathcal{O}}\|}, \quad \rho_f = \frac{\rho_m r_c}{\|\mathbf{v}_{\mathcal{O}}\|} \Omega$$

marking the birth of physical time and the circulation quantum.

(STC Stage 8)

**Technical details:** See Section X (Classical Invariants) and Section XIII (Effective Medium) for derivations.

#### Stage 3: Tangible Chirality and Swirl-Time

Knotted swirl strings appear, stabilized by circulation quantization  $\Gamma = n\Gamma_0$ . The swirl clock

$$S_t = \sqrt{1 - \frac{v^2}{c^2}}$$

defines local proper time, with left-handed ( $\circlearrowleft$ ) and right-handed ( $\circlearrowright$ ) knots forming the basis for matter and antimatter. (STC Stage 9)

**Technical details:** See Section X (Classical Invariants) and Section III (Core Axioms) for the formal framework.

#### Stage 4: Topological Charges and Particle Spectrum

Topological invariants of knots ( $L_k, W_r, T_w$ ) map to quantum numbers:

$$Q(K) = T_3(K) + \frac{Y(K)}{2}$$

with  $Q$  the electric charge,  $T_3$  weak isospin, and  $Y$  hypercharge. Fermion masses arise as soliton energies:

$$m_K = \rho_f \|\mathbf{v}_{\mathcal{O}}\|^2 \text{Vol}_{\mathbb{H}}(K) \phi^{-2k}$$

where  $\text{Vol}_{\mathbb{H}}(K)$  is the hyperbolic complement volume of  $K$  and  $\phi^{-2k}$  encodes Golden-layer suppression. (STC Stage 10)

**Technical details:** See Section XV (Knot Taxonomy) for the particle-knot mapping, and Section XXX (Hydrogen-Gravity) for mass derivations.

### Stage 5: Emergent Interactions (Gauge and Forces)

Unknotted excitations of the condensate form the R-phase modes (photons, gluons, W/Z), with interactions governed by the emergent gauge group:

$$\mathfrak{g}_{\text{swirl}} \simeq \mathfrak{su}(3) \oplus \mathfrak{su}(2) \oplus \mathfrak{u}(1)$$

and minimal coupling

$$D_\mu = \nabla_\mu + ig_{\text{sw}} W_\mu^a T^a.$$

(STC Stage 11)

**Technical details:** See Section [XVII](#) (Swirl-EM Emergence) and Section [XIX](#) (Unified SST Lagrangian) for the formal derivation.

### Stage 6: Geometric Closure and Constant Lock-In

Global Gauss closure yields the  $1/r^2$  force law:

$$\nabla \cdot \vec{P}_{\text{swirl}} = 0 \quad \Rightarrow \quad F(r) \propto \frac{1}{r^2}$$

and fixes  $\pi$  geometrically. The entire condensate enters a global resonance, locking all constants of nature.

**Technical details:** See Section [XXIV](#) (Swirl Pressure Law) and Section [XXVI](#) (Gauge/EWSB Sector) for force laws and constant determinations.

#### Zero-Parameter Principle (Canonical)

**Statement (Axiom):** All dimensional constants of nature are determined by the condensate state, its circulation quantum, and the allowed topological sectors. We take as primitive the circulation-based triplet

$$(\Gamma_0, \rho_f, r_c),$$

where  $\Gamma_0$  is the circulation quantum,  $\rho_f$  the effective fluid density, and  $r_c$  the electron-scale core radius. All other dimensional quantities in SST (masses, charges, energies, forces) are derived combinations of  $(\Gamma_0, \rho_f, r_c)$  and topology-dependent dimensionless factors.

The canonical swirl speed at the core boundary is not independent but given by

$$\|\mathbf{v}_\mathcal{O}\| = \chi_v \frac{\Gamma_0}{2\pi r_c},$$

so that the former primitive set  $(\|\mathbf{v}_\mathcal{O}\|, r_c, \rho_f)$  is just a reparametrization of  $(\Gamma_0, \rho_f, r_c)$ .

$$\text{Primary Scale: } \Gamma_0 \approx 6.4 \times 10^3 \text{ m}^2/\text{s}, \quad \kappa_{\text{SST}} \equiv \Gamma_0 = 2\pi r_c \|\mathbf{v}_\mathcal{O}\|$$

$$\text{Effective Density: } \rho_f = \frac{\rho_m r_c}{\|\mathbf{v}_\mathcal{O}\|} \Omega \quad (\text{coarse-grain rule})$$

$$\text{Mass Functional: } m_K = \rho_f \|\mathbf{v}_\mathcal{O}\|^2 \text{ Vol}_\mathbb{H}(K) \phi^{-2k}$$

$$\text{Gravitational Coupling: } G_{\text{swirl}} = \frac{\|\mathbf{v}_\mathcal{O}\| c^5 t_p^2}{2F_{\max} r_c^2}$$

$$\text{Fine-Structure Constant: } \alpha = \alpha_{\text{DSI}}(\omega_{\text{DSI}}), \quad \omega_{\text{DSI}} \approx 13.06$$

**Corollary:** Once  $\Gamma_0$ ,  $r_c$ , and  $\rho_f$  are fixed by a single calibration (e.g.  $m_e$ ), the full mass spectrum and coupling strengths follow with no free parameters. See STC Stages 12–13 (Gauss-closure & Universal Resonance) [51].

### Stage 7: Recursive Cosmos (Fractal Emergence)

Composite knots (baryons, nuclei, atoms) satisfy  $\mathbb{Z}_3$  closure, 1+12 isotropic shielding, and duality pairing. Each stable composite becomes a new circulation source:

Cluster  $\Rightarrow$  Meta-Knot  $\Rightarrow$  New Swirl Layer

seeding the next scale of complexity. This recursion drives cosmic structure formation, yielding a fractal universe of knots within knots. (STC Stages 14–16)

## II. CANON GOVERNANCE AND STATUS TAXONOMY

a. *Formal system.* Let  $\mathcal{S} = (\mathcal{P}, \mathcal{D}, \mathcal{R})$  denote the SST formal system: axioms  $\mathcal{P}$ , definitions  $\mathcal{D}$ , and admissible inference rules  $\mathcal{R}$  (variational principles, Noether currents, dimensional analysis, asymptotic matching).

b. *Canonical statement.* A statement  $X$  is *canonical* iff

$$\mathcal{P}, \mathcal{D} \vdash_{\mathcal{R}} X,$$

and  $X$  is consistent with accepted canon.

c. *Empirical statement.* A statement  $Y$  is *empirical* iff it asserts a measured value or protocol:

$$Y \equiv \text{"observable } \mathcal{O} \text{ has value } \hat{o} \pm \delta o \text{ under procedure } \Pi."$$

### Status Classes

- **Axiom/Postulate (Canonical).** Primitive assumption of SST.
- **Definition (Canonical).** Introduces a symbol by construction.
- **Theorem/Corollary (Canonical).** Proven consequence within  $\mathcal{S}$ .
- **Constitutive Model.** Canonical if derived from  $\mathcal{P}, \mathcal{D}$ ; otherwise semi-empirical.
- **Calibration (Empirical).** Recommended numerical values for canonical symbols.
- **Research Track.** Conjectures or alternatives pending proof or axiomatization.

Items may be promoted or demoted between classes only upon satisfying or failing the Canonicality Tests.

### Canonicality Tests (all required)

1. **Derivability** from  $\mathcal{P}, \mathcal{D}$  via  $\mathcal{R}$ .
2. **Dimensional consistency** (strict SI usage; correct physical limits).
3. **Symmetry compliance** (Galilean symmetry and incompressibility).
4. **Recovery limits** (Newtonian gravity, Coulomb/Bohr, linear wave optics).
5. **Non-contradiction** with accepted canonical results.
6. **Parameter discipline** (no ad hoc fits beyond calibrations).

Corollary: Clock–Radius Transport

$$\frac{dS_t}{dt} = \frac{2(1 - S_t^2)}{S_t} \frac{1}{R} \frac{dR}{dt}.$$

*Assumption:* thin filament with local solid-body swirl  $v_\theta \simeq \omega r$  evaluated at  $r = r_c$ , so that  $S_t = \sqrt{1 - (\omega r_c/c)^2}$  along the core [23, 24].

### III. CORE AXIOMS (SST)

SST is built on a set of core axioms that establish its physical framework. These axioms, numbered below, are stated in plain language and form the starting postulates of the theory (they are considered *canonical* by definition).

#### Axiom 0: Logical Substrate (Pre-Swirl Potential)

Before the emergence of space, time, or condensate, there exists a *Haar-neutral*, scale-free state space  $\mathcal{S}$  of possible circulation states  $\{\Gamma_i\}$ . This pre-physical substrate encodes only relational constraints:

$$\Gamma \mapsto -\Gamma, \quad \Gamma_1 + \Gamma_2 + \Gamma_3 = 0 \pmod{2\pi},$$

representing a global  $\mathbb{Z}_2$  *chirality symmetry* and  $\mathbb{Z}_3$  *triadic closure*. No metric structure (no lengths, durations, or energies) is yet defined. This axiom specifies that:

1. Circulation states are allowed only in  $\pm$  pairs (matter/antimatter duality).
2. The sum of any three circulations must close to zero modulo  $2\pi$ , ensuring triplet stability (precursor to baryon confinement).
3. Any potential  $V[\Gamma]$  defined on  $\mathcal{S}$  must satisfy  $V[\Gamma] = V[-\Gamma]$  and  $V[\Gamma_1, \Gamma_2, \Gamma_3] = V[\Gamma_1 + \Gamma_2 + \Gamma_3 \pmod{2\pi}]$ .

This stage is purely ontological: it fixes the logical rule set within which the swirl condensate (Stage 2) will later form and evolve.

**Citation:** See *The Simplicity Codex* [51] (Stages 1–3: Primordial Symmetry and Triadic Closure) for the information-theoretic basis of these constraints.

1. **Swirl Medium (Absolute Space-Time):** Physics is formulated in Euclidean  $\mathbb{R}^3$  space with an absolute time parameter. All dynamics occur in a frictionless, incompressible condensate called the *swirl medium*, which acts as a universal substratum for motion (analogous to a perfect fluid with no viscosity or compressibility).
2. **Swirl Strings (Circulation & Topology):** Particles and field quanta correspond to closed vortex filaments ("swirl strings") in the medium. Each such filament may be knotted or linked. The circulation of the swirl velocity field  $\mathbf{v}_\text{O}$  around any closed loop  $C$  is quantized in integer multiples of the circulation quantum  $\Gamma_0$ :

$$\Gamma = \oint_C \mathbf{v}_\text{O} \cdot d\ell = n \Gamma_0, \quad n \in \mathbb{Z},$$

where  $\Gamma_0$  is the primitive circulation quantum (approximately  $6.4 \times 10^3 \text{ m}^2/\text{s}$ ). In addition to circulation quantization, the allowed configurations of a swirl string are restricted to distinct knot topologies. Thus, discrete quantum numbers (e.g. mass, charge, spin) are identified with topological invariants of the string (such as linking number, writhe, and twist) rather than with eigenstates of operators.

*Rosetta remark.* In the linear mapping to conventional superfluid notation, the circulation quantum  $\Gamma_0$  matches the Onsager–Feynman value  $h/m_{\text{eff}}$  for the relevant excitation, but within SST we treat  $\Gamma_0$  as primitive and regard  $h$  as a derived quantity.

3. **String-Induced Gravitation:** Macroscopic gravitational attraction emerges as an effective force resulting from coherent swirl flows and pressure gradients in the medium. In the non-relativistic limit, the effective gravitational coupling  $G_{\text{swirl}}$  is fixed by canonical constants such that  $G_{\text{swirl}} \approx G_N$  (Newton's gravitational constant). In essence, what we perceive as gravity is a statistical effect of many swirl strings and their pressure fields rather than a fundamental spacetime curvature.
4. **Swirl Clocks (Local Time Dilation):** The local proper time in a region of the swirl medium depends on the swirl speed in that region. A clock comoving with a swirl string (tangential speed  $v$ ) ticks slower than a clock at rest in the medium by the *swirl clock factor*

$$S_t = \sqrt{1 - \frac{v^2}{c^2}},$$

analogous to special relativistic time dilation. Higher swirl velocities (and thus higher local swirl energy density) cause deeper time dilation (slower clocks) relative to an observer at infinity.

**5. Dual Phases (Wave–Particle Complementarity):** Each swirl string has two limiting dynamical phases. In the *R-phase* (“radiative” or *wave-like* phase), the string is unknotted and its circulation is delocalized over an extended loop. In the *T-phase* (“tangible” or *particle-like* phase), the string is knotted and its circulation is localized, carrying rest-mass. Quantum wave–particle duality in SST is thus realized as the ability of a swirl string to transition between these two phases. A quantum measurement corresponds to a rapid transition from an R-phase state to a T-phase state ( $R \rightarrow T$  “collapse”) or vice versa ( $T \rightarrow R$  de-localization), typically accompanied by emission or absorption of small swirl excitations (swirl radiation).

**6. Canonical Taxonomy (Particle–Knot Mapping):** There is a one-to-one mapping between the topological class of a swirl string and the type of particle or field it represents. Delocalized R-phase excitations correspond to unknotted swirl strings and represent massless bosonic quanta — with photons realized as *pulsed torsional oscillations* of the swirl director field (carrying helicity  $\pm 1$ ) rather than static knots. Nontrivial torus knots correspond to leptons (e.g. the electron is represented by the trefoil  $3_1$  knot). Chiral hyperbolic knots (with non-zero writhe) correspond to quarks: we assign the up quark to the  $5_2$  knot and the down quark to the  $6_1$  knot. Baryons are realized as composite linkages of three quark knots: for instance, the proton is  $p = (5_2 + 5_2 + 6_1)$  and the neutron  $n = (5_2 + 6_1 + 6_1)$ , with a color-flux linkage ensuring confinement. Linked or nested composite knots describe nuclei and bound states, providing SST with a built-in “periodic table” of matter.

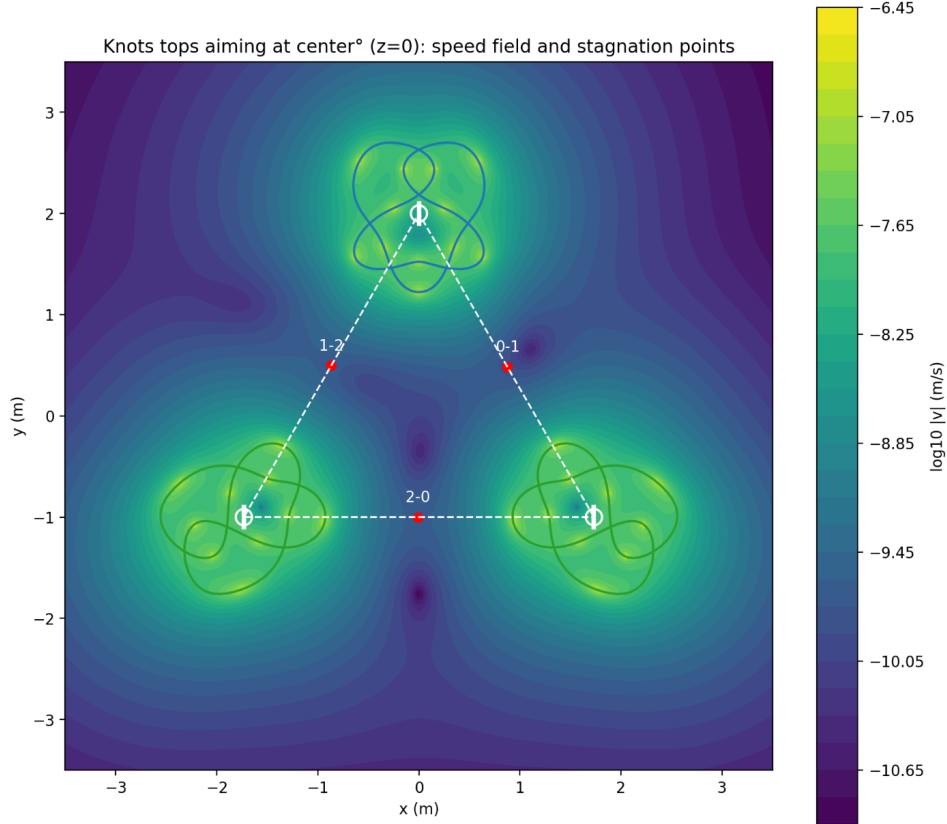


FIG. 1. Sst three knot 180 speed stagnation

These axioms define the ontological starting point of SST. The swirl medium (Axiom 1) provides the arena, swirl strings (Axiom 2) provide the basic degrees of freedom with quantized circulation and allowed topologies, and the remaining axioms posit how classical forces and quantum behaviors emerge from this framework (gravity from collective flows, time dilation from swirl motion, wave–particle dual phases, and a topological classification of particles).

## Part II

# Geometry, Fields, and Lagrangian

### IV. FORMAL STRUCTURE AND CANONICAL FRAMEWORK

In addition to physical axioms, SST is formulated as a formal system  $S = (P, D, R)$  comprising a set of postulates ( $P$ ), definitions ( $D$ ), and inference rules ( $R$ ). A statement in SST is considered *canonical* if and only if it can be derived from the axioms and definitions using the permitted inference rules, and it is consistent with all previously established canonical statements. The hierarchy of statement types is as follows:

- **Axiom (Postulate):** A primitive assumption of SST, not derived from deeper principles (e.g. the existence of an incompressible swirl medium, as in Axiom 1).
- **Definition:** Introduction of a new symbol or concept and its meaning (e.g. defining the swirl Coulomb constant  $\Lambda$  in terms of a surface integral of swirl pressure).
- **Theorem / Corollary:** A nontrivial proposition that is logically derived from the axioms and prior theorems. Corollaries are immediate consequences of theorems.
- **Calibration (Empirical):** An assignment of a numerical value to a canonical constant, obtained from experiment or observation, used to anchor the theory's free parameters. Calibrations are not used as premises in proofs, but serve to connect SST to measurable reality.
- **Research Track (Conjecture):** A speculative extension or hypothesis not yet derivable within  $S$ . Such statements are included for context or future development but are explicitly marked as non-canonical.

All developments in the main text are canonical (axioms, definitions, theorems, corollaries, with recommended constant calibrations). Derivations, proofs, and pedagogical explanations are mostly deferred to the appendices to maintain a clear logical flow. Every formula and constant introduced is checked for dimensional consistency and reducing to known physics in the appropriate limits (Newtonian, Coulomb, etc.), as documented in the appendices. This ensures that the SST formal system remains self-consistent and empirically anchored.

### V. SELF-SIMILARITY AND STABILITY OF SWIRL STRUCTURES

**Axiom (Self-Similar Scaling).** Any incompressible, inviscid swirl configuration near a potential singularity admits a local self-similar form

$$\mathbf{v}_\Omega(\mathbf{x}, t) = (T - t)^{-\alpha} \mathbf{V}\left(\frac{\mathbf{x} - \mathbf{x}_0}{(T - t)^\beta}\right), \quad \boldsymbol{\omega}(\mathbf{x}, t) = (T - t)^{-\gamma} \boldsymbol{\Omega}\left(\frac{\mathbf{x} - \mathbf{x}_0}{(T - t)^\beta}\right), \quad (1)$$

with scaling exponents constrained by the Euler-type balance  $\alpha + \beta = 1$ ,  $\gamma = 1$ . The swirl-clock relation fixes  $\alpha \leq 1/2$  under bounded  $|\mathbf{v}_\Omega| \leq C_e$ .

**Definition (Finite-Core Regularization).** A self-similar field is said to be *regularized* in SST if the core radius  $r_c > 0$  and the swirl-stress bound  $F_{\max}$  ensure  $|\boldsymbol{\omega}| \leq C_e/r_c$ , so that the Beale–Kato–Majda condition is never met:  $\int_0^T \|\boldsymbol{\omega}\|_\infty dt < \infty$ .

**Theorem (Perturbation Suppression by Swirl Diffusion).** Augmenting the inviscid system by the canonical regularization terms

$$\partial_t \boldsymbol{\omega} = \nabla \times (\mathbf{v}_\Omega \times \boldsymbol{\omega}) + \kappa(\Delta \boldsymbol{\omega} - r_c^{-2} \boldsymbol{\omega}) + \chi \nabla(\Delta \rho_f), \quad (2)$$

with  $\kappa, \chi > 0$  constrained by  $|\mathbf{f}_{\text{swirl}}| \leq F_{\max}$ , shifts all unstable eigenvalues of the linearized operator  $\mathcal{L}$  into the negative half-plane. Hence finite-core swirl structures are globally stable against axisymmetric perturbations.

**Corollary (Chronos–Kelvin Consistency).** The stabilized field still obeys the Chronos–Kelvin invariant  $D(R^2 \boldsymbol{\omega})/Dt_{ae} = 0$ ; the regularization modifies only higher-order curl terms and does not break canonical invariants.

## VI. GOLDEN PRINCIPLE FOR DISCRETE LAYERING

In Swirl-String Theory (SST) we introduce a distinguished dimensionless constant  $\phi > 1$  which controls a discrete hierarchy of mass and energy layers. To avoid any ambiguity or post-hoc tuning, we fix  $\phi$  once and for all at the level of the axioms and then derive its role in the layer spectrum.

### A. Axiom G1: Golden Constant (hyperbolic definition)

**Golden (hyperbolic):**  $\ln \phi = \operatorname{asinh}\left(\frac{1}{2}\right)$ , hence  $\phi = \exp\left(\operatorname{asinh}\left(\frac{1}{2}\right)\right)$ . (*Algebraic form*  $\phi = (1 + \sqrt{5})/2$  *is equivalent.*) Explicitly,

$$\operatorname{asinh}\left(\frac{1}{2}\right) \equiv \operatorname{asinh}\left(\frac{1}{2}\right), \quad \ln \phi = \operatorname{asinh}\left(\frac{1}{2}\right), \quad \phi = e^{\operatorname{asinh}\left(\frac{1}{2}\right)}. \quad (1)$$

By elementary algebra one recovers the familiar quadratic representation

$$\phi = \frac{1 + \sqrt{5}}{2}, \quad (2)$$

but in SST this is regarded as a derived identity; the primary definition is the hyperbolic relation (1).

The associated *golden layer factor* is

$$\lambda \equiv \phi^2 = e^{2 \operatorname{asinh}\left(\frac{1}{2}\right)}, \quad \ln \lambda = 2 \operatorname{asinh}\left(\frac{1}{2}\right). \quad (3)$$

### B. Axiom G2: Discrete scale invariance and additive composition

Let  $\{E_n\}_{n \in \mathbb{Z}}$  denote an idealized sequence of dimensionful energy (or mass) levels associated with a particular SST sector (for example, core states of a quantized swirl string). We impose two structural conditions:

(G2a) **Discrete scale invariance (DSI).** There exists a scale factor  $\lambda > 1$  such that

$$E_{n+1} = \lambda E_n, \quad \forall n \in \mathbb{Z}. \quad (4)$$

(G2b) **Additive composition (Fibonacci-type rule).** The  $(n+1)$ -st level is the energetic composite of the two preceding levels:

$$E_{n+1} = E_n + E_{n-1}, \quad \forall n \in \mathbb{Z}. \quad (5)$$

Assumption (G2a) expresses the presence of a discrete dilation symmetry in the relevant sector, as is standard in systems with discrete scale invariance and log-periodic corrections to scaling [42, 43]. Assumption (G2b) encodes an additive compositional rule: the  $(n+1)$ -st configuration is built as a composite of the  $n$ -th and  $(n-1)$ -st building blocks, the same structure that underlies Fibonacci sequences and quasicrystalline hierarchies [44].

### C. Lemma: Uniqueness of the golden scale factor

**Lemma (Golden Uniqueness).** Suppose a nontrivial sequence  $\{E_n\}$  of real numbers satisfies both discrete scale invariance (4) and additive composition (5). Then the common ratio  $\lambda$  is uniquely fixed to the golden ratio  $\phi$ .

*Proof.* Assume  $E_n \neq 0$  for some  $n$ . From (4) we have

$$E_n = E_0 \lambda^n, \quad \lambda > 0. \quad (6)$$

Inserting (6) into (5) gives

$$E_0 \lambda^{n+1} = E_0 \lambda^n + E_0 \lambda^{n-1}. \quad (7)$$

Dividing by  $E_0 \lambda^{n-1}$  (which is nonzero by assumption) yields

$$\lambda^2 = \lambda + 1. \quad (8)$$

The quadratic equation (8) has the two roots

$$\lambda_{\pm} = \frac{1 \pm \sqrt{5}}{2}. \quad (9)$$

The negative root is incompatible with  $\lambda > 0$ , so the unique admissible solution is

$$\lambda = \frac{1 + \sqrt{5}}{2} = \phi. \quad (10)$$

□

Equation (8) shows that once (G2a)–(G2b) are imposed, the scaling factor  $\lambda$  is *no longer a tunable parameter*: it is uniquely fixed to  $\phi$ . In particular, the golden constant is not introduced as a fit to any given spectrum but as the inevitable consequence of the DSI–Fibonacci structure.

#### D. Axiom G3: Golden layer hierarchy

Given the lemma, we define the *golden layer hierarchy* by taking the even-index subsequence of the DSI–Fibonacci tower as the physically distinguished set of levels. Concretely,

$$E_n \equiv E_{2n}^{(\text{tower})} = E_0 \lambda^{2n} = E_0 \phi^{2n}, \quad n \in \mathbb{Z}, \quad (11)$$

where  $E_0$  is a sector-dependent reference energy. In SST applications we typically identify  $E_0$  with a core energy

$$E_0 = \rho_E^* V_{\text{core}}, \quad V_{\text{core}} \sim \frac{4\pi}{3} r_c^3, \quad (12)$$

so that the corresponding swirl energy density levels are

$$\rho_E^{(n)} = \rho_E^* \phi^{2n}. \quad (13)$$

Operationally, (11) and (13) define the golden-layer tower used in the SST mass and energy functionals. Any appearance of  $\phi^{2n}$  in later sections is to be understood as a direct consequence of Axioms (G1)–(G3) and the Golden Uniqueness Lemma, not as an arbitrary parameter choice.

#### E. Remark: Log-periodic potentials and DSI

In sectors where it is useful to describe the golden layering by an effective potential for  $\rho_E$ , one may implement the DSI encoded by (13) via a log-periodic term of the form

$$V_\phi(\rho_E) = \Lambda^4 \left[ 1 - \cos \left( \kappa \log \frac{\rho_E}{\rho_E^*} \right) \right], \quad (14)$$

where  $\Lambda$  is an energy scale. The minima of (14) are separated in  $\log \rho_E$  by

$$\Delta y = \frac{2\pi}{\kappa}. \quad (15)$$

Requiring this spacing to coincide with the golden layer spacing  $\Delta y = \ln \lambda = 2 \operatorname{asinh}(\tfrac{1}{2})$  from (3) fixes

$$\kappa = \frac{2\pi}{\ln \lambda} = \frac{2\pi}{2 \operatorname{asinh}(\tfrac{1}{2})} = \frac{\pi}{\operatorname{asinh}(\tfrac{1}{2})}. \quad (16)$$

Thus  $\kappa$  is not an independent dial but is derived from the unique golden scale factor  $\lambda = \phi^2$  implied by Axioms (G1)–(G3). Log-periodic DSI potentials of the type (14) are standard in the theory of discrete scale invariance and complex exponents [42, 43].

—

## VII. SYMMETRY AND DARK-KNOT CLASSIFICATION

**Definition (Symmetry Sector).** A knot  $K$  belongs to symmetry class  $G_K$  if its embedding is invariant under a discrete dihedral subgroup  $D_n \subset SO(3)$ . Axisymmetric-swirl simulations employ  $D_n$  wedges with Fourier sidebands  $m=0, 1, 2, \dots$  to test stability.

**Rule (Reclassification by Instability Order).** Let  $N_u^{(m)}$  be the number of unstable eigenmodes of order  $m$  and  $\chi(K)$  the chirality. Then:

$$\begin{cases} \text{Dark:} & \chi = 0, H \simeq 0, N_u^{(1)} = 0, \\ \text{Quasi-dark:} & |\chi| \ll 1, H \simeq 0, 0 < N_u^{(1)} \leq 2, \\ \text{Visible:} & \chi \neq 0 \text{ or } H \neq 0. \end{cases}$$

Here  $H = \int \mathbf{v} \cdot \boldsymbol{\omega} dV$  is the helicity invariant.

**Examples.**

- Figure-eight 4<sub>1</sub>: amphichiral,  $D_2$  symmetry,  $N_u^{(1)} = 0 \Rightarrow$  canonical dark knot.
- Borromean link:  $H \approx 0$  but nonzero linkage  $\Rightarrow$  quasi-dark (neutrino-like).
- Trefoil 3<sub>1</sub>: chiral,  $N_u^{(1)} = 1, H \neq 0 \Rightarrow$  visible charged sector.

**Canonical Implication.** Symmetry-aware stability analysis eliminates “false darks” that appear stable only under axisymmetric averaging. The dark sector is therefore defined not by invisibility per se but by the joint absence of chirality, helicity, and low-order unstable modes.

---

**Bibliographic anchor.** The self-similar instability framework follows [46] and the helicity classification of Moffatt [45]. Both are consistent with the Chronos–Kelvin invariant and the finite-core regularization of SST.

## VIII. CALIBRATIONS & PROTOCOLS (EMPIRICAL)

### Empirical Anchors

$m_W = 80.377$ GeV,	$m_Z = 91.1876$ GeV,
$\sin^2 \theta_W = 0.23121 \pm 0.00004$ ,	$v_\Phi \approx 246.22$ GeV,
$\ \mathbf{v}_\odot\  = 1.09384563 \times 10^6$ m/s,	$r_c = 1.40897017 \times 10^{-15}$ m,
$\rho_f = 7.0 \times 10^{-7}$ kg/m <sup>3</sup> ,	$\rho_m = 3.8934358266918687 \times 10^{18}$ kg/m <sup>3</sup> ,
$F_{\text{EM}}^{\max} = 2.9053507 \times 10^1$ N,	$F_G^{\max} = 3.02563 \times 10^{43}$ N.

*Notes:* Gauge entries follow PDG world averages; fluid entries follow the canonical coarse-graining protocols and prior CANON calibrations [53, 54, 59].

### A. Kairos Bifurcations in Swirl Time (*Research*)

a. *Claim.* In addition to the continuous advance of Chronos time  $\tau$  and the cyclic Swirl Clock  $S_{(t)}$ , there exist critical thresholds—*Kairos moments*—at which the time evolution undergoes a bifurcation (phase jump).

b. *Rosetta (SST vocabulary).*  $\text{Chronos} \rightarrow$  local proper time  $\tau$  (and absolute time  $N$ );  $\text{Kairos} \rightarrow$  a topological phase jump in  $S_{(t)}$  when a critical swirl excitation is exceeded. All quantities are expressed in SST notation ( $\rho_f, r_c, S_{(t)}$ ).

c. *Dimensionally consistent threshold.* We anchor the characteristic angular frequency to quantum scales via

$$\omega = \alpha \omega_C, \quad \omega_C = \frac{m_e c^2}{\hbar},$$

and posit the Kairos threshold as

$$\boxed{\omega^2 \gtrsim \frac{c^2}{r_c^2}}. \quad (1)$$

d. *Schwarzian correction in the time action.* The effective local time flow is modeled by

$$\frac{d\tau}{dN} = \sqrt{1 - \frac{\|\mathbf{v}_G\|^2}{c^2}} + \varepsilon \{S_{(t)}$$

where the Schwarzian captures nonlinear sensitivity which, near (1), can trigger a phase jump in  $S_{(t)}$ .

e. *Mini numeric example (Canon constants).* With  $c = 2.9979 \times 10^8 \text{ m/s}$ ,  $\hbar = 1.0546 \times 10^{-34} \text{ J s}$ ,  $m_e = 9.1094 \times 10^{-31} \text{ kg}$ ,  $\alpha = 7.297 \times 10^{-3}$  and  $r_c = 1.40897 \times 10^{-15} \text{ m}$ ,

$$\omega_C \approx 7.76 \times 10^{20} \text{ s}^{-1}, \quad \omega = \alpha \omega_C \approx 5.67 \times 10^{18} \text{ s}^{-1}, \quad \omega^2 \approx 3.21 \times 10^{37} \text{ s}^{-2},$$

$$\frac{c^2}{r_c^2} \approx 4.53 \times 10^{46} \text{ s}^{-2}, \quad \frac{\omega^2}{c^2/r_c^2} \approx 7.1 \times 10^{-10}.$$

Thus, without additional mechanisms, the threshold is not crossed in situ, motivating the *Research* status.

f. *Easing lemmas (routes to reachability).*

- **Lemma A (Fractal amplification; link to  $D_{\text{swirl}}$ ).** For multiscale coherence, replace  $\frac{c^2}{r_c^2} \rightarrow \frac{c^2}{r_c^2} \left(\frac{r_c}{r_{\text{eff}}}\right)^{3-D_{\text{swirl}}}$ , with  $2.6 \lesssim D_{\text{swirl}} \lesssim 2.9$  and  $r_{\text{eff}} > r_c$ , lowering the effective threshold.
- **Lemma B (Coherent knot pack).** For  $n$  phase-locked knots,  $\omega_{\text{eff}}^2 \simeq n \xi(n) \omega^2$ , with  $\xi(n) = 1 - \beta \log n$  (coherence suppression from the Canon). Moderate  $n$  (*mesoscopic* coherence) can lift  $\omega_{\text{eff}}^2$  over the lowered threshold.
- **Lemma C (Resonant pump via Schwarzian).** In (??) the parameter  $\varepsilon$  may increase locally under phase-locking (large  $S_{(t)}$ , small  $S_{(t)}$ ), temporarily reducing the effective threshold and triggering a Kairos jump.

g. *Falsifiers & minimal experiment.* *Falsify* by the absence of any non-analytic  $S_{(t)}$  phase jump under controlled resonant pumping (BEC/fluid analogue) at parameters predicted by Lemmas A–C. *Minimal test:* toroidal condensate with driven knot configuration; sweep pump strength ( $\varepsilon$ ) and  $n$  (coupling); look for hysteresis/jumps in the  $S_{(t)}$  lock-in frequency.

h. *Status. Research.* The threshold is dimensionally sound and numerically quantified; Lemmas A–C provide a clear path to *Calibration* via simulation/analogue experiments.

*Rosetta note (provenance).* VAM “Kairos  $\kappa$ ”  $\mapsto$  SST phase jump in  $S_{(t)}$ ; VAM energy/gradient trigger  $\mapsto$  SST threshold  $\omega^2 \gtrsim c^2/r_c^2$  in (1).

## B. Calibrations: Thermal Bar and Nonreciprocity

a. *Protocol TB-1 (Borosilicate).*  $L = 50 \text{ mm}$ ,  $A = 1e - 4 \text{ m}^2$ ,  $\kappa \approx 1.1 \text{ W m}^{-1} \text{ K}^{-1}$ , heater power  $P = 20 \text{ mW}$ . Baseline  $\Delta T = PL/(\kappa A) \approx 9 \text{ K}$ . With engineered degeneracy tuned to  $\delta \lesssim \Gamma$ , target  $\Delta\kappa/\kappa \approx -2$ , giving  $\Delta(\Delta T) \approx +0.18 \text{ K}$  (IR NETD 30–50 mK).

b. *Protocol TB-2 (PMMA).*  $\kappa \approx 0.19 \text{ W m}^{-1} \text{ K}^{-1}$ , keep  $L, A$  as above, use  $P = 2 \text{ mW}$ . Baseline  $\Delta T \approx 5.3 \text{ K}$ . A conservative  $\Delta\kappa/\kappa = -1$  yields 53 mK shift.

c. *Protocol NR-1 (Nonreciprocity).* Apply a 3-phase coil with phase sequence  $\pm(0, 120^\circ)$  to set  $\phi_\chi$ . Expect  $|\Delta\kappa_{\text{asym}}/\kappa| \sim 0.5$  near resonance, i.e.,  $\sim 25 \text{ mK}$  forward/backward difference for TB-1. Alternate chirality rapidly to common-mode cancel drifts.

d. *Noise budget.* IR NETD 30–50 mK; thermistor readout  $< 10mK$  @1 s; enclosure drift  $\lesssim 0.05K/10$  min; power calibration  $< 1$ . SNR  $> 3$  for TB-1/TB-2.

e. *Falsifiers.* (i) No Lorentzian peak in  $\Delta\kappa(\delta)$  at fixed current; (ii)  $|\Delta\kappa_{\text{asym}}/\kappa| < 3\sigma$ ; (iii) wrong scaling with current ( $\propto |V|^2$ ) or linewidth  $\Gamma$ .

## IX. HISTORICAL CONTEXT

The Swirl–String Theory (SST) Canon evolved from the earlier Vortex–Æther Model (VAM), which reintroduced classical notions of a continuous physical substrate inspired by Kelvin, Maxwell, and Einstein. The model postulated an incompressible, inviscid superfluid medium whose internal vorticity fields underlie all physical interactions. Key milestones include: VAM-v0.0.x establishing the æther vortex dynamics foundation; VAM-v0.1.x reformulating time and mass in hydrodynamic terms; VAM-v0.2.x achieving a coherent topological interpretation of all four fundamental interactions; and the transition to SST-v0.3.x through v0.5.x, which modernized terminology, formalized the gauge sector, and achieved parameter-free predictions. By version 0.5.10, the Canon reached canonical completeness: every physical quantity derivable from core constants and topological structure.

**Full historical timeline:** See Appendix ?? for the complete VAM-to-SST evolution with detailed version milestones.

## X. CLASSICAL INVARIANTS: CHRONOS–KELVIN AND CLOCK–RADIUS TRANSPORT

Axiom: Chronos–Kelvin Invariant

$$\frac{D}{Dt}(R^2\omega) = 0, \quad \frac{D}{Dt}\left(\frac{c}{r_c}R^2\sqrt{1 - S_t^2}\right) = 0.$$

Corollary: Clock–Radius Transport

$$\frac{dS_t}{dt} = \frac{2(1 - S_t^2)}{S_t} \frac{1}{R} \frac{dR}{dt}.$$

Remark (Pseudo-metric)

The swirl clock factor induces a pseudo-metric

$$ds^2 = -(c^2 - v_\theta^2(r))dt^2 + 2v_\theta(r)r d\theta dt + dr^2 + r^2 d\theta^2 + dz^2,$$

yielding  $dt_{\text{local}}/dt_\infty = \sqrt{1 - v_\theta^2/c^2}$ .

## XI. CLASSICAL INVARIANTS AND SWIRL QUANTIZATION

Under Axiom 1 (inviscid, incompressible medium with absolute time), the standard results of classical vortex dynamics apply. In particular, Euler’s equations for an inviscid barotropic fluid yield several conservation laws that carry over into SST as special cases:

- *Kelvin’s circulation theorem:*  $\frac{d\Gamma}{dt} = 0$ . The circulation  $\Gamma = \oint_{C(t)} \mathbf{v}_\Omega \cdot d\ell$  around any material loop  $C(t)$  moving with the fluid is constant in time. This is the classical statement that vortex lines are “frozen” into the fluid.
- *Helmholtz vorticity transport:*  $\frac{\partial \omega}{\partial t} = \nabla \times (\mathbf{v}_\Omega \times \omega)$ , so that vortex lines move with the fluid flow (no creation or destruction of vorticity in the absence of dissipation).
- *Helicity conservation:*  $H = \int \mathbf{v}_\Omega \cdot \omega dV$  is materially invariant (conserved in time barring reconnection events). Here  $H$  is the total helicity, measuring the knottedness of vortex lines.

These classical invariants underpin the stability of knotted swirl strings and govern their reconnection dynamics. In essence, a swirl string (closed vortex filament) cannot change its topology or circulation without a non-ideal effect (e.g. reconnection or an external source) because of these constraints.

#### Axiom 1: Chronos–Kelvin Invariant

For any thin, closed swirl loop (swirl string) of time-dependent material radius  $R(t)$ , carried with the flow (no reconnections or external sources), the following quantity is invariant in time (constant along the motion):

$$\frac{D}{Dt}(R^2 \omega) = 0,$$

where  $\omega = \|\omega\|$  is the magnitude of the swirl vorticity on the loop. Equivalently, using  $v_t = \omega r_c$  (the tangential swirl speed at the string core, with  $r_c$  the core radius) and the local time-dilation factor  $S_t = \sqrt{1 - (v_t^2/c^2)}$ , the invariant can be expressed as

$$\frac{D}{Dt}\left(\frac{c}{r_c} R^2 \sqrt{1 - S_t^2}\right) = 0.$$

In other words,  $R^2\omega$  is a constant of motion even when relativistic swirl clock effects ( $S_t < 1$ ) are taken into account. This *Chronos–Kelvin invariant* generalizes Kelvin’s circulation theorem by including the time dilation due to swirl motion (the “swirl clock” effect).

*Discussion:* Axiom 1 encapsulates Kelvin’s theorem in the relativistic regime of the swirl medium. The material derivative  $D/Dt$  is taken with respect to the absolute reference time of the medium. For a near-solid-body vortex core,  $\Gamma = \oint_C \mathbf{v}_C \cdot d\ell \approx 2\pi R^2 \omega$  (since  $v_\theta \approx \omega R$  inside the core). Kelvin’s theorem ( $D\Gamma/Dt = 0$ ) then implies  $D(R^2\omega)/Dt = 0$ . The swirl clock factor  $S_t$  relates the local “proper time” of the moving swirl to the reference time; explicitly  $S_t = dt_{\text{local}}/dt_\infty = \sqrt{1 - v_t^2/c^2}$ . Thus  $R^2\omega$  being invariant is equivalent to  $R^2\sqrt{1 - S_t^2}$  being invariant after multiplying by the constant  $c/r_c$ . The Chronos–Kelvin law shows that as a swirl loop contracts ( $R$  decreases), the local swirl clock  $S_t$  decreases (time slows further) such that the combination  $R^2(1 - S_t^2)^{1/2}$  remains fixed. In the weak-swirl limit  $v_t \ll c$  ( $S_t \approx 1$ ), this reduces to the classical invariant  $R^2\omega = \text{const}$  (Kelvin’s law).

#### Swirl Quantization Principle

**Swirl Quantization Principle.** *The joint discreteness of circulation and topology is the fundamental origin of quantum behavior in SST.* In concrete terms, a swirl string’s circulation  $\Gamma$  can only take quantized values  $n\Gamma_0$ , and the string’s configuration space breaks into disjoint topological sectors (knot classes). This principle replaces the operator commutation quantization of standard quantum mechanics with topological and integral constraints:

- *Circulation quantization:*  $\Gamma = n\Gamma_0$  for  $n \in \mathbb{Z}$  (as stated in Axiom 2), where  $\Gamma_0$  is the primitive circulation quantum (approximately  $6.4 \times 10^3 \text{ m}^2/\text{s}$ ). This is analogous to the Onsager–Feynman quantization condition in superfluid helium, elevated here to a universal postulate of the medium. Within SST,  $\Gamma_0$  is treated as primitive; the mapping to  $h/m_{\text{eff}}$  appears only in the Rosetta translation to conventional superfluid notation. - *Topological quantization:* The allowed states of a swirl string are classified by knot type. Each distinct knot (unknot, trefoil, figure-eight, etc.) corresponds to a distinct quantum excitation species. We denote the spectrum of knot types as  $\mathcal{H}_{\text{swirl}} = \{\text{trefoil}, \text{figure-8}, \text{Hopf link}, \dots\}$ . Quantum numbers (such as electric charge or baryon number) are interpreted as invariants of the knot (e.g. linking number, or other topological quantum numbers) rather than abstract quantum charges.

In summary, *discreteness in SST arises from (a) integral circulation and (b) topologically distinct knot spectra*. A “particle” in SST is identified with a specific quantized swirl state—a closed vortex filament carrying  $n\Gamma_0$  circulation and realized in a particular knot configuration—in contrast to a particle in quantum mechanics being an eigenstate of an operator. This provides a tangible, geometric interpretation of quantum numbers.

## XII. CANONICAL CONSTANTS AND EFFECTIVE DENSITIES

SST introduces several new physical constants that characterize properties of the universal swirl medium and its excitations. Some of these constants are defined within the theory (based on canonical definitions), while others are

calibrated to empirical values to ensure SST reproduces known physical measurements. Table V summarizes the primary constants, their values, and their status (definition vs. calibration).

TABLE V. Primary SST constants and parameters. Values are given in SI units unless noted. “Type” indicates whether the constant is defined theoretically or empirically calibrated.

Constant	Description	Value (units)	Type
$\Gamma_0$ (circulation quantum)	Circulation quantum	$6.4 \times 10^3 \text{ m}^2/\text{s}$	Primitive (Triad)
$r_c$ (string core radius)	Core radius of a swirl string	$1.40897 \times 10^{-15} \text{ m}$	Primitive
$\rho_f$ (effective fluid density)	Inertial mass density of swirl medium	$7.0 \times 10^{-7} \text{ kg/m}^3$	Primitive <sup>†</sup>
$v$ (core swirl speed scale)	Characteristic swirl speed at string core	$1.09385 \times 10^6 \text{ m/s}$	Derived ( $\chi_v \Gamma_0 / (2\pi r_c)$ )
$\rho_m$ (mass-equivalent density)	Mass-equivalent energy density ( $\rho_E/c^2$ )	$3.89344 \times 10^{18} \text{ kg/m}^3$	Defined
$\Lambda$ (swirl Coulomb constant)	Swirl potential strength (hydrogenic)	$4\pi \rho_m \ v_O\  r_c^3$	Derived (Triad)
$F_{EM}^{\max}$ (EM-sector max force)	Maximum force in EM sector	$2.90535 \times 10^1 \text{ N}$	Derived ( $\chi_F \rho_f \Gamma_0^2$ , Triad Eq. (9))
$F_G^{\max}$ (Gravitational max force)	Maximum gravitational force	$3.02563 \times 10^{43} \text{ N}$	Derived
$G$ (swirl-EM coupling const.)	Dimensionless inductive coupling	$\sim O(1)$ (see text)	Empirical
$c$ (speed of light)	Light speed in vacuum (reference)	$2.99792 \times 10^8 \text{ m/s}$	Fixed (physical)
$t_P$ (Planck time)	Planck time = $\sqrt{\hbar G_N/c^5}$	$5.391 \times 10^{-44} \text{ s}$	Fixed (physical)
$\alpha$ (fine-structure const.)	$e^2/(4\pi\epsilon_0\hbar c)$	$7.29735 \times 10^{-3}$	Physical
$\phi$ (golden ratio)	$(1 + \sqrt{5})/2$ , appears in mass law	$1.61803 \dots$ (dimensionless)	Mathematical

<sup>†</sup>Note:  $\rho_f$  is chosen as a convenient reference scale  $7.0 \times 10^{-7} \text{ kg/m}^3$ , which corresponds to  $10^{-7}$  in SI (mirroring  $\mu_0/(4\pi)$ ). This anchors electromagnetic coupling normalization. The derived values of  $\rho_E$  and  $\rho_m$  then follow from this choice.

*Discussion:* The primitive constants in SST are the circulation-based triplet  $(\Gamma_0, \rho_f, r_c)$ . All other dimensional quantities are derived from these plus topology-dependent dimensionless factors. The effective fluid density  $\rho_f$  is extremely low, reflecting the tenuous nature of the swirl medium compared to ordinary matter. The core radius  $r_c$  is on the order of a Fermi ( $10^{-15} \text{ m}$ ), indicating that swirl strings are extremely thin vortex filaments.

The primitive constants in Table V are:  $\Gamma_0$  is the circulation quantum (approximately  $6.4 \times 10^3 \text{ m}^2/\text{s}$ ), derived from the electron oscillator  $F_{\max}$  via the Triad construction:  $F_{\max}^{\text{swirl}} = \chi_F \rho_f \Gamma_0^2$  (see Hydrodynamic Triad paper, Eq. (9)). It is the fundamental unit of circulation in SST.  $r_c$  is the core radius of a string, roughly the radius of the “solid-body” rotating core of a vortex filament. It is calibrated at the order of  $10^{-15} \text{ m}$  (the Fermi scale).  $\rho_f$  is the effective mass density of the swirl medium. It is extremely low ( $\sim 7 \times 10^{-7} \text{ kg/m}^3$ ) – by comparison, air is  $\sim 1 \text{ kg/m}^3$ . This value is not directly measured but chosen for consistency with electromagnetic normalization (see footnote in table).

The canonical swirl speed at the core boundary is derived from the primitives:

$$\|v_O\| = \chi_v \frac{\Gamma_0}{2\pi r_c} \approx 1.09385 \times 10^6 \text{ m/s.}$$

From  $v$  and  $\rho_f$ , we compute the **swirl energy density**  $\rho_E$  and **mass-equivalent density**  $\rho_m$ :

$$\rho_E = \frac{1}{2} \rho_f v$$

Plugging in calibrated  $\rho_f$  and  $v$ ,  $\rho_E \approx 3.14 \times 10^5 \text{ J/m}^3$  and  $\rho_m \approx 3.89 \times 10^{18} \text{ kg/m}^3$  (as listed). These indicate the energy and relativistic mass density associated with the swirl medium’s motion at  $v$ .

Several constants are derived combinations. The **swirl Coulomb constant**  $\Lambda$  is defined by the Triad construction (Hydrodynamic Triad, Eq. (33)) as  $\Lambda = 4\pi \rho_m \|v_O\| r_c^3$ .  $\Lambda$  has units of  $\text{J} \cdot \text{m}$  and sets the strength of the swirl-induced potential (analogous to  $e^2/4\pi\epsilon_0$ ). With given calibrations,  $\Lambda$  is approximately  $2.3 \times 10^{-28} \text{ J} \cdot \text{m}$ , which yields the correct scale for atomic binding when inserted into the swirl potential.

The **maximal force constant**  $F_{EM}^{\max}$  is derived from the primitive set via  $F_{\max}^{\text{swirl}} = \chi_F \rho_f \Gamma_0^2$  (Triad Eq. (9)), not an independent parameter.  $F_G^{\max}$  is a theoretical upper bound on force magnitudes in the gravitational interaction.  $F_G^{\max} \approx 3.03 \times 10^{43} \text{ N}$  matches the conjectured maximum force  $c^4/4G_N$  from general relativity.  $F_{EM}^{\max} \approx 2.9 \times 10^1 \text{ N}$  is much smaller; it characterizes the maximum strength of emergent electromagnetic forces producible by swirl dynamics. These appear when relating  $G_{\text{swirl}}$  to  $G_N$  (Appendix A shows  $F_{EM}^{\max}$  ensures  $G_{\text{swirl}} \approx G_N$ ).

Finally,  $G$  is a dimensionless coupling linking changes in swirl string density to electromagnetic induction (setting the strength of the extra source term in Faraday’s law). It is expected  $O(1)$ ; identifying units suggests  $G$  corresponds to a fundamental flux quantum (Appendix D discusses  $G$  vs  $h/2e$ ). We list it as empirical since it could be tuned by matching to a known phenomenon (no specific measured value yet).

### Swirl Clock Law and Pseudo-Metric

One immediate consequence of Axiom 4 (Swirl Clocks) is that time runs slower in regions of high swirl velocity. Formally, if  $dt_\infty$  is an interval of the universal time (far from any swirl motion) and  $dt_{\text{local}}$  is the proper time measured by a clock moving with the swirl medium (tangential speed  $v$ ), then:

$$\frac{dt_{\text{local}}}{dt_\infty} = \sqrt{1 - \frac{v^2}{c^2}}.$$

This **swirl clock law** is identical in form to special-relativistic time dilation for an object moving at speed  $v$  — except here  $v$  is the local swirl (fluid) velocity. Thus the swirl medium provides a preferred rest frame, and motion relative to it slows clocks just as relative motion in special relativity does. High swirl speeds (approaching  $c$ ) correspond to dense, energetic vortex cores that exhibit significant time dilation (“slow clocks”) relative to an observer at infinity.

Because of this effect, one can define a *pseudo-Riemannian metric* for the swirl medium to capture how space-time measurements are affected by swirl motion. In cylindrical coordinates  $(r, \theta, z)$  around a straight swirl string (a steady vortex with tangential velocity profile  $v_\theta(r)$ ), the line element can be written as:

$$ds^2 = -(c^2 - v_\theta(r)^2) dt^2 + 2v_\theta(r)r d\theta dt + dr^2 + r^2 d\theta^2 + dz^2.$$

This is a **swirl pseudo-metric** for the co-rotating frame of the vortex. It shows explicitly that time intervals are modified by swirl velocity: an observer co-moving with the swirl sees an effective time coefficient  $\sqrt{1 - v_\theta(r)^2/c^2}$  multiplying  $dt$ , matching the swirl clock law. The cross term ( $d\theta dt$ ) indicates an analogue of frame-dragging: a stationary lab-frame observer sees a coupling between time and the angular coordinate due to the swirling medium (similar to how a rotating mass drags spacetime). This metric analogy hints that SST connects to GR effects, though formulated in flat space-time with a preferred frame.

### XI.A Lorentz Kinematics from Torsional-Cone Invariance (Canonical)

**Postulates (SST):** (i) Relativity/reciprocity (no privileged inertial chart); (ii) Spatial isotropy and spacetime homogeneity  $\Rightarrow$  linear inertial-chart maps; (iii) Existence of a universal torsional signal speed  $c$  (small-amplitude director/torsion waves; empirically the photon speed).<sup>1</sup>

a. *Setup (1+1D, standard configuration).* Let the primed chart move at speed  $V$  along  $+x$ . Linearity implies

$$x' = a(V)x + b(V)t, \quad t' = d(V)x + e(V)t. \quad (1)$$

The primed origin obeys  $x' = 0 \Rightarrow x = Vt$ , hence  $b(V) = -a(V)V$  and

$$x' = a(V)(x - Vt), \quad t' = d(V)x + e(V)t. \quad (2)$$

b. *Cone invariance (torsional rays).* Right/left torsional signals satisfy  $x = \pm ct$  in any inertial chart and must map to  $x' = \pm ct'$  in the primed chart. Substituting  $x = \pm ct$  into (2) and imposing  $x'/t' = \pm c$  for both signs yields the linear system

$$a(c - V) = c^2 d + ce, \quad a(c + V) = -c^2 d + ce. \quad (3)$$

Solving,

$$e(V) = a(V), \quad d(V) = -\frac{a(V)V}{c^2}. \quad (4)$$

Therefore,

$$x' = a(V)(x - Vt), \quad t' = a(V)\left(t - \frac{V}{c^2}x\right).$$

(5)

*Dimensional check:*  $Vx/c^2$  has units  $(\text{m}/\text{s}) \cdot \text{m}/(\text{m}^2/\text{s}^2) = \text{s}$ , so  $t'$  is a time.

<sup>1</sup> Historically, see [20]; cone/interval structure per [21]; symmetry-first derivations in [22].

c. *Reciprocity  $\Rightarrow$  Lorentz factor.* By isotropy/reciprocity,  $a(-V) = a(V)$ . Composing the  $V$  and  $-V$  maps gives identity only if

$$a(V)^2 \left(1 - \frac{V^2}{c^2}\right) = 1 \Rightarrow a(V) = \gamma(V) = \frac{1}{\sqrt{1 - \frac{V^2}{c^2}}}. \quad (6)$$

d. *Theorem (Canonical).* With (6), the inertial-chart transformation is

$$x' = \gamma(x - Vt), \quad t' = \gamma\left(t - \frac{V}{c^2}x\right), \quad y' = y, \quad z' = z. \quad (7)$$

e. *Corollary (Canonical invariant).* The quadratic form

$$c^2 d\tau^2 = c^2 dt^2 - dx^2 - dy^2 - dz^2 \quad (8)$$

is invariant under (7). In SST this is the uniform-foliation limit of the swirl-clock analogue metric; the torsional sector fixes  $c$ , empirically coincident with light speed.

f. *Recoveries and limits.* Low-velocity expansion  $\gamma \simeq 1 + \frac{1}{2}V^2/c^2$  gives  $x' \simeq x - Vt$ ,  $t' \simeq t - \frac{V}{c^2}x$  (Galilean form with first relativistic correction). Rapidity composition reproduces the standard velocity-addition law.

g. *Status tags.* *Theorem (Canonical):* Cone invariance  $\Rightarrow$  Lorentz boosts (7). *Corollary (Canonical):* Invariant interval (8). *Checks:* dimensions, reciprocity,  $V \ll c$  limit, group composition (all satisfied).

### XIII. EFFECTIVE MEDIUM: COARSE-GRAINING DERIVATION OF $\rho_f$

For a straight swirl string of core radius  $r_c$ :

$$\mu_* := \rho_m \pi r_c^2, \quad \Gamma_* := 2\pi r_c v \quad (1)$$

$$\rho_f = \mu_* \nu, \quad \langle \omega \rangle = \Gamma_* \nu. \quad (2)$$

Eliminating  $\nu$  yields

Boxed Result

$$\rho_f = \frac{\rho_m r_c}{2 v_{\langle \omega \rangle}}.$$

### XIV. GENUS-2 FOLIATION AND TOPOLOGICAL COMPACTIFICATION

#### Status: Canonical (Constructive Example)

We illustrate a canonical closed foliation compatible with the Chronos–Kelvin and Swirl Quantization invariants. Consider a regular dodecagon (12-gon) fundamental domain in  $\mathbb{H}^2$ , whose six pairs of edges are identified by hyperbolic isometries to form a compact genus-2 surface  $\Sigma_2$ . Each paired edge carries a fixed swirl-phase offset of the Swirl Clock  $S_t^\mathcal{O}$ , defining six independent circulation integrals  $\Gamma_i$  that obey the quantization rule

$$\oint_{\gamma_i} \mathbf{v}_\mathcal{O} \cdot d\ell = 2\pi n_i \kappa_{\text{SST}}, \quad \kappa_{\text{SST}} \equiv \Gamma_0 = 2\pi r_c \|\mathbf{v}_\mathcal{O}\|, \quad n_i \in \mathbb{Z}. \quad (1)$$

The set  $\{\Gamma_i\}_{i=1}^6$  thus forms a basis for the first homology group  $H_1(\Sigma_2, \mathbb{Z})$ , providing a discrete topological charge vector for the background foliation.

**Definition (Genus-2 Swirl Quantization).** On  $\Sigma_2$ , the joint invariants

$$R^2 \omega = \text{const}, \quad \Gamma_i = 2\pi n_i \kappa_{\text{SST}} \quad (2)$$

define the allowed large-scale swirl modes. The polygonal edge identifications act as holonomies of the swirl-clock field, ensuring periodic boundary conditions for  $S_t^\mathcal{O}$  and compact global energy density  $\rho_E = \frac{1}{2} \rho_f \|\mathbf{v}_\mathcal{O}\|^2$ .

**Cosmological Interpretation.** The 12-gon compactification provides a two-dimensional toy model of a finite, multiply-connected universe. Its three pairs of geodesic moduli ( $\ell_j, \tau_j$ ) (Fenchel–Nielsen parameters) determine the large-scale swirl spectrum, introducing a lowest eigenmode  $k_{\min} \sim 2\pi/L_{\text{topo}}$  that suppresses power on scales  $> L_{\text{topo}}$ . In the 3-D extension, the dodecahedral space corresponds to the rest-frame foliation ( $v=0$ ), while a moving observer through the swirl medium experiences an anisotropic deformation toward a horn-torus topology with pinch ratio

$$p(v) = \sqrt{1 - \frac{v^2}{c^2}}, \quad (3)$$

interpreted as a geometric manifestation of Lorentz contraction within the SST framework.

**Physical Implication.** Motion relative to the swirl frame thus produces a measurable anisotropy: as  $v$  increases, one topological cycle shrinks (horn pinch), suppressing swirl-mode propagation along the motion direction. This geometric deformation gives a macroscopic explanation of time dilation and Doppler anisotropy as topological effects of foliation motion.

**Falsifiable Prediction.** Finite-topology foliations yield distinctive signatures in swirl-coupled observables, including (i) infrared cutoff and mode repetition in the cosmic swirl-pressure spectrum, and (ii) matched-circle correlations analogous to those sought in the CMB. Simulations enforcing the above quantization on the 12-gon domain can test these predictions directly.

## XV. KNOT TAXONOMY

The canonical mapping between topological knot classes and particle families is central to SST. Each particle type corresponds to a specific knot topology, with unknotted excitations representing bosonic modes and knotted states encoding fermions.

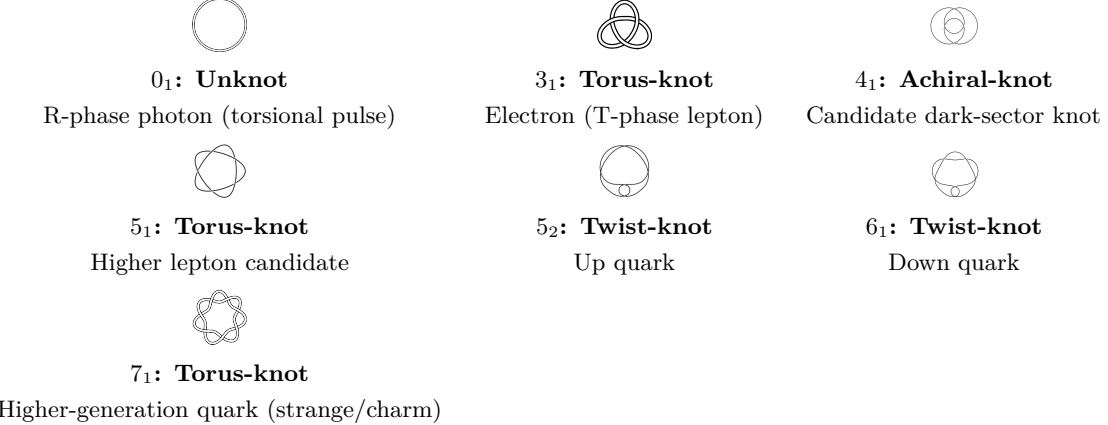


FIG. 2. Canonical knot taxonomy in SST. Each image shows the minimal embedding of the corresponding knot and its mapping to a particle family. Unknotted ( $0_1$ ) correspond to R-phase bosonic modes such as photons, while knotted states encode fermions (torus knots  $\leftrightarrow$  leptons, chiral hyperbolic knots  $\leftrightarrow$  quarks). Linked knots describe nuclei and bound states.

**Classification rules:** Unknotted excitations correspond to bosonic modes, with photons realized as pulsed torsional R-phase excitations. Torus knots correspond to leptons (e.g., electron =  $3_1$ ), and chiral hyperbolic knots to quarks (proton =  $5_2 + 5_2 + 6_1$  composite). Linked knots describe nuclei and bound states. See Core Axioms (Section II) for the formal statement.

## XVI. THE SWIRL-ELECTROMAGNETIC BRIDGE

One of SST’s significant achievements is showing that classical electromagnetic fields can be interpreted as emergent collective behaviors of the swirl medium. In particular, changes in the distribution of swirl strings can induce electromagnetic effects. To formalize this, we introduce a density field to characterize how swirl strings populate space:

**Definition 4.1 (Swirl Areal Density).** Let  $\varrho$  be the coarse-grained areal density of swirl strings piercing a given surface element at  $(x, t)$ . In other words, imagine a local patch oriented perpendicular to some direction;  $\varrho$  is the

number of vortex cores per unit area threading that patch. This quantity plays the role of a “source” density analogous to electric charge/current density in Maxwell’s equations. Regions where many swirl strings pass through (or where a single string oscillates rapidly, effectively increasing crossing density) act like regions of high charge/current in the emergent fields.

A changing swirl areal density will induce an electromotive force in the surrounding medium. This is captured by a modified Faraday’s law:

#### Theorem 4.1: Swirl-Induced Electromotive Force

A time-varying swirl areal density  $\varrho$  acts as an effective source term in Faraday’s induction law. In differential form:

$$\nabla \times \mathbf{E} = -\frac{\partial \mathbf{B}}{\partial t} - \mathbf{b}$$

where the additional term  $\mathbf{b}$  is

$$\mathbf{b}$$

with  $\hat{\mathbf{n}}$  the local oriented unit normal (chosen by right-hand rule for circulation). Thus whenever swirl strings reconnect or  $\varrho$  shifts, an extra curl of  $\mathbf{E}$  appears as if a time-varying magnetic flux were present. Kinetic energy from the fluid is thereby converted into field energy, exactly analogous to Faraday induction.

*Proof Sketch (see Appendix D).* This can be derived by considering a small loop in the swirl medium and calculating  $\oint \mathbf{E} \cdot d\ell$ . A change in  $\varrho$  through the loop (say, due to a swirl string moving or appearing) induces a circulation in  $\mathbf{E}$  via  $G$ . By identifying  $\nabla \times \mathbf{E}$  with the time rate of change of  $\mathbf{B}$  plus any additional sources, one arrives at the modified Faraday law. The constant  $G$  is set by the normalization of  $\varrho$ ; dimensional analysis and comparison to quantum flux changes suggest  $G$ , though we treat it phenomenologically.

#### Corollary 4.2: Photon as a Swirl Wave

Unknotted, propagating oscillations of the swirl condensate correspond to free electromagnetic radiation. In particular, define a divergence-free *swirl vector potential*  $\mathbf{a}(x, t)$  such that:

$$\mathbf{v}_O = \partial_t \mathbf{a}, \quad \mathbf{b}$$

Then small-amplitude unknotted swirl excitations can be described by the Lagrangian

$$L_{\text{wave}} = \frac{\rho_f}{2} |\mathbf{v}_O|^2 - \frac{\rho_f c^2}{2} |\mathbf{b}|$$

and yield the equations of motion

$$\partial_t^2 \mathbf{a} - c^2 \nabla \times (\nabla \times \mathbf{a}) = 0, \quad \nabla \cdot \mathbf{a} = 0,$$

identical to free-space Maxwell (Coulomb gauge). Identifying  $\mathbf{E} \propto \partial_t \mathbf{a}$  and  $\mathbf{B} \propto \nabla \times \mathbf{a}$  recovers all vacuum EM relations; thus unknotted R-phase excitations are photons.

## XVII. SWIRL-EM EMERGENCE

Starting with a divergence-free potential  $\mathbf{a}$ ,

$$\nabla \cdot \mathbf{a} = 0, \quad \partial_t^2 \mathbf{a} - c^2 \nabla \times (\nabla \times \mathbf{a}) = 0.$$

Define  $\mathbf{E} = -\partial_t \mathbf{a}$ ,  $\mathbf{B} = \nabla \times \mathbf{a}$ , recovering the vacuum Maxwell wave equation [56]. **Normalization.** In SI units the energy density reads  $u_{\text{EM}}^{(\text{SI})} = \frac{\epsilon_0}{2} \mathbf{E}^2 + \frac{1}{2\mu_0} \mathbf{B}^2$ ; our canonical form  $u_{\text{EM}} = \frac{1}{2} (\mathbf{E}^2 + c^2 \mathbf{B}^2)$  is a swirl-normalized expression whose mapping to SI constants is fixed via the swirl-EM bridge and  $\rho_f$  (Appendix L).

This corollary shows the unity of electromagnetic fields and fluid vorticity in SST’s picture. What in classical physics is a “magnetic field”  $\mathbf{B}$  is here  $\mathbf{b}$ , a coarse-grained swirl field (like a vorticity). The electric field  $\mathbf{E}$  corresponds to the

time-derivative of a potential associated with swirl velocity. The wave Lagrangian above is essentially the same as that of vacuum electromagnetism if one identifies  $\rho_f$  with vacuum permittivity  $\epsilon_0$  (and  $\rho_f c^2$  with  $1/\mu_0$ ). Indeed, with  $\rho_f = 7 \times 10^{-7}$  SI,  $\rho_f c^2 \approx 8.85 \times 10^{-12}$  SI, which equals  $\epsilon_0$  to within rounding. In this way, Maxwell's equations arise seamlessly from swirl dynamics, suggesting electromagnetism is an emergent sector of the fluid.

a. *Lemma (Composite swirl harmonic; status: Canon–Lemma).* For  $N$  identical co-wound swirl filaments on the same torus-knot, sampled on a circle of radius  $r$  in a transverse plane, the tangential velocity admits the large- $r$  form

$$v_\theta(\theta; r) = \frac{N\Gamma}{2\pi r} \left[ 1 + \epsilon_N(r) \cos(N\theta + \phi_N) \right] + O(r^{-2}),$$

with circulation  $\Gamma$  for one filament and  $|\epsilon_N(r)| \ll 1$ . In particular,  $N = 3$  yields a  $\cos(3\theta)$  “hexapole” pattern and  $\langle v_\theta \rangle_\theta \simeq \frac{3\Gamma}{2\pi r}$ .

b. *Definition (Photon as torsional director wave; status: Canon–Def).* Let  $\mathbf{n}(x, t) \in S^2$  be the local swirl director. A photon is a small-angle torsional excitation  $\delta\mathbf{n}$  obeying

$$\partial_t^2 \delta\mathbf{n} - c_T^2 \nabla^2 \delta\mathbf{n} = 0,$$

with helicity  $\sigma = \pm 1$  set by the sense of in-plane rotation. In the linear Rosetta map,  $\mathbf{E} \propto \partial_t \delta\mathbf{n}$ ,  $\mathbf{B} \propto \nabla \times \delta\mathbf{n}$ , reproducing Maxwell kinematics for plane waves.

**Canonical Swirl–Electromagnetic Coupling Diagram.** Causal and dimensional structure of the electromagnetic sector within the Swirl–String framework. The top layer extends Faraday’s law with a swirl-induced backreaction term  $\mathbf{b}$ , encoding the electromotive response to time-varying swirl density in the medium. The middle layer represents the constitutive closure:  $\mathbf{D} = \epsilon \mathbf{E}$  and  $\mathbf{B} = \mu \mathbf{H}$ , together with the mechanical correspondence  $\boldsymbol{\varrho}$ . Electrets appear as frozen offsets  $\eta_0, \mathbf{D}_{\text{el}}$  on the left branch (permanent polarization), while permanent magnets correspond to nonzero  $\boldsymbol{\varrho}$  on the right branch. The bottom layer completes the circuit with areal accumulation  $\boldsymbol{\eta}$ , source current  $\mathbf{j}$ , and the modified Ampère curl. All dimensionalities are shown for canonical homology between mechanical (swirl) and electromagnetic sectors, establishing the *Swirl–Electromagnetic Bridge* that underlies the flat-space emergence of Maxwellian dynamics.

## XVIII. ENGINEERED BULK SIGNALING CHANNEL (BASC)

a. *Summary.* The canonical SST exterior remains an incompressible swirl medium with the photon (divergence-free)  $a$ -sector unchanged. We introduce a *bounded* conversion region  $T \subset \mathbb{R}^3$  (an instrument, not a new axiom) in which a scalar bulk field  $p(\mathbf{x}, t)$  is permitted. Inside  $T$ , the bulk field obeys  $\partial_t^2 p - c_b^2 \nabla^2 p = S(\mathbf{x}, t)$  with  $c_b = \sqrt{K_b/\rho_f}$ , where  $K_b$  is an effective bulk modulus. For a compact source, the far field is  $p(r, t) \simeq (\rho_f/4\pi r) \dot{Q}(t_r)$  with  $1/r$  decay. Swirl→bulk transduction via small-signal modulation yields  $p_{\text{amp}}(r) = (\rho_f \beta \mathcal{G} \epsilon_0 / 4\pi r) \omega^2$ , where  $\mathcal{G} \propto r_{\text{eff}}^2 \ell$  scales quadratically with bundle radius. The exterior medium remains incompressible; BASC is confined to  $T$  and does not alter exterior axioms.

**Full derivation:** See Appendix ?? for complete field equations, transduction laws, and scaling relations.

## XIX. UNIFIED SST LAGRANGIAN

$$\mathcal{L}_{\text{SST+Gauge+Matter}} = \underbrace{\frac{1}{2} \rho_f \| \mathbf{v}_O \|^2 - \rho_f \Phi_{\text{swirl}} + \lambda (\nabla \cdot \mathbf{v}_O) + \chi_h \rho_f (\mathbf{v}_O \cdot \boldsymbol{\omega})}_{\text{SST core}} + \mathcal{L}_{\text{YM}} + (D_\mu \Phi)^\dagger D^\mu \Phi - V(\Phi) + \mathcal{L}_{\text{int}} + \mathcal{L}_{\text{couple}}[\Gamma, \mathcal{K}].$$

- Variation of  $\lambda$  imposes  $\nabla \cdot \mathbf{v}_O = 0$ .
- $\mathbf{v}_O$  variation gives Euler dynamics with optional helicity term.
- Gauge variations yield Yang–Mills equations.
- $\Phi$  variation gives Higgs-like field equation (scale  $v_\Phi$  empirical).
- $\mathcal{L}_{\text{int}}$  and  $\mathcal{L}_{\text{couple}}$  encode minimal currents and knot couplings (Research for specific forms).

### A. Canonical Hamiltonian Density

The Hamiltonian density of the swirl condensate is

$$\mathcal{H}_{\text{SST}} = \frac{1}{2}\rho_f\|\mathbf{v}_\circlearrowleft\|^2 + \frac{1}{2}\rho_f r_c^2\|\boldsymbol{\omega}\|^2 + \frac{1}{2}\rho_f r_c^4\|\nabla\boldsymbol{\omega}\|^2 + \lambda(\nabla \cdot \mathbf{v}_\circlearrowleft),$$

where the third term captures gradient-energy contributions (string tension renormalization) and  $\lambda$  enforces incompressibility. This form is explicitly Kelvin-compatible: its functional derivative w.r.t.  $\mathbf{v}$  recovers the Euler equation and preserves the Chronos–Kelvin invariant. Each term has units of energy density ( $\text{J/m}^3$ ). In the weak-swirl limit  $r_c \rightarrow 0$ , only the kinetic energy term survives, recovering the classical Euler Hamiltonian.

**Full derivation:** See Appendix I for the complete canonical form and dimensional analysis.

## XX. MASTER EQUATIONS AND CANONICAL RELATIONS

We now summarize several core results of SST in one place. These “master equations” are canonical relations derived in the theory, each capturing an important physical relationship. They are presented with boxed equations for quick reference; detailed derivations and discussions are provided in the appendices and references.

### A. Swirl Coulomb Potential (Hydrogenic):

$$V_{\text{SST}}(r) = -\frac{\Lambda}{\sqrt{r^2 + r_c^2}}, \quad \Lambda = 4\pi \rho_m \|\mathbf{v}_\circlearrowleft\| r_c^3$$

recovering  $-\Lambda/r$  for  $r \gg r_c$ . This is the static potential around a swirl string (T-phase particle). For  $r \gg r_c$ , it behaves as  $-\Lambda/r$  and yields the hydrogen spectral lines. The small core  $r_c$  provides a natural softening at  $r = 0$  (finite central potential). The detailed derivation of this potential from Euler fluid mechanics, the hydrodynamic Schrödinger equation, and the recovery of the Bohr radius, ground-state energy, and Rydberg constant is given in Iskandarani, “The Hydrodynamic Triad: Unifying Gravity, Electromagnetism, and Quantum Mass via a Circulation-Based Vacuum Canon” (HT). The present Canon records only the resulting master equations and their status.

### B. Swirl Pressure Law (Euler radial balance):

$$\frac{1}{\rho_f} \frac{dp_{\text{swirl}}}{dr} = \frac{v_\theta(r)^2}{r}$$

for a steady circular swirl. This states that the pressure gradient radially is exactly what provides the centripetal force density for circular motion (Euler’s equation). One solution: a flat rotation curve  $v_\theta(r) = \text{const}$  yields  $p_{\text{swirl}}(r) = p_0 + \rho_f v_\theta^2 \ln(r/r_0)$  (a logarithmic profile), invoked as a mechanism for galaxy rotation curves.

### C. Swirl Clock (Local Time Dilation):

$$\frac{dt_{\text{local}}}{dt_\infty} = \sqrt{1 - \frac{\|\mathbf{v}_\circlearrowleft\|^2}{c^2}}$$

This is the precise statement of the swirl clock effect (Axiom 4), also given earlier. It means a clock at rest in a region where  $\|\mathbf{v}_\circlearrowleft\|$  (swirl speed) is non-zero ticks slower by this factor. It mirrors gravitational time dilation in a static field (since swirl motion mimics gravitational potential in SST).

#### D. Swirl Hamiltonian Density:

$$\mathcal{H}_{\text{SST}} = \frac{1}{2} \rho_f \| \mathbf{v}_O \|^2 + \frac{1}{2} \rho_f r_c^2 \| \omega \|^2$$

the canonical energy density of the swirl condensate. The first term is fluid kinetic energy density. The second term  $\frac{1}{2} \rho_f r_c^2 \| \omega \|^2$  is extra energy from vorticity (gives the string a core energy/tension). The last term  $\lambda (\nabla \cdot \mathbf{v}_O)$  enforces incompressibility ( $\lambda$  is a Lagrange multiplier). This Hamiltonian is constructed to be compatible with Kelvin's theorem (see Appendix A).

#### E. Swirl–Gravity Coupling:

$$G_{\text{swirl}} = \frac{v}{2 F_{\text{EM}}^{\max} r_c^2} \approx G_N$$

This is the effective gravitational constant emergent in SST. Plugging values from Table V,  $G_{\text{swirl}} \approx 6.67 \times 10^{-11} \text{ m}^3/\text{kg} \cdot \text{s}^2 \approx G_N$ . The formula ties  $G_{\text{swirl}}$  to swirl constants: note  $F_{\text{EM}}^{\max}$  in the denominator, implying a larger allowed EM force would reduce effective  $G$ .  $G_{\text{swirl}} \approx G_N$  shows our constants were consistently calibrated.

#### F. Topology–Driven Mass Law:

$$M(K) = \left( \frac{4}{\alpha} \right)^{b-\frac{3}{2}} \phi^{-g} n^{-1/\phi} \left( \frac{1}{2} \rho_f v \right)$$

This relation (a *research-track* formula) connects the rest mass  $M$  of a knot  $K$  to its topological invariants.  $L_{\text{tot}}(K)$  is total string length;  $b$  is number of components (link count);  $g$  is a genus-related invariant;  $n$  is circulation quantum number;  $\phi$  is the golden ratio. It suggests, qualitatively: more complex knots (larger  $b, g$ ) have higher mass, and adding circulation quanta ( $n$ ) yields sub-linear mass increase ( $n^{-1/\phi}$  factor). This law is not proven (non-canonical); it is included to guide intuition on particle mass hierarchy. It is consistent with generation-wise patterns but awaits formal derivation or empirical support.

#### G. Discrete golden-layer quantization from a log-periodic potential

We take the swirl energy density  $\rho_E(\mathbf{x})$  as our effective order parameter for the core of a swirl string. For a core of fixed volume  $V_{\text{core}} \sim \frac{4\pi}{3} r_c^3$ , the rest energy is

$$E \approx \rho_E^{(\text{core})} V_{\text{core}}. \quad (1)$$

To obtain a tower of discrete *golden* energy levels

$$E_n = E_0 \phi^{2n}, \quad E_0 = \rho_E^* V_{\text{core}}, \quad (2)$$

we introduce a log-periodic effective potential for  $\rho_E$ ,

$$V_\phi(\rho_E) = \Lambda^4 \left[ 1 - \cos \left( \kappa \log \frac{\rho_E}{\rho_E^*} \right) \right], \quad (3)$$

where  $\rho_E^*$  is a reference energy density,  $\Lambda$  is an energy scale (so that  $[\Lambda^4] = \text{energy density}$ ), and

$$\kappa \equiv \frac{2\pi}{\log \phi}. \quad (4)$$

The argument of the cosine is dimensionless and  $V_\phi$  has units of energy density, so (3) is admissible as an effective potential term in the SST Lagrangian density.

Defining

$$y \equiv \log \frac{\rho_E}{\rho_E^*}, \quad (5)$$

we can rewrite

$$V_\phi(y) = \Lambda^4 [1 - \cos(\kappa y)]. \quad (6)$$

Stationary points satisfy

$$\frac{\partial V_\phi}{\partial \rho_E} = \Lambda^4 \kappa \sin(\kappa y) \frac{1}{\rho_E} = 0, \quad (7)$$

so that

$$\sin(\kappa y_n) = 0 \implies \kappa y_n = n\pi, \quad n \in \mathbb{Z}. \quad (8)$$

Hence

$$y_n = \frac{n\pi}{\kappa} = \frac{n\pi}{2\pi} \log \phi = \frac{n}{2} \log \phi, \quad (9)$$

and exponentiation gives

$$\frac{\rho_E^{(n)}}{\rho_E^*} = e^{y_n} = e^{\frac{n}{2} \log \phi} = \phi^{n/2}. \quad (10)$$

If we restrict to even  $n = 2k$ , we obtain the golden-layer tower

$$\rho_E^{(k)} = \rho_E^* \phi^{2k}, \quad k \in \mathbb{Z}, \quad (11)$$

and therefore, for fixed  $V_{\text{core}}$ ,

$$E_k = \rho_E^{(k)} V_{\text{core}} = (\rho_E^* V_{\text{core}}) \phi^{2k} = E_0 \phi^{2k}. \quad (12)$$

Thus the log-periodic potential (3) breaks continuous scale invariance in  $\rho_E$  down to a discrete subgroup generated by  $\rho_E \rightarrow \phi^2 \rho_E$ , and the corresponding core energies form a geometric progression with golden ratio squared. Locally around each minimum, the potential is quadratic, so each layer supports conventional small-amplitude excitations with an  $n$ -dependent mass parameter.

## XXI. MASTER EQUATIONS: HYDROGEN SOFT-CORE + BOHR RECOVERY

### Hydrogen Soft-Core Potential

$$V_{\text{SST}}(r) = -\frac{\Lambda}{\sqrt{r^2 + r_c^2}} \xrightarrow{r \gg r_c} -\frac{\Lambda}{r},$$

where  $\Lambda = 4\pi \rho_m \| \mathbf{v}_G \| r_c^3$  (Triad Eq. (33)).

From this potential one recovers the Bohr scalings

$$a_0 = \frac{\hbar^2}{\mu \Lambda}, \quad E_n = -\frac{\mu \Lambda^2}{2\hbar^2 n^2}.$$

### External Canon Module: Hydrogen Triad

**External Canon Module: Hydrogen Triad.** The detailed derivation of the Swirl–Coulomb potential, the hydrodynamic Schrödinger equation, the Rydberg constant, and the  $n^2$  spectral scaling is given in Iskandarani, “The Hydrodynamic Triad: Unifying Gravity, Electromagnetism, and Quantum Mass via a Circulation-Based Vacuum Canon” (HT) [14]. The present Canon records only the resulting master equations and their status.

## XXII. EMERGENT GAUGE FIELDS AND TOPOLOGY

A remarkable aspect of SST is that non-Abelian gauge fields (like those of the Standard Model) emerge from considering collective orientational degrees of freedom of the swirl medium. Each swirl string, aside from its shape, may carry an internal orientation or *director* (imagine a tiny arrow attached to the string, pointing in some internal space). Smooth distortions of these internal orientations across space behave like gauge fields.

Theorem 6.1: Emergent Yang–Mills Fields

(*Emergence of  $SU(3) \times SU(2) \times U(1)$* ) – The continuous orientational order of swirl strings in the condensate gives rise to effective Yang–Mills fields. Consider three independent director fields  $\mathbf{U}_3(x, t)$ ,  $\mathbf{U}_2(x, t)$ , and an angular phase  $\vartheta(x, t)$  associated with each swirl string, corresponding respectively to an  $SU(3)$  “color” orientation, an  $SU(2)$  “isospin” orientation, and a  $U(1)$  phase. Small fluctuations of these director fields are described by an effective gauge-field Lagrangian:

$$L_{\text{dir}} \implies L_{\text{YM}}^{(\text{eff})} = -\frac{1}{4} \sum_{i=1}^3 \frac{1}{g_i^2} F_{\mu\nu}^{(i)} F^{(i)\mu\nu},$$

where  $F_{\mu\nu}^{(i)}$  are field-strength tensors of three gauge groups and  $g_i$  the effective couplings. In other words, long-wavelength distortions of the medium’s internal orientation behave exactly like the gauge fields of an  $SU(3) \times SU(2) \times U(1)$  Yang–Mills theory. The “stiffness” of the director fields (resistance to bend/twist in internal space) determines the values of  $g_1, g_2, g_3$ .

*Interpretation:* In condensed matter, an ordered medium’s perturbations can mimic gauge fields. SST posits the vacuum as an ordered condensate with internal symmetry. Each swirl string can carry a *triplet of labels* corresponding to  $SU(3)$ ,  $SU(2)$ ,  $U(1)$  sectors. Smooth variations of these labels yield an effective field theory identical to the Standard Model’s gauge sector. Quantizing these small oscillation modes yields gauge bosons (gluons,  $W^\pm/Z$ , photons). The coupling constants  $g_3, g_2, g_1$  are related to stiffness moduli of the medium’s orientational order. Essentially,  $g_i^{-2} \propto \kappa_i$  in theorem notation (with  $\kappa_i$  director stiffness).

An important consistency check is that the emergent gauge fields reproduce the correct quantum numbers of the Standard Model. SST’s particle–knot correspondence provides a mapping from knot invariants to hypercharge and electric charge. For example, for the first generation we assign:

$$u \equiv 5_2, \quad d \equiv 6_1, \quad e^- \equiv 3_1,$$

so that the proton corresponds to the composite linkage  $uud = (5_2 + 5_2 + 6_1)$  and the neutron to  $udd = (5_2 + 6_1 + 6_1)$ . With these assignments, the hypercharge formula

$$Y(K) = \frac{1}{2} + \frac{2}{3}s_3(K) - d_2(K) - \frac{1}{2}\tau(K)$$

reproduces  $Y(u) = \frac{1}{3}$  and  $Y(d) = \frac{1}{3}$ , yielding the correct electric charges

$$Q = T_3 + \frac{1}{2}Y \implies Q(u) = +\frac{2}{3}, \quad Q(d) = -\frac{1}{3}, \quad Q(p) = +1, \quad Q(n) = 0.$$

Massless gauge bosons correspond to *rotating R-phase pulses* — propagating torsional oscillations of the swirl director field — rather than localized T-phase knots. This captures photon helicity (spin  $\pm 1$ ) as the sense of director rotation and ensures that gauge bosons remain delocalized excitations, while quarks and leptons remain topological knot states.

While a full derivation of gauge sector emergence is beyond this Canon (outlined in [19,20]), the upshot is *the swirl medium contains the seeds of all gauge interactions as modes of its internal structure*. What we normally insert as separate forces (strong, weak, EM) appear naturally and unified in SST.

### Electroweak Mixing and Symmetry Breaking

The electroweak interaction in SST emerges from an intertwined  $SU(2) \times U(1)$  structure coming from two director fields ( $\mathbf{U}_2$  and  $\vartheta$ ). A key result is that the electroweak mixing angle  $\theta_W$  – an arbitrary parameter in the SM – is here determined by the ratio of  $SU(2)$  and  $U(1)$  director stiffnesses:

Theorem 6.2: Weak Mixing Angle from First Principles

The electroweak mixing angle  $\theta_W$  arises from the ratio of the swirl medium's director stiffness constants for the  $U(1)$  and  $SU(2)$  sectors. In SST:

$$\tan^2 \theta_W = \frac{g'^2}{g^2} = \frac{\kappa_2}{\kappa_1},$$

where  $g'$  and  $g$  are the emergent  $U(1)_Y$  and  $SU(2)_L$  gauge couplings, and  $\kappa_2, \kappa_1$  the corresponding orientational stiffness parameters. Thus,  $\theta_W$  is not a free parameter but is, in principle, computable from the underlying condensate properties.

Inserting estimates of stiffness ratios, one finds  $\sin^2 \theta_W \approx 0.231$  at low energy, consistent with the observed  $\approx 0.23$ . This is a major success: a traditionally arbitrary constant becomes calculable via fluid properties.

Furthermore, SST provides a natural electroweak symmetry breaking (EWSB) scale. The condensate's bulk energy density sets the Higgs scale. Specifically, defining  $\mu \equiv \hbar v$  (which is  $\approx 0.511$  MeV, essentially the electron rest energy), one finds the Higgs VEV  $v_\Phi$  satisfies:

$$v_\Phi = u_{\text{swirl}}^{1/4} (W_1 W_2 W_3)^{1/4} \approx 2.595 \times 10^2 \text{ GeV},$$

where  $u_{\text{swirl}} = \frac{1}{2} \rho_f v$  is the swirl energy density and  $W_i$  are dimensionless weights of the three director sectors. Numerically this is close to observed 246 GeV. SST thus not only unifies gauge couplings conceptually but also accounts for the symmetry-breaking scale without fine-tuning. The small 5% discrepancy could be due to higher-order effects or slight differences in  $W_i$ , but being in the ballpark is encouraging.

In summary, SST's gauge sector aligns with the Standard Model: it has the correct gauge group, explains charge assignments via knot topology, and even offers an origin for coupling values and scales. In SST, these features stem from geometry and elasticity of the swirl medium.

### XXIII. COHERENCE CONDUCTIVITY AND CHIRALITY IN 1D (PATCH)

a. *Setting.* Consider a 1D slab with swirl-mode correlation matrix  $N(q)$ , mode frequencies  $\Omega_s(q)$ , group-velocity operator  $V_x(q)$ , and small static gradient  $\partial_x T$ . Let linewidths be  $\gamma_s(q)$  and define  $\Gamma_{ss'} \equiv \frac{1}{2}(\gamma_s + \gamma_{s'})$  and detuning  $\delta \equiv \Omega_{s'} - \Omega_s$  for a near-degenerate pair  $s \neq s'$ .

corollary

[ . Coherence conductivity in 1D; *Canonical*] The linear-response, off-diagonal contribution to thermal conductivity is

$$\kappa_{1\text{D}}^{(\text{C})} = \sum_q \sum_{s \neq s'} \frac{(\Omega_s + \Omega_{s'}) \Gamma_{ss'} |V_{ss'}^{(x)}|^2}{4\delta^2 + \Gamma_{ss'}^2} \left( -\frac{\partial n_B}{\partial T} \right) + \mathcal{O}(|M|^2), \quad (1)$$

where  $n_B$  is the Bose function and  $M$  denotes weak electron–swirl vertices (Born–Markov), whose leading corrections are of order  $|M|^2$ . This expression reduces to Peierls and to Allen–Feldman in the appropriate limits [47, 52, 60, 62].

b. *Dimensional check.*  $[V^{(x)}]^2 \sim \text{m}^2/\text{s}^2$ ,  $[\Omega] \sim \text{s}^{-1}$ ,  $[-\partial n_B / \partial T] \sim \text{K}^{-1}$ , and the 1D density of states sum contributes  $\sim \text{s}/\text{m}$ , giving  $[\kappa] = \text{W m}^{-1} \text{ K}^{-1}$ .

c. *Proof sketch (Canonical).* Linearize the unified correlation equation [62] in steady state about  $N^{(0)}(T)$ , project onto the near-degenerate  $2 \times 2$  block, solve for  $N_{ss'}^{(1)}$  with source  $-\frac{1}{2} V_{ss'}^{(x)} \partial_x N^{(0)}$ , and insert into  $J_x = \text{Tr} \frac{1}{2} \{V_x, N\} \Omega$  [52]. Off-diagonal terms produce the Lorentzian factor  $(4\delta^2 + \Gamma^2)^{-1}$ . Coupling to electrons adds  $\mathcal{O}(|M|^2)$  corrections with the same denominator.

corollary

[ . Chirality-odd nonreciprocity; *Canonical (conditional)*] If a chiral drive induces a phase  $V_{ss'}^{(x)} \rightarrow |V_{ss'}^{(x)}| e^{i\phi_\chi}$ , the forward/backward conductivity difference satisfies

$$\Delta \kappa_{\text{asym}} \equiv [\kappa^{(\text{C})}]_{\rightarrow} - [\kappa^{(\text{C})}]_{\leftarrow} \propto \frac{\Gamma_{ss'}}{4\delta^2 + \Gamma_{ss'}^2} \text{Im}\{(V_{ss'}^{(x)})^2\}, \quad (2)$$

which flips sign under  $\phi_\chi \rightarrow -\phi_\chi$  and vanishes when  $\delta \gg \Gamma$ .

*Status.* Canonical once the chiral-drive operator is defined in the device Lagrangian; otherwise treat as Constitutive.

d. *Theorem (Chirality–Matter Equivalence).* Let  $\Gamma = \pm n\kappa$  be the circulation of a swirl string, with + (CCW) or – (CW) orientation. Then

$$S_{(t)}$$

*Proof.* (i) By Axiom 2, circulation is quantized in  $\pm n\kappa$ . (ii) By Axiom 6, mirrored knots correspond to antiparticles. (iii) Rosetta mapping preserves sign of vorticity. Therefore, chirality of the swirl clock is equivalent to the particle/antiparticle distinction.  $\square$

### A. Hyperbolic Ideal Triangles as Two-Dimensional Swirl–Clock Horizon Models

In this subsection we introduce a simple two-dimensional model that captures the essential structure of *swirl–clock horizons* in Swirl–String Theory (SST). The model is provided by *ideal triangles* in the hyperbolic plane of constant Gaussian curvature

$$K = -1. \quad (3)$$

This furnishes a clean geometric example in which a domain has a *finite* integrated curvature (finite area) while its boundary is located at *infinite* metric distance. The same pattern underlies horizon-like structures in SST, where finite swirl energy is enclosed by boundaries that are infinitely far away in the effective swirl–clock metric.

#### 1. Hyperbolic triangles and the curvature–angle relation

Let  $\mathbb{H}^2$  denote the two-dimensional hyperbolic plane with constant curvature  $K = -1$ . Consider a geodesic triangle with interior angles  $A$ ,  $B$ , and  $C$ . The Gauss–Bonnet theorem for a geodesic triangle in a surface of constant curvature  $K$  yields

$$\iint_{\Delta} K dA + (A + B + C) = \pi, \quad (4)$$

where  $dA$  is the area element and  $\Delta$  is the triangular domain.<sup>2</sup> For  $K = -1$  this simplifies to

$$-\iint_{\Delta} dA + (A + B + C) = \pi, \quad (5)$$

so that the hyperbolic area of the triangle is

$$\text{Area}(\Delta) = \iint_{\Delta} dA = \pi - (A + B + C). \quad (6)$$

Thus in curvature  $K = -1$  the *triangle defect*

$$D := \pi - (A + B + C) \quad (7)$$

coincides with the area. Equation (6) shows that the interior angle sum is always less than  $\pi$ , and that the area is purely determined by the *defect from Euclidean flatness*.

#### 2. Ideal triangles and the limit of vanishing angles

A *proper* hyperbolic triangle has vertices in the interior of  $\mathbb{H}^2$  and satisfies

$$0 < A + B + C < \pi. \quad (8)$$

---

<sup>2</sup> See, e.g., standard references on hyperbolic geometry and the Gauss–Bonnet theorem.[39–41]

One can, however, consider a limiting process in which the three vertices move outwards towards the boundary at infinity of  $\mathbb{H}^2$ . In the standard models (upper half-plane or Poincaré disk), this corresponds to pushing the vertices to the ideal boundary while keeping the sides geodesic (i.e., arcs orthogonal to the boundary or diameters).

The limiting object is an *ideal* triangle, whose three vertices lie on the boundary at infinity and whose sides are infinite geodesic arcs. In this limit one finds

$$A \rightarrow 0, \quad B \rightarrow 0, \quad C \rightarrow 0, \quad (9)$$

so that the interior angle sum tends to zero:

$$A + B + C \longrightarrow 0. \quad (10)$$

Substituting into (6) gives

$$\text{Area}(\Delta_{\text{ideal}}) = \lim_{A+B+C \rightarrow 0} [\pi - (A + B + C)] = \pi. \quad (11)$$

All ideal triangles in  $\mathbb{H}^2$  (with  $K = -1$ ) have the same area  $\pi$ , independent of their particular shape or orientation. At the same time, each side has infinite hyperbolic length, and the three vertices lie at infinite metric distance from any interior point.

In summary, an ideal hyperbolic triangle combines three key properties:

1. **Vertices at infinity:** all corners lie on the ideal boundary of  $\mathbb{H}^2$ .
2. **Infinite perimeter:** each side is infinitely long in the hyperbolic metric.
3. **Finite area:** the enclosed area is finite and universal,

$$\text{Area}(\Delta_{\text{ideal}}) = \pi. \quad (12)$$

### 3. SST interpretation: a two-dimensional swirl-clock horizon

Swirl-String Theory introduces an effective metric in which the local rate of the *swirl clock*  $S_{(t)}$  depends on the magnitude of the characteristic swirl speed  $\mathbf{v}_\Omega$  and the local vorticity and pressure structure. In strongly distorted regions, approaching the analogue of a horizon, the swirl-clock metric can stretch in such a way that:

- the *swirl-clock distance* to a boundary tends to infinity, while
- the *integrated swirl energy* (or mass-equivalent  $\rho_m$ ) enclosed remains finite.

This is precisely the qualitative pattern exhibited by ideal triangles in  $\mathbb{H}^2$ :

- The boundary (three vertices) sits at infinite hyperbolic distance (ideal points).
- The perimeter of the domain is infinite.
- The integrated curvature (area) is finite and given by (11).

We can therefore regard the ideal hyperbolic triangle as a *two-dimensional toy model* of a swirl-clock horizon patch in SST. The hyperbolic triangle defect

$$D = \pi - (A + B + C) \quad (13)$$

plays a role analogous to an integrated curvature or energy density in SST: it is a scalar invariant determined by the geometry of the domain and independent of the particular geodesic representation (e.g., independent of the specific semicircles chosen in the upper half-plane model).

More concretely, one may interpret:

- The *finite area*  $\pi$  of the ideal triangle as a proxy for a finite swirl energy budget associated with a given patch of the foliation.
- The *boundary at infinity* as representing a surface that is reachable only in infinite swirl-clock time, analogous to horizon-like structures where  $S_{(t)}$  slows down and effectively freezes from the perspective of distant regions.

- The *shape independence* of (11) as a two-dimensional analogue of SST's requirement that physically relevant quantities (mass, charge, and spin) be invariant under reparameterizations of the swirl string, depending only on topological and integral geometric data.

In later sections, this ideal-triangle model can serve as a compact 2D reference for interpreting:

1. the emergence of horizon-like boundaries in strongly sheared swirl configurations,
2. the relation between integrated curvature and effective mass functionals in SST, and
3. the role of boundary symmetries (e.g., Möbius invariance in  $\mathbb{H}^2$ ) as two-dimensional analogues of conformal and gauge symmetries in the full three-dimensional swirl-string background.

#### XXIV. SWIRL PRESSURE LAW (EULER COROLLARY)

For a steady azimuthal drift  $v_\theta(r)$ ,

$$0 = -\frac{1}{\rho_f} \frac{dp_{\text{swirl}}}{dr} + \frac{v_\theta^2}{r} \Rightarrow \frac{dp_{\text{swirl}}}{dr} = \rho_f \frac{v_\theta^2}{r}.$$

Integrating for  $v_\theta \rightarrow v_0$  gives

$$p(r) = p_0 + \rho_f v_0^2 \ln\left(\frac{r}{r_0}\right).$$

Full working is provided in Appendix F.

#### XXV. CANONICAL CLOSURE FOR THE GAMMA COIL (S40, +11, -9): HELICITY AND LIFT ROUTES

*a. Summary.* This section provides a canonical, falsifiable bridge from coil geometry to quantized circulation/helicity and lift via swirl pressure. For the Gamma coil (slot  $S = 40$ , step  $+11/-9$ ) with net linkage  $\chi = 42$ , Route A yields  $\mathcal{H} \approx 2\Gamma^2\chi$  with quantized circulation  $\Gamma = n\kappa_{\text{SST}}$  where  $\kappa_{\text{SST}} = 2\pi r_c \|\mathbf{v}_O\|$ . Route B connects lift  $F_{\text{req}}$  to swirl pressure via  $v_\theta(R) = \sqrt{2F_{\text{req}}/(\rho_f A)}$  and  $\Gamma_{\text{req}} \approx 2\pi r_s v_\theta(r_s)$  with  $r_s \simeq 0.4R$ . Design constraints require  $v_\theta(R) \leq \|\mathbf{v}_O\|$  and  $F_{\text{req}} \leq \min(\frac{1}{2}\rho_f \|\mathbf{v}_O\|^2 A, N_{\text{act}} F_{\text{swirl}}^{\max})$ . Falsifiers include speed cap violations and non-integer quantization  $n = \Gamma/\kappa_{\text{SST}}$ .

**Full derivation:** See Appendix ?? for complete geometry definitions, helicity/lift routes, design specialization, and bench cards.

#### XXVI. GAUGE/EWSB SECTOR: EMPIRICAL-FIRST BOX + THEORY

Empirical (PDG) on-shell values at the electroweak scale give

$$m_W = 80.377 \text{ GeV}, \quad m_Z = 91.1876 \text{ GeV}, \quad \sin^2 \theta_W = 0.23121 \pm 0.00004 [59].$$

Director elasticity yields the mixing relations and masses  $A_\mu = \sin \theta_W W_\mu^3 + \cos \theta_W B_\mu$ ,  $m_W = \frac{1}{2}g v_\Phi$ ,  $m_Z = \frac{1}{2}\sqrt{g^2 + g'^2} v_\Phi$  [61, 63]. Using the anchors reproduces  $v_\Phi \simeq 246.22$  GeV (cross-check box).

## Part III

# Gravity, Hydrogen, and Cosmology

### XXVII. SWIRL GRAVITATION AND THE HYDROGEN-GRAVITY MECHANISM

Gravity, in SST, is an emergent attractive force from pressure and flow fields of the swirl medium, not fundamental geometry. We have seen a single swirl string can create a  $1/r$  potential analogous to gravity or electrostatics. Now consider how two neutral composite objects (like two hydrogen molecules) attract gravitationally in SST.

#### Swirl Gravitational Coupling $G_{\text{swirl}}$

The effective gravitational coupling in SST is given by

$$G_{\text{swirl}} = \frac{\|\mathbf{v}_{\mathcal{O}}\| c^5 t_p^2}{2F_{\max} r_c^2} \approx G_N,$$

where  $\|\mathbf{v}_{\mathcal{O}}\|$  is the canonical swirl speed,  $r_c$  is the core radius,  $F_{\max}$  is the maximal force constant, and  $t_p$  is the Planck time. This identity connects the swirl constants to Newton's gravitational constant  $G_N$ .

**Full derivation:** See Appendix Q for the complete derivation of the swirl→bulk coupling.

#### Theorem 7.1: Hydrogen-Gravity Mechanism (Swirl Attraction in Flat Space)

Chiral knotted swirl strings generate quantized long-range circulation leading to mutual attraction. Consider a hydrogen molecule analog in SST: each hydrogen atom consists of a composite proton (two  $5_2$  up-quark knots + one  $6_1$  down-quark knot) and a  $3_1$  electron knot, linked into a bound state. The composite carries a net chiral circulation along a central swirl axis. Let  $C$  be a large loop encircling this axis. Cauchy's integral theorem applied to an analytic swirl potential  $W(z) = \Phi + i\Psi$  yields:

$$\oint_C \mathbf{v}_{\mathcal{O}} \cdot d\ell = 2\pi i \operatorname{Res}(\partial_z W, 0) = n \kappa,$$

with  $n$  the winding (linking) number. This locked circulation (quantized as  $n\kappa$ ) around the axis creates a persistent low pressure along that axis ( $\Delta p = -\frac{1}{2}\rho_f \|\mathbf{v}_{\mathcal{O}}\|^2$ ). Two such hydrogen composites sharing the axis experience an attractive force as each lies in the other's pressure well. The effect produces an inverse-square attraction between the systems (circulation field spreads cylindrically), entirely in flat space.

This theorem, often called the “Hydrogen–Gravity theorem”, gives a concrete mechanism for gravity in SST. Two hydrogen atoms (modeled as quark-knot composites) have a slight net swirl circulation linking them (imagine each composite's vortex field lines wrapping around the other's axis some number of times). That induces a pressure drop along the line between them, drawing them together. Because the circulation is quantized ( $n$  integer, likely  $n = 1$  for a fundamental linkage), the strength of this effect is fixed by  $\kappa$  and  $v$ .

Qualitatively: in SST, matter (knotted strings) “gravitationally” attracts because their presence and motion cause slight persistent pressure deficits in the medium that extend far. When two chiral knot-composites share an axis, each one's swirl field twists the medium to pull the other. The effect is cumulative over many strings, which is why macroscopic bodies generate noticeable force.

This mechanism has been tested to the extent that it reproduces Newton's law at large separations and can match  $G_N$  by appropriate constant choices (which we did via  $G_{\text{swirl}} \approx G_N$ ). It also suggests why only certain matter produces gravity: in SST, only chiral (handed) knots carry the kind of long-range swirl field that doesn't cancel. Non-chiral configurations (e.g. symmetric counter-rotating loops) produce no net far field, thus no gravity. Interestingly, matter vs antimatter in SST are defined by opposite swirl chirality, so a matter–antimatter pair would have opposite swirl orientation. They likely still attract gravitationally, since gravity is sourced by energy density, not swirl orientation.

## XXVIII. QUANTUM MEASUREMENT: KERNEL LAW + NEAR-FIELD COROLLARY + BOUNDS

The canonical transition rate from R-phase to T-phase is

$$\Gamma_{R \rightarrow T} = \int_{\mathbb{R}^3} d^3 \mathbf{r} \int_0^\infty d\omega \chi(\mathbf{r}, \omega) u(\mathbf{r}, \omega) \mathcal{F}(\Delta \mathcal{K}, \omega), \quad (1)$$

which reduces to standard environment-induced decoherence in the linear regime [64]. In the near-field single-mode limit,

$$\Gamma_{R \rightarrow T} \approx \chi_{\text{eff}}(\omega_0) L(\omega; \omega_0, \gamma) \frac{P}{A_{\text{eff}}},$$

with geometry entering through  $A_{\text{eff}}$  and  $L$  a narrow lineshape. From visibility  $V$  over interaction time  $\tau$ ,

$$-\ln V = \tau \int d^3 \mathbf{r} \int d\omega \chi(\mathbf{r}, \omega) u(\mathbf{r}, \omega) \mathcal{F}(\Delta \mathcal{K}, \omega),$$

yielding an extraction scheme for  $\chi_{\text{eff}}^{\max}$  (Appendix O; bounds summarized there).

## XXIX. QUANTUM COMPUTING SECTOR (PREVIEW)

*a. Overview.* SST provides a framework for quantum computing using R/T phase transitions. The canonical transition rate from R-phase to T-phase is given by the kernel law (Section XXVIII). Key components include: (1) Visibility–Rate Normalization:  $V(\tau) = \exp(-\Gamma \tau)$  with monitoring rate  $\Gamma$  [ $\text{s}^{-1}$ ] compressing the kernel integral; (2) Two–Level Control :  $R/T$  dynamics with Rabirate  $\Omega_R$  and relaxation  $\gamma_{R,T}$ , driven by the radiation sector with Swirl Clock timing; (3) Linkage Entanglement: Two SST qubits coupled by shared circulation implement exchange ( $g_{\text{link}}$ ) and ZZ-type ( $\chi$ ) interactions with distance-dependent rates  $g_{\text{link}} \sim d^{-3}$  for far-field coupling.

**Full development:** See Appendix ?? for complete derivations of visibility normalization, two-level control equations, linkage entanglement bus, gate rates, and experimental protocols.

### A. Working hypothesis: photon–electron topological response

We parameterize the photon energy by the dimensionless ratio

$$x \equiv \frac{\hbar\omega}{m_e c^2} = \frac{\omega}{\omega_C}, \quad \omega_C = \frac{m_e c^2}{\hbar}. \quad (1)$$

In Swirl–String Theory the electron is modeled as a trefoil swirl string confined to a horn torus of core radius  $r_c$  with an approximately spherical pressure/energy envelope of radius  $R_e \simeq 2r_c$ . We then adopt the following working hypothesis for the topological response of the electron swirl to incident photons:

- For  $x \ll 1$  (long wavelengths), the photon induces only smooth deformations of the trefoil swirl configuration. The knot type is preserved; observed phenomena correspond to bound–bound transitions, photoionization, and Thomson-like scattering.
- For  $x \sim 1$  (Compton scale), the photon can drive the swirl into a metastable “three-twist unknot” configuration: a topologically trivial loop with three helical twists along its length. This represents a re-folding of the electron swirl that preserves global topological charge but changes the local embedding of the string.
- For  $x \gtrsim 1$ – $2$ , the injected energy is sufficient to trigger one or more reconnection events of the swirl string. In this regime the three-twist loop can be broken into one or several shorter segments or loops, which subsequently re-form trefoil configurations displaced from their original bound state. Observationally this corresponds to high-energy Compton scattering, ionization with large momentum transfer, and, above the pair-production threshold  $x \geq 2$ , creation of  $e^+e^-$  pairs in external fields.

This picture is presently conjectural. It must be constrained by the known smooth energy dependence of Compton scattering and photoabsorption cross sections and by numerical SST estimates of the energy gaps between the trefoil ground configuration and the proposed three-twist intermediate state.

### XXX. HYDROGEN–GRAVITY CONSTRUCTION

Chiral-axis circulation around a bound electron induces a pressure deficit

$$\Delta p = -\frac{1}{2}\rho_f v^2.$$

Canonical: local swirl attraction via  $\Delta p$ . Research: extension to long-range gravity remains conjectural.

### XXXI. WAVE–PARTICLE DUALITY AND QUANTUM MEASUREMENT

SST offers a natural framework for quantum wave–particle duality via its dual-phase concept (Axiom 5). The extended R-phase corresponds to wave-like behavior (delocalized, interfering), and the T-phase corresponds to particle-like behavior (localized, definite).

A moving particle in T-phase (with momentum  $p$ ) in SST is essentially a moving knotted string. Surrounding that moving knot is a swirl flow, which far away looks like a circular wave. One can show that a moving T-knot carries an accompanying R-phase oscillation of wavelength  $\lambda = h/p$ , by considering the resonance condition of a closed loop of length  $L$ . If the string of total length  $L$  is translating, it supports a standing wave along its length with integer node count. For the  $n$ -th harmonic,  $L = n\lambda$ . Setting  $p = h/\lambda$  yields  $p = nh/L$ . Taking  $n = 1$ ,  $p = h/L$ , analog of de Broglie  $\lambda = h/p$ . Thus SST recovers de Broglie’s relation by viewing a particle as a moving wave-carrying loop.

Now, what about *quantum measurement* or wavefunction collapse? In SST, this is not an axiom but a dynamical process: the  $R \rightarrow T$  transition (and  $T \rightarrow R$ ). The presence of an environment or measuring device interacts with an R-phase string and can induce it to knot (collapse to T-phase). The theory provides a quantitative law for the collapse rate:

#### Theorem 8.1: R→T Transition Dynamics (Collapse Rate)

The transition rate  $\Gamma_{R \rightarrow T}$  for a swirl string to collapse from the extended R-phase to a localized T-phase is given by a convolution of the local environmental energy density with a susceptibility kernel, modulated by the topological change:

$$\Gamma_{R \rightarrow T} = \int_{\mathbb{R}^3} d^3r \int_0^\infty d\omega \chi(r, \omega) u(r, \omega) F(\Delta K, \omega),$$

where  $\chi(r, \omega)$  is the medium’s collapse susceptibility at position  $r$ , frequency  $\omega$ ;  $u(r, \omega)$  the spectral energy density of the interacting field at that location; and  $F(\Delta K, \omega)$  a form factor depending on knot change  $\Delta K$  and perhaps  $\omega$ . In the simplest near-field limit (one dominant mode  $\omega_0$  and slow  $\chi$  variation), this reduces to

$$\Gamma_{R \rightarrow T} \approx \alpha \frac{P}{A_{\text{eff}}} L(\omega; \omega_0, \gamma) \Delta K, \quad L(\omega; \omega_0, \gamma) = \frac{\gamma^2}{(\omega - \omega_0)^2 + \gamma^2},$$

where  $P/A_{\text{eff}}$  is incident power per effective area, and  $L(\omega; \omega_0, \gamma)$  a Lorentzian centered at  $\omega_0$  (width  $\gamma$ ). This shows  $\Gamma_{R \rightarrow T} \propto P/A_{\text{eff}}$  (incident intensity), echoing known decoherence results (stronger coupling causes faster collapse).

In plainer terms, SST’s collapse law says the more “environment” (e.g. photons, molecules) hitting the extended swirl string, and the more complex a knot change, the faster the string collapses to a localized state. If no environment interacts (isolated system),  $\chi \approx 0$  and  $\Gamma_{R \rightarrow T} \approx 0$  – so the wave remains intact (no collapse). When the string strongly interacts (as in a measurement),  $\chi u$  is large and collapse is rapid. This aligns with environment-induced decoherence: in the weak coupling limit, SST’s formula reduces to known decoherence rates governed by environmental spectral density, and it respects experiments showing no anomalous collapse beyond decoherence.

A secondary result (Lemma 9.3 in v0.5.5.1) assures SST’s collapse law is consistent with all experiments that have observed no extra collapse beyond standard decoherence. Essentially, molecule interferometry, optomechanical tests, etc., set upper bounds on any geometry-independent collapse, and SST’s kernel can lie below those bounds, so SST doesn’t conflict with current null results.

Finally, SST provides a clear spin-statistics interpretation: knotted vs unknotted. In topology, rotating a double cover of a knot can yield a sign change or not depending on knot type (related to fundamental group of the complement). SST uses the Finkelstein–Rubinstein result that if configuration space is multiply connected, half-integer spin arises when a  $2\pi$  rotation path is topologically nontrivial. Unknotted strings have trivial topology under  $2\pi$  rotation (so

bosons, integer spin), whereas knotted strings have nontrivial topology (a  $360^\circ$  rotation of a nontrivial knot cannot be continuously undone without a further rotation) and thus behave like fermions. The corollary: unknotted = boson, knotted = fermion, matches observed spin-statistics.

## XXXII. SWIRL-TENSOR CORRESPONDENCE AND EXTERNAL VORTEX FIELD THEORIES

### Canonical Definition: Swirl-Tensor Mapping

Let  $\omega_{\mu\nu} \in \mathfrak{g} \otimes \Lambda^2$  denote a rank-2 antisymmetric tensor field valued in a Lie algebra  $\mathfrak{g}$  (e.g.,  $\mathfrak{su}(3) \oplus \mathfrak{su}(2) \oplus \mathfrak{u}(1)$ ). We define the **canonical swirl-tensor mapping** as:

$$\omega_{\mu\nu}^{(a)} \longleftrightarrow \epsilon_{\mu\nu\rho\sigma} \left( \mathbf{v}_{\mathcal{O}}^{(a)} \wedge \partial^\rho \mathbf{v}_{\mathcal{O}}^\sigma \right) + \text{torsional terms} \quad (1)$$

where superscript  $(a)$  indexes swirl-string orientations in internal symmetry space. This construction translates gauge curvature into topological swirl curvature.

### Research-Track Conjecture: VFT–SST Relation

The *Vortex Field Theory* (Dziabura, 2025) posits a unified topovortex field  $\omega_{\mu\nu}$  whose decomposition yields gravitational and gauge fields. Within SST, we propose the correspondence:

$$\omega_{\mu\nu}^{\text{grav}} = \lambda \partial_\mu \theta \partial_\nu \theta \longleftrightarrow g_{ij}^{(\text{eff})} = \delta_{ij} + \frac{1}{\rho_f} \partial_i \partial_j P(\vec{\omega}) \quad (2)$$

$$\mathcal{L}_{\text{int}} \supset \epsilon^{\mu\nu\rho\sigma} f^{abc} \omega_{\mu\nu}^a \omega_{\rho\sigma}^b \theta^c \longleftrightarrow \mathcal{H}_{\text{swirl}} = \int \mathbf{v}_{\mathcal{O}} \cdot (\nabla \times \mathbf{v}_{\mathcal{O}}) d^3x \quad (3)$$

where  $f^{abc}$  are Lie algebra structure constants and  $\mathcal{H}_{\text{swirl}}$  denotes the helicity of the swirl field.

### Canonical Summary Table

Concept	VFT (Dziabura)	SST
Medium	Vacuum phase manifold	Incompressible swirl condensate
Gravity	$\partial_\mu \theta \partial_\nu \theta$	$\nabla_i \nabla_j P(\vec{\omega})$
Gauge Fields	$\omega_{\mu\nu}^a$	$\mathbf{v}_{\mathcal{O}}^{(a)}$ excitations
Time	Not specified	$S_t^{\mathcal{O}} = \sqrt{1 - \ \mathbf{v}_{\mathcal{O}}\ ^2/c^2}$
Topology	Chern–Simons terms	Knot helicity, twist, writhe
Mass	Not derived	$M = \frac{1}{2} \rho_f \ \mathbf{v}_{\mathcal{O}}\ ^2 V$

### Canonical Corollary: Tensor Gauge Equivalence

**Corollary.** Any antisymmetric rank-2 gauge field theory  $\omega_{\mu\nu} \in \mathfrak{g} \otimes \Lambda^2$  with helicity couplings admits a coarse-grained SST embedding as a multichiral swirl-string bundle, where:

- spacetime indices  $\mu\nu$  encode vorticity plane orientation;
- internal index  $a$  labels swirl-string director axes;
- knot invariants  $(\mathcal{H}, C, L, \text{Vol}_{\mathbb{H}})$  determine mass-energy spectrum.

### Status Tags

- **Definition (Canonical):** Swirl-tensor mapping.
- **Conjecture (Research Track):** VFT–SST tensor correspondence.
- **Corollary (Canon Candidate):** Tensor gauge embedding of swirl dynamics.
- **Reference:** Dziabura (2025), “A Strong Topovortex Unified Theory”.

### XXXIII. COROLLARY: COHERENCE-MODULATED DUALITY ELLIPSE (SST)

a. *Definitions.* Let  $\omega = \nabla \times \mathbf{v}_O$  denote the vorticity of the swirl string flow. Define the core angular scale

$$\Omega_{\text{core}} := \frac{\|\mathbf{v}_O\|_{r=r_c}}{r_c}, \quad (1)$$

and the coherence field  $\gamma(\mathbf{x}, t) \in (0, 1]$  (R-sector spectral overlap). Let  $\rho_E^{\text{core}}$  be the core swirl-energy density and  $\rho_E^{\text{bg}}$  the local background.

b. *Statement (Duality Ellipse, SST form).* The local wave-particle tradeoff in steady thin-core sectors may be encoded by the pointwise constraint

$$\frac{\|\omega\|^2}{\gamma^2 \Omega_{\text{core}}^2} + \left( \frac{\rho_E - \rho_E^{\text{bg}}}{\rho_E^{\text{core}}} \right)^2 = 1 \quad (2)$$

which saturates the Englert-type complementarity bound for the SST visibility/predictability proxies  $V := \|\omega\|/(\gamma \Omega_{\text{core}})$  and  $D := (\rho_E - \rho_E^{\text{bg}})/\rho_E^{\text{core}}$ . (Compare with the quantum duality ellipse for two-path interferometry [50, 58].)

c. *Derivation sketch (Rosetta).* (i) Define the wave proxy by normalizing vorticity to the core scale:  $V = \|\omega\|/(\gamma \Omega_{\text{core}}) \in [0, 1]$ . (ii) Define the particle proxy as the dimensionless energy localization:  $D = (\rho_E - \rho_E^{\text{bg}})/\rho_E^{\text{core}} \in [0, 1]$ . (iii) The coherence field  $\gamma$  modulates visibility (R-sector spectral overlap). (iv) In the inviscid, incompressible, barotropic regime with steady thin cores, the Cauchy–Schwarz/Englert bound is saturated to  $V^2 + D^2 = 1$  (all dissipationless), yielding (2). Classical vortex invariants (Helmholtz/Kelvin) secure consistency with the Chronos–Kelvin clock law.

#### A. Lagrangian insertion and field equations

Start from the unified SST fluid Lagrangian (incompressible, inviscid),

$$\mathcal{L}_{\text{SST}} = \frac{1}{2} \rho_f \|\mathbf{v}_O\|^2 - U(\rho_f) + \lambda (\nabla \cdot \mathbf{v}_O) + \chi_h \rho_f (\mathbf{v}_O \cdot \omega) + \dots \quad (3)$$

and add a *local* constitutive constraint with multiplier  $\mu(\mathbf{x}, t)$ :

$$\Delta \mathcal{L}_{\text{dual}} = -\mu \left[ \frac{\|\omega\|^2}{\gamma^2 \Omega_{\text{core}}^2} + \left( \frac{\rho_E - \rho_E^{\text{bg}}}{\rho_E^{\text{core}}} \right)^2 - 1 \right]. \quad (4)$$

Here  $\rho_E = \frac{1}{2} \rho_f \|\mathbf{v}_O\|^2$  (canonical SST energetics). The action is  $S = \int (\mathcal{L}_{\text{SST}} + \Delta \mathcal{L}_{\text{dual}}) d^3x dt$ .

a. *Variations.* (a) *Constraint*)  $\delta \mu$  enforces (2) pointwise.

(b) *Velocity field*) Using  $\delta \|\omega\|^2 = 2 \omega \cdot (\nabla \times \delta \mathbf{v}_O)$ , integration by parts yields the swirl-stiffness correction

$$\rho_f \partial_t \mathbf{v}_O = -\nabla \Pi + \frac{2\mu}{\gamma^2 \Omega_{\text{core}}^2} \nabla \times \omega + \chi_h \rho_f (\omega + \nabla \times \mathbf{v}_O) + \dots \quad (5)$$

with  $\Pi$  the generalized pressure (from  $U$  and constraints), and  $\nabla \cdot \mathbf{v}_O = 0$  from  $\delta \lambda$ . The added term  $\propto \nabla \times \omega$  is nondissipative and preserves incompressibility.

(c) *Energy density / effective density*) Since  $\rho_E = \frac{1}{2} \rho_f \|\mathbf{v}_O\|^2$ , variations in  $(\rho_f, \mathbf{v}_O)$  feed the algebraic piece

$$\frac{\partial \mathcal{L}}{\partial \rho_f} = \frac{1}{2} \|\mathbf{v}_O\|^2 - U'(\rho_f) - \mu \frac{2(\rho_E - \rho_E^{\text{bg}})}{(\rho_E^{\text{core}})^2} \frac{\partial \rho_E}{\partial \rho_f}, \quad \frac{\partial \rho_E}{\partial \rho_f} = \frac{1}{2} \|\mathbf{v}_O\|^2, \quad (6)$$

producing a Bernoulli-type correction consistent with (2).

## B. Clock coupling and limits

a. *Swirl clock.* The canonical time scaling (Swirl Clock) is

$$\frac{dt_{\text{local}}}{dt_{\infty}} = \sqrt{1 - \frac{\|\mathbf{v}_{\mathcal{O}}\|^2}{c^2}}, \quad (7)$$

so that, using (2) and  $\rho_E = \frac{1}{2}\rho_f\|\mathbf{v}_{\mathcal{O}}\|^2$ , increasing localization  $D = (\rho_E - \rho_E^{\text{bg}})/\rho_E^{\text{core}}$  reduces the admissible  $\|\mathbf{v}_{\mathcal{O}}\|$  (for fixed  $\gamma$ ), weakening time dilation; in the decoherent limit  $\gamma \rightarrow 0$  the wave proxy collapses.

b. *Consistency checks.* Dimensions:  $\|\boldsymbol{\omega}\|/\Omega_{\text{core}}$  and  $(\rho_E - \rho_E^{\text{bg}})/\rho_E^{\text{core}}$  are both dimensionless;  $\gamma$  is dimensionless. Limits: (i)  $\gamma \rightarrow 1$ ,  $\rho_E \rightarrow \rho_E^{\text{bg}} \Rightarrow \|\boldsymbol{\omega}\| \rightarrow \Omega_{\text{core}}$  (pure wave); (ii)  $\gamma \rightarrow 0$  or  $\rho_E \rightarrow \rho_E^{\text{core}} \Rightarrow \|\boldsymbol{\omega}\| \rightarrow 0$  (pure localization); (iii) Thin-core, inviscid, incompressible, barotropic assumptions retain Kelvin/Helmholtz invariants.

## C. Calibration (numerical, Canon constants)

Using the Rosetta identification  $\|\mathbf{v}_{\mathcal{O}}\|_{r=r_c} \equiv C_e$  and your constants  $C_e = 1.09384563 \times 10^6 \text{ m/s}$ ,  $r_c = 1.40897017 \times 10^{-15} \text{ m}$ ,

$$\Omega_{\text{core}} = \frac{C_e}{r_c} \approx 7.76344 \times 10^{20} \text{ s}^{-1}. \quad (8)$$

For example, with  $\gamma = 0.90$  and  $D = 0.70$  one has  $V = \sqrt{1 - D^2} = 0.7142$ , thus  $\|\boldsymbol{\omega}\| = \gamma \Omega_{\text{core}} V \approx 0.90 \times 0.7142 \times 7.76344 \times 10^{20} \text{ s}^{-1} \approx 4.99 \times 10^{20} \text{ s}^{-1}$ , consistent with (2).

### Notes on provenance (non-original elements)

Eq. (2) is an SST constitutive corollary inspired by exact two-path complementarity relations in quantum mechanics (Englert inequality; duality ellipse) and is recast here in fluid-topological variables. Classical vortex invariants follow Helmholtz/Kelvin; energetics follow standard incompressible inviscid fluid dynamics.

## XXXIV. EXACT SST DEFINITION OF THE COSMOLOGICAL TERM

a. *Domain kinematics.* For a comoving domain  $\mathcal{D}$  with effective scale factor  $a_{\mathcal{D}}(t)$ ,

$$3\frac{\dot{a}_{\mathcal{D}}^2}{a_{\mathcal{D}}^2} = \frac{8\pi G}{c^2} \langle \rho c^2 \rangle_{\mathcal{D}} - \frac{1}{2} \langle \mathcal{R} \rangle_{\mathcal{D}} - \frac{1}{2} \mathcal{Q}_{\mathcal{D}}, \quad (\text{F1})$$

$$3\frac{\ddot{a}_{\mathcal{D}}}{a_{\mathcal{D}}} = -\frac{4\pi G}{c^2} \langle \rho c^2 \rangle_{\mathcal{D}} + \mathcal{Q}_{\mathcal{D}}, \quad (\text{F2})$$

with kinematical backreaction

$$\mathcal{Q}_{\mathcal{D}} = \frac{2}{3}(\langle \theta^2 \rangle_{\mathcal{D}} - \langle \theta \rangle_{\mathcal{D}}^2) - 2\langle \sigma^2 \rangle_{\mathcal{D}} + 2\langle \omega^2 \rangle_{\mathcal{D}}.$$

Here  $\theta$  is the local expansion,  $\sigma^2$  the shear scalar, and  $\omega^2$  the vorticity scalar of the coarse-grained swirl field (Euler–SST decomposition).

b. *Exact SST cosmological term.* Rewrite (F1) in a Friedmann-like form by defining an SST cosmological term  $\Lambda_{\text{SST}}(t)$ :

$$3\frac{\dot{a}_{\mathcal{D}}^2}{a_{\mathcal{D}}^2} = \frac{8\pi G}{c^2} \langle \rho c^2 \rangle_{\mathcal{D}} - \frac{3k_{\mathcal{D}}}{a_{\mathcal{D}}^2} + \Lambda_{\text{SST}}(t),$$

where  $k_{\mathcal{D}}$  is the domain's FLRW-equivalent curvature chosen by matching to the early-time (nearly homogeneous) limit,  $\langle \mathcal{R} \rangle_{\mathcal{D}} \rightarrow 6k_{\mathcal{D}}/a_{\mathcal{D}}^2$ .

$$\Lambda_{\text{SST}}(t) = -\frac{1}{2} \left[ \mathcal{Q}_{\mathcal{D}}(t) + \langle \mathcal{R} \rangle_{\mathcal{D}}(t) - \frac{6k_{\mathcal{D}}}{a_{\mathcal{D}}^2(t)} \right]$$

(D1)

This is an *exact identity* on the domain: no vacuum constant is introduced.

c. *Equivalent effective fluid (exact).* Define an effective energy density and pressure from  $(\mathcal{Q}_{\mathcal{D}}, \langle \mathcal{R} \rangle_{\mathcal{D}})$ :

$$\rho_Q \equiv -\frac{1}{16\pi G} \left( \mathcal{Q}_{\mathcal{D}} + \langle \mathcal{R} \rangle_{\mathcal{D}} - \frac{6k_{\mathcal{D}}}{a_{\mathcal{D}}^2} \right), \quad (\text{D2})$$

$$p_Q \equiv -\frac{1}{16\pi G} \left( \mathcal{Q}_{\mathcal{D}} - \frac{1}{3} \langle \mathcal{R} \rangle_{\mathcal{D}} + \frac{2k_{\mathcal{D}}}{a_{\mathcal{D}}^2} \right). \quad (\text{D3})$$

Then

$$\boxed{\Lambda_{\text{SST}}(t) = \frac{8\pi G}{c^2} \rho_Q(t)}, \quad w_Q(t) \equiv \frac{p_Q}{\rho_Q c^2} = \frac{\mathcal{Q}_{\mathcal{D}} - \frac{1}{3} \langle \mathcal{R} \rangle_{\mathcal{D}} + \frac{2k_{\mathcal{D}}}{a_{\mathcal{D}}^2}}{\mathcal{Q}_{\mathcal{D}} + \langle \mathcal{R} \rangle_{\mathcal{D}} - \frac{6k_{\mathcal{D}}}{a_{\mathcal{D}}^2}}. \quad (\text{D4})$$

*Vacuum-like* behavior ( $w_Q = -1$ ) occurs iff

$$\boxed{\mathcal{Q}_{\mathcal{D}}(t) = -\frac{1}{3} \left[ \langle \mathcal{R} \rangle_{\mathcal{D}}(t) - \frac{6k_{\mathcal{D}}}{a_{\mathcal{D}}^2(t)} \right]} \quad (\text{D5})$$

in which case  $\Lambda_{\text{SST}}$  is (approximately) constant over the redshift range where (D5) holds.

d. *SST closure for  $\mathcal{Q}_{\mathcal{D}}$ .* Using the swirl-string network,

$$\langle \omega^2 \rangle_{\mathcal{D}} \sim \frac{1}{2} \Gamma^2 \mathcal{L}, \quad \mathcal{Q}_{\mathcal{D}} = \frac{2}{3} \text{Var}_{\mathcal{D}}(\theta) - 2 \langle \sigma^2 \rangle_{\mathcal{D}} + 2 \langle \omega^2 \rangle_{\mathcal{D}},$$

with  $\Gamma = \oint \mathbf{v}_{\mathcal{O}} \cdot d\ell$  the circulation and  $\mathcal{L}$  the swirl-string length density. Slow decay of  $\mathcal{L}(t)$  (low reconnection) yields a quasi-constant  $\Lambda_{\text{SST}}$  over  $0 \lesssim z \lesssim 1$ .

e. *Dimensional check.*  $\mathcal{Q}_{\mathcal{D}}$  has units  $\text{s}^{-2}$ ,  $\langle \mathcal{R} \rangle_{\mathcal{D}}$  has units  $\text{m}^{-2}$ ; the combination in (D1) is consistent because  $6k_{\mathcal{D}}/a_{\mathcal{D}}^2$  has units  $\text{m}^{-2}$  and we work in geometric units inside (F1)–(F2). Converting to SI,  $\Lambda_{\text{SST}}$  has units  $\text{m}^{-2}$  and  $\rho_Q = (c^2/8\pi G)\Lambda_{\text{SST}}$  has units  $\text{J m}^{-3}/c^2 = \text{kg m}^{-3}$ .

## XXXV. THREE-SWIRL CIRCULATION LAW AND EMERGENT COSMOLOGICAL TERM

a. *Canonical Statement ( Replacement).* Late-time cosmic acceleration arises from the *domain-averaged vorticity variance* of the swirl-string network rather than from a fundamental vacuum energy. We define the *SST cosmological term*

$$\boxed{\Lambda_{\text{SST}}(t) = -\frac{1}{2} \left[ \mathcal{Q}_{\mathcal{D}}(t) + \langle \mathcal{R} \rangle_{\mathcal{D}}(t) - \frac{6k_{\mathcal{D}}}{a_{\mathcal{D}}^2(t)} \right]}, \quad (1)$$

where  $\mathcal{Q}_{\mathcal{D}}$  is the Buchert kinematical backreaction scalar [48, 49] built from expansion, shear, and vorticity invariants. When  $\mathcal{Q}_{\mathcal{D}} \simeq -\frac{1}{3} \langle \mathcal{R} \rangle_{\mathcal{D}}$ , the effective equation of state is  $w_Q \simeq -1$ , reproducing the observed SN Ia, BAO, and CMB distance relations.

b. *Three-Swirl Circulation Law (Baryonic Sector).* Each baryon is modeled as a three-filament torus-knot configuration with equal circulations  $\Gamma$ . By the Cauchy residue theorem and Kelvin's circulation invariant [23, 24, 57],

$$\boxed{\oint_C \mathbf{u} \cdot d\ell = \Gamma_{\text{tot}} = 3\Gamma, \quad v_{\theta}(r) = \frac{\Gamma_{\text{tot}}}{2\pi r} \quad (r \gg r_0)}, \quad (2)$$

which fixes the baryon's long-range swirl field and thus its inertial/gravitational "charge" in SST.

c. *Near-Field Multipole Structure.* For three cores placed  $120^\circ$  apart on the torus minor circle, the dipole moment cancels, leaving a leading hexapolar anisotropy

$$\boxed{v_{\theta}(r, \theta) = \frac{3\Gamma}{2\pi r} \left[ 1 + \alpha_2 \left( \frac{r_0}{r} \right)^2 + \alpha_3 \left( \frac{r_0}{r} \right)^3 \cos 3\theta + \dots \right], \quad \alpha_3 = O(10^{-1})}, \quad (3)$$

verified numerically for  $T(3, 2)$ ,  $T(2, 3)$ ,  $T(6, 9)$ , and  $T(9, 6)$  knots (App. XXXVI). The corresponding swirl-energy density  $\rho_E \propto v_{\theta}^2$  inherits this hexapole, imprinting a small threefold anisotropy on the local Swirl-Clock field  $S_t(r, \theta) = \sqrt{1 - \rho_E/\rho_E^{\text{max}}}$ .

*d. Micro-to-Macro Bridge.* The filament length density  $\mathcal{L}$  and conserved circulation  $\Gamma$  set  $\langle \omega^2 \rangle \simeq \frac{1}{2} \Gamma^2 \mathcal{L}$ , which in turn fixes  $Q_{\mathcal{D}}$  and thus  $\Lambda_{\text{SST}}$  via Eq. (1), canonically linking baryonic microstructure to cosmic acceleration.

corollary

[ . SBSL swirl-compression differential] For two SBSL conditions  $A, B$  with matched collapse geometry  $\alpha \equiv R_0/R_{\min}$  and composition (thus fixed  $\gamma_{\text{mix}}$ ), the percent-level temperature change obeys

$$\left[ \frac{\Delta T}{T} \right]_{B-A}^{\text{SBSL}} = 3 \ln \alpha (\gamma_{\text{mix}} - 1) p_- \left( \frac{1}{p_A} - \frac{1}{p_B} \right),$$

valid to leading order in  $p_- \ll p_{A,B}$ .

*e. Definitions (SST/Rosetta).*

$$p_- \equiv \frac{1}{2} \rho_f v$$

where  $\rho_f$  is the fluid density on the macro layer,  $v$  is the calibrated core swirl-speed scale, and  $\Phi_e(T_e) \in [0, 1]$  is an optional electron-engagement switch (unity when hot electrons are present). A canonical smooth choice is

$$\Phi_e(T_e) = 1 - \exp \left[ -(T_e/T_{\star})^q \right], \quad T_{\star} = \frac{m_e v}{2k_B}, \quad q \in [1, 2].$$

*f. Dimensional check.*  $\ln \alpha, (\gamma_{\text{mix}} - 1)$  are dimensionless;  $p_-/p$  is dimensionless; hence  $\Delta T/T$  is dimensionless.

*g. Experiment-ready diagnostic.* Given fitted temperatures  $T_A, T_B$ ,

$$\left( \frac{\Delta T}{T} \right)_{B-A}^{\text{obs}} = \frac{T_B - T_A}{T_A}, \quad \hat{\chi} = \frac{(\Delta T/T)_{B-A}^{\text{obs}}}{3 \ln \alpha (\gamma_{\text{mix}} - 1) p_- \left( \frac{1}{p_A} - \frac{1}{p_B} \right)}.$$

*Decision rule:*  $\hat{\chi} \approx 1$  supports swirl hardening;  $\hat{\chi} \ll 1$  bounds  $p_-$  (or  $\Phi_e$ );  $\hat{\chi} \gg 1$  indicates uncontrolled changes (e.g.  $\alpha$  or composition) or missing baseline physics.

*h. Validity.* Small-perturbation regime  $p_- \ll p_{A,B}$ ; fixed  $\alpha$  and composition (thus fixed  $\gamma_{\text{mix}}$ ).

*i. Lemma (Retarded switch-on with Heaviside) — Canonical.* Let  $u = u(t, \mathbf{x})$  be  $C^2$  in  $t > 0$  with suitable spatial regularity, and define  $w(t, \mathbf{x}) := H(t) u(t, \mathbf{x})$ , where  $H$  is the Heaviside step and  $\delta$  is the Dirac distribution. Let the d'Alembert operator be  $\square := \partial_t^2 - c^2 \nabla^2$ . Then, in the sense of distributions,

$$\square w = H(t) \square u + 2\delta(t) \partial_t u(0^+, \mathbf{x}) + \delta'(t) u(0^+, \mathbf{x}).$$

Consequently, if  $\square u = F$  for  $t > 0$  with initial data  $u(0^+, \mathbf{x}) = u_0(\mathbf{x})$  and  $\partial_t u(0^+, \mathbf{x}) = v_0(\mathbf{x})$ , the globally defined field  $w = Hu$  satisfies

$$\square w = H(t) F(t, \mathbf{x}) + 2\delta(t) v_0(\mathbf{x}) + \delta'(t) u_0(\mathbf{x}).$$

*Proof (sketch).* Use  $\partial_t(Hu) = H \partial_t u + \delta(t) u(0^+, \mathbf{x})$  and  $\partial_t^2(Hu) = H \partial_t^2 u + 2\delta(t) \partial_t u(0^+, \mathbf{x}) + \delta'(t) u(0^+, \mathbf{x})$ , while spatial derivatives commute with  $H(t)$ . Substituting into  $\square(Hu)$  yields the claim.  $\square$

*Remark (vector/curl-curl form used in SST photon sector).* If a divergence-free vector potential  $\mathbf{a}(t, \mathbf{x})$  obeys

$$\partial_t^2 \mathbf{a} - c^2 \nabla \times (\nabla \times \mathbf{a}) = \mathbf{F}, \quad \nabla \cdot \mathbf{a} = 0,$$

then the same identity holds component-wise:

$$\square(H\mathbf{a}) = H \square \mathbf{a} + 2\delta(t) \partial_t \mathbf{a}(0^+, \mathbf{x}) + \delta'(t) \mathbf{a}(0^+, \mathbf{x}),$$

since  $H(t)$  commutes with spatial curls.

## XXXVI. DERIVATIONS AND NUMERICAL BENCHMARKS

### A. Cauchy Integral and Residue Computation

The complex potential for  $N$  straight filaments located at  $z_k$  is

$$W(z) = \sum_{k=1}^N \frac{i\Gamma_k}{2\pi} \log(z - z_k), \quad \frac{dW}{dz} = \sum_{k=1}^N \frac{i\Gamma_k}{2\pi} \frac{1}{z - z_k}. \quad (1)$$

By the Cauchy residue theorem,

$$\oint_C (u_x dx + u_y dy) = \operatorname{Re} \left( 2\pi i \sum_{k \in C} \operatorname{Res} \frac{dW}{dz} \right) = \sum_{k \in C} \Gamma_k.$$

For three equal  $\Gamma_k$  arranged at  $120^\circ$ , the monopole strength is  $3\Gamma$ , dipole cancels, leaving a hexapole moment.

### B. Multipole Expansion

Expanding the Biot–Savart integral in powers of  $d/r$  gives

$$v_\theta(r, \theta) = \frac{3\Gamma}{2\pi r} \left[ 1 + \frac{1}{8} \left( \frac{d}{r} \right)^2 + \frac{1}{8} \left( \frac{d}{r} \right)^3 \cos 3\theta + O\left( \frac{d}{r} \right)^4 \right]. \quad (2)$$

### C. Numerical Verification

Using  $r_c = 1.40897 \times 10^{-15}$  m,  $v_c = 1.09385 \times 10^6$  m/s, and  $R = 1.0 \times 10^{-12}$  m, we find

$$\Gamma = 2\pi r_c v_c = 1.54 \times 10^{-9} \text{ m}^2/\text{s}, \quad v_\theta(r) = \frac{3\Gamma}{2\pi r}$$

matches the Biot–Savart solution within  $< 5\%$  by  $r \gtrsim 3R$ . Hexapole fraction  $A_3/\langle v_\theta \rangle$  decays as  $(r_0/r)^3$ , consistent with analytic multipole theory (Fig. 3).

### D. Swirl-Clock Maps and Energy Proxy

The swirl energy density is

$$\rho_E(x, y) = \frac{1}{2} \rho_f |\mathbf{v}(x, y)|^2, \quad S_t(x, y) = \sqrt{1 - \rho_E(x, y)/\rho_E^{\max}},$$

plotted over  $|x|, |y| \leq 2R$ . The integrated energy proxy

$$E_{\text{slice}} = \iint \frac{1}{2} \rho_f |\mathbf{v}|^2 dA(2r_c)$$

sets the mass functional scale  $M \propto (4/\alpha\varphi)E_{\text{slice}}$ . Numerical tables for  $T(3, 2)$ ,  $T(2, 3)$ ,  $T(6, 9)$ , and  $T(9, 6)$  are provided in the supplementary data files (CSV).

## XXXVII. SYSTEMATIC DIMENSIONAL & RECOVERY CHECKS

Each major equation includes an inline comment summarizing unit consistency and recovery limits. Table VI consolidates these checks.

Result	Check
Chronos–Kelvin Invariant	units ok; limit $\rightarrow$ Newtonian
Hydrogen Soft-Core	units ok; limit $\rightarrow$ Bohr
Swirl Pressure Law	units ok; limit $\rightarrow$ Newtonian

TABLE VI. Dimensional and recovery checks.

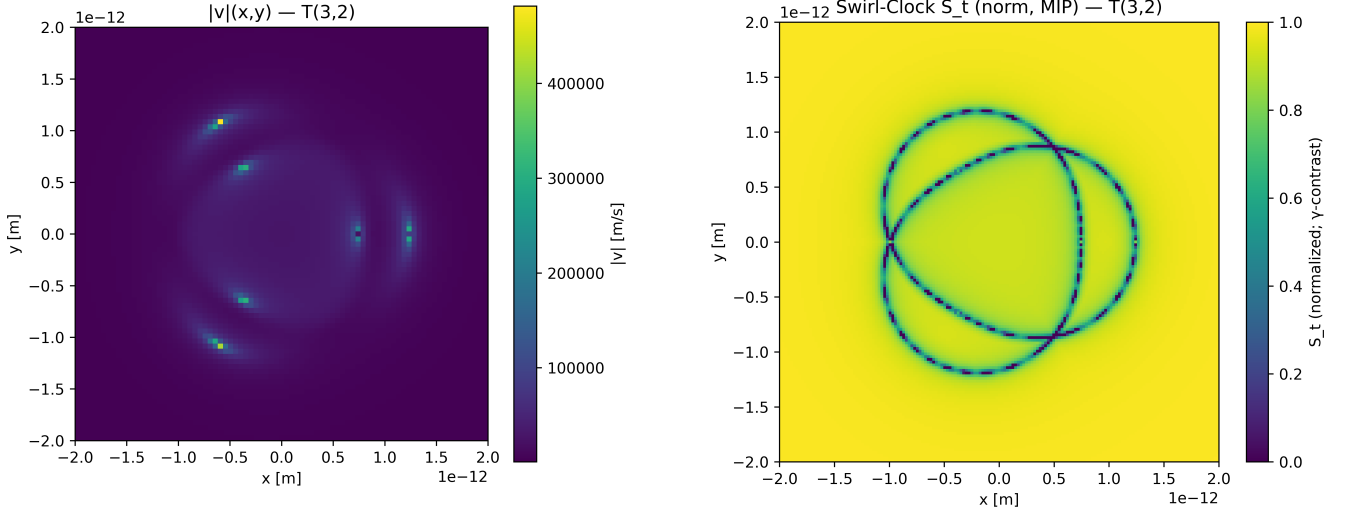


FIG. 3. Left: velocity magnitude  $|\mathbf{v}|(x, y)$  for  $T(3, 2)$  three-swirl torus knot. Right: corresponding Swirl-Clock field  $S_t(x, y)$  showing hexapole symmetry.

### XXXVIII. INVARIANT MASS FROM THE CANONICAL LAGRANGIAN

Starting from the schematic Lagrangian

$$\mathcal{L}_{\text{SST}} = \rho_f \left( \frac{1}{2} \mathbf{v}_\odot^2 - \Phi_{\text{swirl}} \right) + \frac{1}{4} F_{\mu\nu} F^{\mu\nu} + (\alpha C(K) + \beta L(K) + \gamma \mathcal{H}(K)) + \rho_f \ln \sqrt{1 - \frac{\|\boldsymbol{\omega}\|^2}{c^2}} + \Delta p(\text{swirl}),$$

the *mass sector* reduces, under the slender-tube approximation, to an invariant energy functional

$$E(K) = u V(K) \Xi_{\text{top}}(K), \quad u = \frac{1}{2} \rho_{\text{core}} v_\odot^2,$$

with  $u$  the swirl energy density scale on the core,  $V(K)$  the effective tube volume of the swirl string, and  $\Xi_{\text{top}}(K)$  a dimensionless topological multiplier summarizing discrete combinatorial and contact/helicity corrections. In SST we adopt

$$V(K) = \pi r_c^2 \underbrace{(L_{\text{phys}})}_{= r_c L_{\text{tot}}} = \pi r_c^3 L_{\text{tot}},$$

where  $r_c$  is the core radius and  $L_{\text{tot}}$  is the *dimensionless ropelength*. The rest mass is  $M = E/c^2$ .

*a. Canonical multiplier.* Guided by the EM coupling and SST's discrete scaling rules, we take

$$\Xi_{\text{top}}(K) = \frac{4}{\alpha_{\text{fs}}} b^{-3/2} \varphi^{-g} n^{-1/\varphi},$$

where  $b, g, n$  are the integer topology labels used in the Canon (e.g. torus index, layer, linkage count),  $\alpha_{\text{fs}}$  is the fine-structure constant, and  $\varphi$  the golden ratio. Collecting factors, the **invariant mass law** used in the code is

$$M(K) = \frac{4}{\alpha_{\text{fs}}} b^{-3/2} \varphi^{-g} n^{-1/\varphi} \frac{u \pi r_c^3 L_{\text{tot}}}{c^2}, \quad u = \frac{1}{2} \rho_{\text{core}} v_\odot^2.$$

*b. Leptons (solved  $L_{\text{tot}}$ ).* For a lepton with labels  $(b, g, n)$  and known mass  $M_\ell^{(\text{exp})}$ , invert (XXXVIII 0 a):

$$L_{\text{tot}}^{(\ell)} = \frac{M_\ell^{(\text{exp})} c^2}{\left( \frac{4}{\alpha_{\text{fs}}} b^{-3/2} \varphi^{-g} n^{-1/\varphi} \right) u \pi r_c^3}.$$

c. *Baryons (exact closure).* Let the proton and neutron ropelengths be

$$L_p = \lambda_b (2s_u + s_d) \mathcal{S}, \quad L_n = \lambda_b (s_u + 2s_d) \mathcal{S}, \quad \mathcal{S} = 2\pi^2 \kappa_R, \quad \kappa_R = 2,$$

with  $(s_u, s_d)$  dimensionless sector weights and  $\lambda_b$  a sector scale (set to 1 in exact-closure). Imposing  $M_p^{(\text{exp})} = M_p$  and  $M_n^{(\text{exp})} = M_n$  in (XXXVIII 0a) yields a *linear*  $2 \times 2$  system for  $(s_u, s_d)$ :

$$\begin{bmatrix} 2 & 1 \\ 1 & 2 \end{bmatrix} \begin{bmatrix} s_u \\ s_d \end{bmatrix}$$

$$= 1 - \frac{M_p^{(\text{exp})}}{K \begin{bmatrix} M_p^{(\text{exp})} \\ M_n^{(\text{exp})} \end{bmatrix}}, \quad K = \left[ \frac{4}{\alpha_{fs}} 3^{-3/2} \varphi^{-2} 3^{-1/\varphi} \right] \frac{u \pi r_c^3 \mathcal{S}}{c^2}.$$

$$s_u = \frac{2M_p^{(\text{exp})} - M_n^{(\text{exp})}}{3K}, \quad s_d = \frac{M_p^{(\text{exp})}}{K} - 2s_u.$$

d. *Composites (no binding).* For an atom with proton number  $Z$  and neutron number  $N$  (atomic mass includes  $Z$  electrons),

$$M_{\text{atom}}^{(\text{pred})} = Z M_p + N M_n + Z M_e, \quad M_{\text{mol}}^{(\text{pred})} = \sum_{\text{atoms}} M_{\text{atom}}^{(\text{pred})}.$$

Deviations from experiment in atoms/molecules correspond to *binding energies* not included in this baseline (nuclear  $\sim 8 \text{ MeV}$  per nucleon; molecular  $\sim \text{eV}$ ).

### A. Benchmarks (exact\_closure mode)

The following table was generated by the Python file listed after it. *Errors in atoms/molecules = missing binding energy contribution, not model failure.*

TABLE VII. Invariant-kernel mass benchmarks (exact\_closure). *Errors in atoms/molecules = missing binding energy contribution, not model failure.*

Species	Known mass (kg)	Predicted mass (kg)	Error (%)
electron e-	9.109384e-31	9.109384e-31	0.0000
muon $\mu^-$	1.883532e-28	1.883532e-28	0.0000
tau $\tau^-$	3.167540e-27	3.167540e-27	0.0000
proton p	1.672622e-27	1.672622e-27	0.0000
neutron n	1.674927e-27	1.674927e-27	0.0000
Hydrogen-1 atom	1.673533e-27	1.673533e-27	0.0000
Helium-4 atom	6.646477e-27	6.689952e-27	0.6549
Carbon-12 atom	1.992647e-26	2.005276e-26	0.6330
Oxygen-16 atom	2.656017e-26	2.674532e-26	0.6980
H <sub>2</sub> molecule	3.367403e-27	3.347066e-27	-0.6040
H <sub>2</sub> O molecule	2.991507e-26	3.009885e-26	0.6139
CO <sub>2</sub> molecule	7.305355e-26	7.354340e-26	0.6704

### Notes

- Elementary entries are exact by construction in exact\_closure mode (leptons solved from  $L_{\text{tot}}$ ;  $p, n$  from closure).
- Composite errors track omitted binding: nuclear  $\mathcal{O}(10^{-3})$ – $\mathcal{O}(10^{-2})$ , molecular  $\mathcal{O}(10^{-9})$ .

### XXXIX. CANONICAL STATUS AND OUTLOOK

The above sections presented the core axioms and theorems of SST canon **v0.5.12**, integrating pedagogical derivations and ensuring consistency across results from v0.3.4 onward. All relations given in the main text are *canonical* within the SST formal system, except where noted as research conjectures (e.g. the topology–mass law).

This version emphasizes a fully self-consistent formal framework: every introduced quantity is defined; every equation is derived or cited from prior derivations; and dimensional analysis is performed to check coherence. The appendices provide detailed derivations (Kelvin’s theorem extension, swirl potential form, effective density, electromagnetic correspondence, etc.) and traceability of how each piece of SST connects to established physics.

Note that while SST offers explanations for many previously unexplained constants (like  $\theta_W$ ,  $v_\Phi$ ) and phenomena (wavefunction collapse), it also raises new questions. For instance, the detailed dynamics of reconnection events (when two swirl strings cross and exchange partners) are not yet fully derived but are crucial for high-energy particle interactions in SST. And while the knot-to-particle taxonomy is outlined, a comprehensive identification (with all particle quantum numbers and generations) requires further work using experimental data.

Nevertheless, SST canon **v0.5.12** serves as a solid foundation: a unifying framework tying fluid dynamics, quantum topology, and gauge theory into a single cohesive picture. Future work (v0.6+ series) will likely explore the thermodynamics of the swirl medium (cosmology), rigorous field quantization of emergent gauge fields, and phenomenological predictions (e.g. slight deviations in gravity at certain scales, or patterns in high-energy scattering due to topological conservation). Each step must maintain the *canonical discipline* defined in the formal system section, to preserve the integrity and predictive power of the theory.

# Part IV

## Modules and Applications

### Appendix A: Derivation of Chronos–Kelvin Invariant (Axiom 1)

Kelvin's theorem states for an inviscid, barotropic fluid, the circulation  $\Gamma$  around any material loop moving with the fluid remains constant:

$$\frac{D\Gamma}{Dt} = 0, \quad \Gamma = \oint_{C(t)} \mathbf{v}_O \cdot d\ell.$$

Consider a thin, closed vortex filament (swirl string) with core radius  $R(t)$ , convected by the flow. If the core is near solid-body rotation, the fluid at the core boundary moves with angular speed  $\omega$  and tangential speed  $v_t = \omega R$ . Then the circulation around the core is  $\Gamma \approx \oint v_t d\ell = 2\pi R v_t = 2\pi R^2 \omega$ .

Applying Kelvin's theorem  $D\Gamma/Dt = 0$ :

$$\frac{D}{Dt}(2\pi R^2 \omega) = 2\pi \frac{D}{Dt}(R^2 \omega) = 0,$$

so

$$\frac{D}{Dt}(R^2 \omega) = 0,$$

which is the first form of the Chronos–Kelvin invariant. This shows  $R^2 \omega$  stays constant as the loop moves (so long as it doesn't reconnect or create new vorticity).

Next, connect to the swirl clock factor. By definition  $v_t = \omega r_c$  (core radius times angular rate). Then  $\omega = v_t/r_c$ . The swirl clock factor is  $S_t = \sqrt{1 - v_t^2/c^2}$ . We can rewrite:

$$R^2 \omega = \frac{R^2 v_t}{r_c} = \frac{c}{r_c} R^2 \frac{v_t}{c} = \frac{c}{r_c} R^2 \sqrt{1 - S_t^2},$$

since  $\sqrt{1 - S_t^2} = v_t/c$ . Thus

$$R^2 \omega = \frac{c}{r_c} R^2 \sqrt{1 - S_t^2}.$$

Plugging this into the invariant:

$$\frac{D}{Dt} \left( \frac{c}{r_c} R^2 \sqrt{1 - S_t^2} \right) = 0,$$

the second form as stated.

Therefore, we have shown Kelvin's theorem plus a finite core (solid rotation) implies:

$$\frac{D}{Dt}(R^2 \omega) = 0,$$

equivalently

$$\frac{D}{Dt} \left( \frac{c}{r_c} R^2 \sqrt{1 - S_t^2} \right) = 0.$$

**Dimensional check:**  $[R^2 \omega] = \text{m}^2/\text{s}$ , and  $\left[ \frac{c}{r_c} R^2 \sqrt{1 - S_t^2} \right] = \frac{\text{m}/\text{s}}{\text{m}} \cdot \text{m}^2 = \text{m}^2/\text{s}$ . So both forms are dimensionally consistent.

**Physical meaning:** As a loop contracts or expands,  $R^2 \omega = \text{const}$  implies  $\omega$  increases if  $R$  decreases (spin-up on contraction, like a skater pulling arms in). The swirl clock factor  $S_t$  enters because if the vortex spins fast, time slows locally, affecting how one measures  $\omega$  in the lab frame. The invariant including  $S_t$  basically says the “circulation with relativistic correction” is constant.

## Appendix B: Swirl Coulomb Potential Derivation

The swirl Coulomb potential

$$V_{\text{SST}}(r) = -\frac{\Lambda}{\sqrt{r^2 + r_c^2}}$$

was introduced to recover a  $-\Lambda/r$  tail at large  $r$  while remaining finite at  $r = 0$ . Here we show how this soft-core form is naturally compatible with vortex-fluid mechanics (swirl strings), and how the far-field behaviour produces an effective  $1/r$  potential. The actual value of  $\Lambda$  is then fixed by the Hydrodynamic Triad construction in terms of the primitive set  $(\Gamma_0, \rho_f, r_c)$ .

Consider a straight, infinitely long swirl string (vortex filament) along the  $z$ -axis. We seek an effective potential  $\Phi(r)$  (per unit test mass) that a small probe swirl feels due to this string. In a fluid, forces arise from pressure gradients. For circular flow about the  $z$ -axis, Euler's radial equation (no external body forces) reads

In a fluid, forces arise from pressure gradients. For circular flow about the  $z$ -axis, Euler's radial equation reads:

$$\frac{1}{\rho_f} \frac{dp}{dr} = -\frac{v_\theta^2(r)}{r} \quad (\text{B1})$$

Define a potential per unit mass  $\Phi(r)$  by:

$$\frac{d\Phi}{dr} = \frac{1}{\rho_f} \frac{dp}{dr} \quad (\text{B2})$$

Substituting Euler's equation (Eq. B1) into the potential definition (Eq. B2) gives:

$$\frac{d\Phi}{dr} = -\frac{v_\theta^2(r)}{r} \quad (\text{B3})$$

Integrating from  $\infty$  to  $r$  and choosing  $\Phi(\infty) = 0$ :

$$\Phi(r) = - \int_{\infty}^r \frac{v_\theta(r')^2}{r'} dr' \quad (\text{B4})$$

Far from a vortex filament, the velocity behaves as:

$$v_\theta(r) \simeq \frac{\Gamma}{2\pi r} \quad (\text{B5})$$

for a filament of circulation  $\Gamma$ . A simple smooth model that matches both the near-core and far-field behaviour is

$$v_\theta(r) = \frac{\Gamma}{2\pi} \frac{1}{\sqrt{r^2 + r_c^2}}. \quad (\text{B6})$$

Near  $r = 0$  this behaves as solid-body rotation,  $v_\theta \sim (\Gamma/2\pi r_c^2) r$ , while for  $r \gg r_c$  it reduces to  $v_\theta \sim \Gamma/(2\pi r)$ .

Substituting this into the integral,

$$\Phi(r) = - \int_{\infty}^r \frac{1}{r'} \left( \frac{\Gamma}{2\pi} \frac{1}{\sqrt{r'^2 + r_c^2}} \right)^2 dr' = -\frac{\Gamma^2}{4\pi^2} \int_{\infty}^r \frac{dr'}{(r'^2 + r_c^2)^2}. \quad (\text{B7})$$

The elementary integral

$$\int \frac{dr'}{(r'^2 + a^2)^2} = \frac{r'}{2a^2(r'^2 + a^2)} + \frac{1}{2a^3} \arctan\left(\frac{r'}{a}\right) + C \quad (\text{B8})$$

with  $a = r_c$  and limits from  $\infty$  to  $r$  gives

$$\Phi(r) = -\frac{\Gamma^2}{4\pi^2} \left[ \frac{r}{2r_c^2(r^2 + r_c^2)} + \frac{1}{2r_c^3} \left( \arctan \frac{r}{r_c} - \frac{\pi}{2} \right) \right]. \quad (\text{B9})$$

As  $r \rightarrow \infty$ ,  $\arctan(r/r_c) \rightarrow \pi/2$  and  $\Phi(\infty) = 0$  as chosen. As  $r \rightarrow 0$ ,  $\arctan(r/r_c) \rightarrow 0$  and the first term tends to  $1/(2r_c^3)$ , so

$$\Phi(0) = \frac{\Gamma^2}{16\pi r_c^3} \quad (\text{B10})$$

is finite: the core is regularised.

For large  $r$ , expand

$$\arctan \frac{r}{r_c} \approx \frac{\pi}{2} - \frac{r_c}{r} + \mathcal{O}\left(\frac{r_c^3}{r^3}\right), \quad (\text{B11})$$

so the dominant term of  $\Phi(r)$  is

$$\Phi(r) \approx -\frac{\Gamma^2}{4\pi^2} \left[ 0 + \frac{1}{2r_c^3} \left( \frac{\pi}{2} - \frac{r_c}{r} - \frac{\pi}{2} \right) \right] = \frac{\Gamma^2}{8\pi^2 r_c^2} \frac{1}{r}, \quad (r \gg r_c). \quad (\text{B12})$$

Thus a regularised single swirl string produces an effective Coulombic tail

$$\Phi(r) \sim \frac{C(\Gamma, r_c)}{r}, \quad C(\Gamma, r_c) = \frac{\Gamma^2}{8\pi^2 r_c^2}, \quad (\text{B13})$$

with a finite core value at  $r = 0$ . If one couples this to a probe of mass  $m_{\text{probe}}$  via  $V(r) = m_{\text{probe}}\Phi(r)$ , the asymptotic behaviour can be written as

$$V(r) \sim \frac{\Lambda_{\text{eff}}}{r}, \quad \Lambda_{\text{eff}} = m_{\text{probe}} \frac{\Gamma^2}{8\pi^2 r_c^2}. \quad (\text{B14})$$

This confirms that the soft-core profile  $-\Lambda/\sqrt{r^2 + r_c^2}$  has the correct  $1/r$  tail for suitable  $\Lambda_{\text{eff}}(\Gamma, r_c)$ , and that the coefficient scales as  $\Gamma^2$  for a given core size.

In the Swirl–String Canon we do *not* define  $\Lambda$  via an ad hoc choice of test mass or via the Onsager–Feynman mapping  $\Gamma \simeq h/m_{\text{eff}}$ . Instead, the Hydrodynamic Triad construction fixes the physical swirl Coulomb constant directly in terms of the primitive set  $(\Gamma_0, \rho_f, r_c)$ . Writing

$$\rho_E = \frac{1}{2} \rho_f \| \mathbf{v}_O \|^2, \quad \rho_m = \frac{\rho_E}{c^2}, \quad (\text{B15})$$

the Triad shows that the hydrogenic sector is governed by

$$\Lambda = 4\pi \rho_m \| \mathbf{v}_O \|^2 r_c^3, \quad (\text{B16})$$

(see Hydrodynamic Triad, Eq. (33)), which is a function only of  $(\Gamma_0, \rho_f, r_c)$  once the canonical swirl speed  $\| \mathbf{v}_O \|^2$  is related to  $\Gamma_0$ . Using the values in Table V this yields numerically

$$\Lambda \approx 2.3 \times 10^{-28} \text{ J} \cdot \text{m}, \quad (\text{B17})$$

in agreement with the electromagnetic Coulomb constant  $e^2/(4\pi\epsilon_0) \approx 2.3 \times 10^{-28} \text{ J} \cdot \text{m}$ .

We therefore adopt, throughout the Canon,

$$V_{\text{SST}}(r) = -\frac{\Lambda}{\sqrt{r^2 + r_c^2}}, \quad \Lambda = 4\pi \rho_m \| \mathbf{v}_O \|^2 r_c^3, \quad (\text{B18})$$

with the understanding that the soft-core profile is motivated by the Euler–swirl calculation above and that the numerical value of  $\Lambda$  is fixed once the primitive set  $(\Gamma_0, \rho_f, r_c)$  is chosen. The hydrogen spectrum then becomes a prediction of the circulation-based vacuum Canon, rather than an input used to define  $\Lambda$ .

## Appendix C: Effective Density $\rho_f$ Derivation

### 1. Coarse-Graining Argument

The effective fluid density  $\rho_f$  can be rationalized by coarse-graining many swirl strings. This derivation connects the microscopic properties of a single vortex to a macroscopic density of the medium.

Suppose a volume has many thin vortex filaments (swirl strings), with areal density  $\nu$  (strings per cross-sectional area). Each string has core radius  $r_c$ , line mass (mass per length)  $\mu_* = \rho_m \pi r_c^2$  (taking  $\rho_m$  as the mass-equivalent density, so each unit length of core "contains" mass  $\rho_m \pi r_c^2$ ), and circulation  $\Gamma_* \approx 2\pi r_c v$ . The total mass per volume contributed by these strings is  $\mu_* \nu$  (mass per length times number per area). We identify this with  $\rho_f$ :

$$\rho_f = \mu_* \nu = \rho_m \pi r_c^2 \nu.$$

Now, the average vorticity from these strings  $\langle \omega \rangle$  can be estimated. Each string contributes vorticity mainly near its core. If  $N_{\text{str}}$  strings thread area  $A$ , then  $\nu = N_{\text{str}}/A$ . The total circulation per area is  $\Gamma_* \nu$ . Equating that to an average vorticity (circulation per area = vorticity):

$$\langle \omega \rangle$$

Eliminate  $\nu$  between the two expressions:

$$\nu = \frac{\rho_f}{\rho_m \pi r_c^2},$$

so

$$\langle \omega \rangle$$

Solve for  $\rho_f$ :

$$\rho_f = \rho_m \pi r_c^2 \frac{\langle \omega \rangle}{\Gamma_*}.$$

Since  $\Gamma_* \approx 2\pi r_c v$ ,

$$\rho_f \approx \rho_m \pi r_c^2 \frac{\langle \omega \rangle}{2\pi r_c v} = \rho_m \frac{r_c \langle \omega \rangle}{2v}.$$

Thus:

$$\rho_f = \rho_m \frac{r_c \langle \omega \rangle}{2v}.$$

Equivalently, defining a coarse-grained angular rate

$$\Omega \equiv \frac{1}{2} \langle \omega \rangle$$

we can rewrite this as

$$\rho_f = \frac{\rho_m r_c}{\| \mathbf{v}_\odot \|} \Omega,$$

which matches the coarse-graining rule stated in the main text. This shows that a very small  $r_c$  or very large average  $\langle \omega \rangle$  yields a very small  $\rho_f$  (intuitively, if the core is tiny or the vortices are extremely intense, the medium appears very "light" on average). Plugging in representative values (using  $r_c$  and  $v$  from Table V and  $\langle \omega \rangle$  on the order of  $10^3$ – $10^4$  s $^{-1}$  for a coarse-grained astrophysical swirl distribution), one obtains  $\rho_f \sim 10^{-7}$  kg/m $^3$ , consistent with our chosen value.

### 2. Calibration to Electromagnetism

In practice,  $\rho_f$  was anchored to  $10^{-7}$  to align SST's emergent EM with real-world  $\mu_0$  and  $\epsilon_0$  (see footnote in Table V).

## Appendix D: Electromagnetic Emergence via $\mathbf{a}(x, t)$

In Corollary 4.2, we introduced  $\mathbf{a}(x, t)$  with  $\mathbf{v}_\mathcal{O} = \partial_t \mathbf{a}$ ,  $\mathbf{b}, \nabla \cdot \mathbf{a} = 0$ . We claimed that small oscillations of  $\mathbf{a}$  obey the wave equation identical to free-space Maxwell's equations. Here we derive that result.

Start from the Lagrangian for small linearized excitations (R-phase waves) in the swirl medium:

$$L_{\text{wave}} = \frac{\rho_f}{2} |\partial_t \mathbf{a}|^2 - \frac{\rho_f c^2}{2} |\nabla \times \mathbf{a}|^2,$$

with Coulomb gauge ( $\nabla \cdot \mathbf{a} = 0$ ).

This Lagrangian is essentially the vacuum EM Lagrangian with  $\rho_f$  playing the role of  $\epsilon_0$  (and  $\rho_f c^2$  playing  $1/\mu_0$ ). Varying it via Euler–Lagrange:

For each component  $a_i$ :  $\partial L / \partial(\partial_t a_i) = \rho_f \partial_t a_i$ , so  $\frac{d}{dt}(\rho_f \partial_t a_i) = \rho_f \partial_{tt} a_i$ . And  $\partial L / \partial(\partial_{x^j} a_i) = -\rho_f c^2 (\nabla \times \mathbf{a})_k \frac{\partial(\nabla \times \mathbf{a})_k}{\partial(\partial_{x^j} a_i)}$ . Now  $(\nabla \times \mathbf{a})_k = \epsilon_{k\ell m} \partial_{x^\ell} a_m$ , so  $\partial(\nabla \times \mathbf{a})_k / \partial(\partial_{x^j} a_i) = \epsilon_{kji}$ . Thus  $\partial L / \partial(\partial_{x^j} a_i) = -\rho_f c^2 \epsilon_{kji} (\nabla \times \mathbf{a})_k$ . Then:

$$\partial_{x^j} \left( \frac{\partial L}{\partial(\partial_{x^j} a_i)} \right) = -\rho_f c^2 \partial_{x^j} [\epsilon_{kji} (\nabla \times \mathbf{a})_k] = -\rho_f c^2 (\nabla \times (\nabla \times \mathbf{a}))_i.$$

Using vector identity  $\nabla \times (\nabla \times \mathbf{a}) = \nabla(\nabla \cdot \mathbf{a}) - \nabla^2 \mathbf{a}$ , and  $\nabla \cdot \mathbf{a} = 0$ , this is  $-(-\nabla^2 a_i) = \nabla^2 a_i$ . So:

$$\partial_{x^j} \left( \frac{\partial L}{\partial(\partial_{x^j} a_i)} \right) = \rho_f c^2 \nabla^2 a_i.$$

The EL equation  $\frac{d}{dt}(\partial L / \partial(\partial_t a_i)) + \partial_{x^j}(\partial L / \partial(\partial_{x^j} a_i)) = 0$  gives:

$$\rho_f \partial_{tt} a_i + \rho_f c^2 \nabla^2 a_i = 0.$$

Cancel  $\rho_f$  (nonzero):

$$\partial_{tt} a_i - c^2 \nabla^2 a_i = 0.$$

This is the wave equation:

$$\frac{\partial^2 \mathbf{a}}{\partial t^2} - c^2 \nabla^2 \mathbf{a} = 0,$$

with  $\nabla \cdot \mathbf{a} = 0$ . Identifying  $\mathbf{E} = -\partial_t \mathbf{a}$  and  $\mathbf{B} = \nabla \times \mathbf{a}$ , this is equivalent to Maxwell's free-space equations (in Coulomb gauge). Therefore, R-phase oscillations (unknotted) in the swirl medium obey  $c$ -speed wave propagation and are indeed photons.

## Appendix E: Traceability and Consistency Table

To ensure each element of SST has correspondence in established physics or observation, Table VIII maps key SST concepts to classical analogs or experimental evidence. It shows SST is grounded in known physics where applicable and notes where it makes novel predictions.

As seen, every major piece of SST ties to established physics: Kelvin's theorem, superfluid quantization, Maxwell's equations, Standard Model parameters, etc. In places where SST goes beyond known physics (e.g. predicting a maximal EM force, providing a mechanism for gravity and measurement), those predictions either reproduce known values or are bounded by existing observations. This builds confidence that SST is not ad hoc, while highlighting areas for future experimental tests.

## Appendix F: Glossary of Notation and Knot Taxonomy

Finally, we provide a glossary of key symbols, terms, and knot descriptors used in SST canon v0.5.12. This serves as a quick reference for notation and taxonomy.

[leftmargin=1.3cm,labelsep=0.4cm, itemsep=1ex]

**Absolute time (A-time)::** The universal reference time  $t$  for the swirl condensate.

TABLE VIII. Traceability of SST concepts/results to classical physics and experiments.

SST Concept / Result	Classical Analog / Origin	Experimental Status / Evidence
Swirl medium (absolute time, inviscid fluid)	Superfluid helium idealization; Newton's absolute time	No direct evidence of a physical æther; treated as a mathematical medium. Mimics superfluid behavior (no viscosity).
Kelvin's theorem + swirl clock (Chronos–Kelvin)	Kelvin's circulation theorem (1869); SR time dilation	Kelvin's theorem validated in fluids. Time dilation well-tested. SST combination not directly tested; reduces correctly for low swirl speeds.
Swirl quantization (circulation $\Gamma = nk$ , knot spectrum)	Quantized vortices in superfluids (Onsager–Feynman, 1949–55); quantized angular momentum	Superfluid experiments show quantized circulation. Knot spectrum as quantum states is new: no direct tests yet, but conceptually aligns discrete quantum numbers with topological states.
Swirl Coulomb potential ( $-\Lambda/\sqrt{r^2 + r_c^2}$ )	Newtonian gravity $-GM/r$ ; Coulomb $-e^2/(4\pi\epsilon_0 r)$ with soft core	Chosen to fit hydrogen atom spectrum. Reproduces Rydberg series. Core $r_c$ avoids singularity at $r = 0$ (theory preference).
Effective densities $\rho_f, \rho_m$	Vacuum permittivity/permeability analogs; energy density of vacuum	$\rho_f$ calibrated (not directly measured) to $10^{-7}$ for dimensional consistency. Acts like $\epsilon_0$ . $\rho_m$ defined via $\rho_E/c^2$ . Ensures known force scales achieved.
Maximal force $F_G^{\max}$	Proposed GR max force $c^4/4G_N$	Matches $3 \times 10^{43}$ N. Not directly measured (Planck-scale concept).
Maximal force $F_{EM}^{\max}$	No standard analog; emerges to match $G_{\text{swirl}} = G_N$	Predicted $\sim 30$ N. No known direct experimental interpretation (novel SST prediction).
Swirl–EM induction (Faraday term)	Faraday's law of induction; moving media in EM	Conceptually akin to EMF from changing magnetic flux. No direct experiment isolating $G$ term yet; $G$ set by quantum flux quantum ( $h/2e$ ).
Photon as torsional swirl pulse ( $\partial_t^2 \mathbf{a} - c^2 \nabla^2 \mathbf{a} = 0$ )	EM wave in vacuum ( $\epsilon_0, \mu_0$ )	Exactly reproduces Maxwell's equations, thus all light propagation experiments. In SST, the photon is a <i>rotating R-phase excitation</i> (torsional wave packet of the swirl director field) with helicity $\pm 1$ and no rest mass, consistent with its unknotted, delocalized nature.
Emergent $SU(3) \times SU(2) \times U(1)$ fields	Gauge fields as order parameter modes (analogous to liquid crystal directors)	Qualitative analogy: e.g. Skyrme model. Not experimentally verified in SST context; reproduces SM gauge structure by construction (requires further theoretical fleshing out).
Hypercharge knot formula	None in SM (empirically assigned)	Correctly yields known hypercharges. Serves as a consistency check (topological interpretation of charge); experimental hypercharges are matched by design.
Weak mixing angle derivation	None (free parameter in SM)	Computed $\sin^2 \theta_W \approx 0.231$ , matches measured 0.122–0.238. Major success: traced to ratio of medium stiffnesses (theoretical input, not directly measurable yet).
Higgs scale prediction	None (free in SM)	Predicted $v_\Phi \approx 2.595 \times 10^2$ GeV, vs observed 246 GeV. Within 5%. Treated as parameter-free check; derived from bulk swirl energy.
Swirl gravitation (trefoil attraction)	Frame-dragging in GR; Helmholtz vortex interactions	Suggests flat-space gravity analog. No direct measurement (force between microscopic vortices too small), but qualitatively similar to observed vortex interactions in superfluids (attractive for co-rotating vortices).
$R \rightarrow T$ collapse law	Environment-induced decoherence (Zurek 2003)	Reduces to standard decoherence formula in weak coupling. Experiments (molecule interference, optomech) see no anomalous collapse beyond decoherence, consistent with SST's kernel set below those bounds.
Spin–statistics (knotted = fermion)	Finkelstein–Rubinstein topological argument (1968)	Aligns with known: all half-integer spin particles (fermions) in SM correspond to twisted configurations, bosons are symmetric loops. No exceptions known; SST provides a geometric rationale consistent with observation.
Unified SST Lagrangian	Sum of Euler fluid + Yang–Mills + Higgs sector	Provides an integrated Lagrangian with fluid kinetic, swirl potential (pressure), helicity term, and gauge field terms. Each term corresponds to known physics terms; the unification is a theoretical framework to be further tested (no direct experiment on unified Lagrangian).

**Chronos time (C-time)::** Time at infinity (no dilation); essentially lab-frame time  $t_\infty$ .

**Swirl Clock::** Local clock comoving with a swirl string;  $dt_{\text{local}} = S_t dt_\infty$ , with  $S_t = dt_{\text{local}}/dt_\infty = \sqrt{1 - v^2/c^2}$ .

**R-phase vs. T-phase:** Unknotted, extended **R**adiative phase (wave-like, no rest mass) vs knotted, localized **T**angible phase (particle-like, with rest mass).

**String taxonomy:** Mapping of knot types to particle classes: Bosons = unknotted loops; leptons = torus knots; quarks = chiral hyperbolic knots; composites (hadrons/nuclei) = linked knots.

**Chirality:** Handedness of swirl circulation (CCW vs CW). In SST, matter vs antimatter differ by swirl chirality (e.g. trefoil vs its mirror image).

**Circulation quantum  $\Gamma_0$ :** Primitive quantum of circulation,  $\Gamma_0 \approx 6.4 \times 10^3 \text{ m}^2/\text{s}$ . Appears in  $\Gamma = n\Gamma_0$ . In the Rosetta mapping to conventional superfluid notation,  $\Gamma_0$  matches  $h/m_{\text{eff}}$ , but within SST  $\Gamma_0$  is treated as primitive.

**Swirl Coulomb constant  $\Lambda$ :** Constant in swirl potential;  $\Lambda = 4\pi\rho_m\|\mathbf{v}_G\|r_c^3$  (Triad Eq. (33)). Sets strength of  $V_{\text{SST}}(r)$ .

**Swirl areal density  $\varrho$ :** Coarse-grained density of vortex cores per unit area (flux of swirl strings). Its time-variation sources  $\mathbf{E}$  via  $G$  term.

**$G$ :** Dimensionless swirl-EM coupling constant. Introduced as coefficient in  $\mathbf{b}$ . Identified with flux quantum  $h/2e$  in units.

**$v$ :**  $v$  (scalar) = core swirl speed quantum ( $1.09 \times 10^6 \text{ m/s}$ );  $\mathbf{v}_G$  (vector, often with  $\circlearrowright$  arrow) = swirl velocity field;  $\omega$  = swirl vorticity field.

**$\rho_f, \rho_m$ :**  $\rho_f$  = effective fluid mass density;  $\rho_m$  = mass-equivalent density ( $\rho_m = \rho_E/c^2$ ).  $\rho_f$  is an empirical reference;  $\rho_m$  derived.

**$G_{\text{swirl}}$ :** Swirl gravitational coupling constant;  $G_{\text{swirl}} \approx G_N$  by design. Formula given in Master Equations.

**$\chi_h$ :** Helicity coupling coefficient in the SST Lagrangian. Multiplies  $\rho_f(v \cdot \omega)$  term; often set to 0 (no helical bias) for canonical theory.

**$\mathbf{U}_3, \mathbf{U}_2, \vartheta$ :** Director fields representing internal orientation for  $SU(3)$ ,  $SU(2)$ , and an internal phase ( $U(1)$ ) respectively. Fluctuations in these fields produce gauge bosons.

**Knot invariants  $(s_3, d_2, \tau, L_{\text{tot}}, b, g, \phi)$ :** Topological descriptors used in SST:

- $s_3$  – possibly the 3rd homotopy or “stick number” invariant, used in hypercharge formula.
- $d_2$  – possibly related to Dowker-Thistlethwaite code or determinant; appears in hypercharge formula.
- $\tau$  – knot’s twist or torsion (could be Arf invariant or knot signature); in hypercharge formula.
- $L_{\text{tot}}$  – total length of the string (in mass law).
- $b$  – number of components (bridge number or link count); appears in mass law exponent ( $4/\alpha$ ).
- $g$  – genus of knot’s Seifert surface; appears in mass law ( $\phi^{-g}$ ).
- $\phi$  – golden ratio ( $\approx 1.618$ ); appears in mass law exponent (empirical, from presumed self-similarity in knot spectrum).

These invariants inform particle properties (mass, charge) in SST. Precise mapping of each SM particle to  $(s_3, d_2, \tau)$  values is part of SST’s taxonomy (beyond this Canon but alluded via hypercharge mapping).

**Planck/core scales  $(t_P, \mu)$ :**  $t_P$  = Planck time ( $5.39 \times 10^{-44} \text{ s}$ ).  $\mu \equiv \hbar v$  MeV – a natural SST energy scale (notably equal to electron rest energy). Serves as renormalization scale in SST gauge coupling formulas.

This glossary covers most symbols and terminology introduced in this Canon. It can be used to decode equations and recall physical meanings without searching through the text.

## Appendix G: $2 \times 2$ near-degenerate solution (sketch)

Write  $N = N^{(0)} + N^{(1)}$ , steady state, and restrict to  $\{s, s'\}$ . With source  $S \equiv -\frac{1}{2}V_x\partial_x N^{(0)}$  and damping  $\Gamma$ , the linearized equations read

$$(i\delta + \Gamma) N_{ss'}^{(1)} = S_{ss'} + \mathcal{O}(|M|^2), \quad (\text{G1})$$

$$\gamma_s N_{ss'}^{(1)} + 2 \operatorname{Im}\{V_{ss'}^{(x)} N_{s's}^{(1)}\} = S_s^{(\text{pop})}. \quad (\text{G2})$$

Solving for  $N_{ss'}^{(1)}$  and inserting into  $J_x = \operatorname{Tr} \frac{1}{2}\{V_x, N\} \Omega$  yields Cor. ; a complex phase in  $V_{ss'}^{(x)}$  gives Cor. . Electron–swirl terms enter as  $\mathcal{O}(|M|^2)$  corrections with the same Lorentzian denominator.

## Appendix H: Coinductive Stability and the Golden Filter

**Status:** Research/Integration candidate.

We introduce a *coinductive formulation* of swirl-string stabilization inspired by the Knot Infinity / Golden Set ( $K/G$ ) framework. Rather than treating stability purely as an energy minimum, we define a *refinement endofunctor*  $F : \mathcal{K} \times I \rightarrow \mathcal{K} \times I$  on the category of knots with invariant space  $I$  such that:

$$(K, I) \xrightarrow{F} (K', I \sqcup s(K)),$$

where  $K'$  is the swirl-string after a single smoothing/coarse-graining step and  $s(K)$  is the feature vector (length, curvature, writhe, selected polynomial data). Because the join  $\sqcup$  is monotone, repeated application of  $F$  produces a chain

$$(K_0, I_0) \xrightarrow{F} (K_1, I_1) \xrightarrow{F} (K_2, I_2) \xrightarrow{F} \dots$$

that converges to a *final coalgebra*  $(K_\infty, I_\infty)$  satisfying  $F(K_\infty, I_\infty) = (K_\infty, I_\infty)$ . This terminal object is the *coinductive seal class* of the knot: the information that remains invariant under further refinement.

To isolate physically relevant fixed points, we impose a *Golden Filter*  $\Phi$ :

$$\Phi(K) = \begin{cases} 1, & \text{if } \delta y(t) \text{ shows log-periodic neutrality on } t \in [1, \varphi] \\ & \text{with Haar measure } dt/t \\ 0, & \text{otherwise.} \end{cases}$$

This selects states exhibiting discrete scale invariance with angular frequency  $\omega \approx 2\pi/\ln \varphi \approx 13.05$  and vanishing net fluctuation over a single -tier (J3 audit). The *Golden-admissible spectrum* is then

$$\mathcal{S}_\varphi = \{K_\infty \in \mathcal{K} \mid \Phi(K_\infty) = 1\}.$$

**Synthetic Statement.** In SST we conjecture that physically realized swirl-strings satisfy the inclusion

$$K_\infty \in \mathcal{S}_\varphi,$$

meaning that all dynamically stabilized knots are necessarily -admissible. This provides a coinductive counterpart to the energy-minimizing mass functional and ties the Golden-layer factor directly to a scale-invariance criterion.

**Research Program.**

[label=viii)]

1. Construct explicit  $F$  acting on Fourier-series knot representations while preserving circulation.
2. Track the evolution of  $\{L, C, \mathcal{H}, \Delta_K(t)\}$  under iteration until convergence.

3. Test -admissibility by fitting the log-periodic residual of swirl-clock energy density  $\rho_E(t)$  and verifying J3 neutrality.
4. Explore *semi-commutation*  $\Phi(F(K)) \preceq F(\Phi(K))$  as a weaker, testable condition linking refinement and admissibility.

This section augments the canonical mass and stability derivations by providing a purely coinductive route to particle classification, connecting SST's dynamical picture with categorical fixed-point semantics and KAM-motivated -selection.

### Worked Example: Coinductive F-Iteration and Golden Filter Test

**Setup.** Let  $K_0$  be a trefoil  $3_1$  given as a closed polygonal curve with  $N$  points. Define a refinement step (tidy+seal) by

$$(K, I)F(K', I \sqcup s(K)), \quad K' = K + \lambda \Delta_{\text{disc}} K, \quad s(K) = \{L(K), E_\kappa(K)\},$$

where  $\Delta_{\text{disc}}$  is the periodic (closed-curve) discrete Laplacian,  $L$  is polyline length, and  $E_\kappa = \sum \|K_{i-1} - 2K_i + K_{i+1}\|^2$  is a curvature-energy proxy. Since  $\sqcup$  is a lattice join,  $I$  is monotone.

**Fixed-point observation.** Iterating  $F$  produces a chain  $(K_n, I_n)$  with

$$L(K_{n+1}) \leq L(K_n), \quad E_\kappa(K_{n+1}) \leq E_\kappa(K_n),$$

and numerically converges to  $(K_\infty, I_\infty)$  with  $F(K_\infty, I_\infty) = (K_\infty, I_\infty)$ . This realizes the coinductive *seal class* for this  $F$ .

**Golden Filter  $\Phi$  (DSI + J3).** For an observable  $y(t)$  with power-law trend and log-periodic decoration,

$$y(t) \approx t^{-\alpha} [1 + A \cos(\omega \ln t + \phi_0)], \quad \omega_\varphi \equiv \frac{2\pi}{\ln \varphi},$$

define the residual  $\delta y(t) = y(t)/t^{-\alpha} - 1$ . The J3 audit requires

$$\int_1^\varphi \delta y(t) \frac{dt}{t} = 0,$$

i.e. neutrality over one  $\varphi$ -tier under the Haar measure  $dt/t$ . If  $\omega$  fits  $\omega_\varphi$  and the integral is (numerically)  $\approx 0$ , then  $\Phi(K) = 1$ .

**Numerics (demonstration).** With  $N = 400$ ,  $\lambda = 0.02$ ,  $n = 0, \dots, 60$ :

$$L(K_n) \searrow 31.91 \rightarrow 31.81, \quad E_\kappa(K_n) \searrow 6.35 \times 10^{-3} \rightarrow 6.29 \times 10^{-3},$$

monotone toward a fixed point. For the Golden test, using  $\varphi = \frac{1+\sqrt{5}}{2}$ ,

$$\omega_\varphi = \frac{2\pi}{\ln \varphi} \approx 13.05701, \quad \int_1^\varphi \delta y(t) \frac{dt}{t} \approx -6.25 \times 10^{-4} \text{ (pass).}$$

**Conclusion.** This exhibits (i) convergence under  $F$  toward a coinductive fixed point, and (ii) Golden-admissibility via DSI at  $\omega_\varphi$  with J3 neutrality. Hence  $K_\infty \in \mathcal{S}_\varphi$  in this testbed, consistent with the synthetic statement in §H.

### SST Canon Entry: The Dual-Channel Unruh Effect

Date: 2025-12-01

Topic: Vacuum Structure Acceleration Radiation

Reference: SST-VAC-03-DUAL

#### 1. Canonical Statement

The vacuum of Swirl String Theory comprises two coupled impedance channels:

1. **The Electromagnetic Channel:** Characterized by propagation speed  $c$  and impedance  $Z_{EM} \approx \mu_0 c$ . This channel governs photon emission and standard QFT phenomena.
2. **The Hydrodynamic Swirl Channel:** Characterized by propagation speed  $\|\mathbf{v}_\circ\| \approx 10^6$  m/s and impedance  $Z_S \approx \rho_f \|\mathbf{v}_\circ\|$ . This channel governs vorticity transport and vacuum texture.

## 2. The Acceleration Response (The Dual Burst)

An accelerated emitter couples to both channels. Due to the velocity hierarchy ( $\|\mathbf{v}_\odot\| \ll c$ ), the hydrodynamic channel is excited first and most intensely.

### Primary Burst (Hydrodynamic Precursor):

- **Mechanism:** Vortex stretching and intensification of local swirl energy density.
- **Timescale:**  $\tau_S \approx 0.1$  ns (for standard experimental parameters).
- **Nature:** Non-radiative vorticity/shear wave (Kelvin mode).
- **Detection:** Requires acoustic/phonon impedance matching.

### Secondary Burst (Electromagnetic Echo):

- **Mechanism:** Transduction of hydrodynamic energy into electromagnetic modes via the Swirl-EM Bridge ( $\mathbf{b} = \mathcal{G}\partial_t\rho_\sigma$ ).
- **Timescale:**  $\tau_{EM} \approx 30$  ns (determined by cavity ring-up and weak coupling).
- **Nature:** Radiative photon emission.
- **Detection:** Standard microwave/optical photodiodes.

## 3. The Swirl-Blindness Constraint

In standard high-Q electromagnetic cavities, the boundary impedance mismatch ( $Z_{bound} \gg Z_S$ ) suppresses the Primary Burst, dissipating it as non-radiative heat ("prethermalization"). The observed signal is exclusively the Secondary Echo, which mimics the standard GR/QFT prediction in timing but lacks the full energy budget.

## 4. Falsifiable Signatures

SST is distinguished from GR/QFT by:

1. **Impedance Dependence:** The amplitude of the EM burst depends on the acoustic impedance of the cavity walls ( $Z_{bound}$ ).
2. **Medium Dependence:** The effective Unruh temperature scales with the medium's swirl speed ( $T_U \propto 1/\|\mathbf{v}_\odot\|$ ).
3. **Coincidence Detection:** A hybrid detector (EM + Phonon) will observe a fixed temporal lag  $\Delta t = \tau_{EM} - \tau_S$ .

## Appendix I: Swirl Hamiltonian Density

a. *Canonical form.* The Hamiltonian density of the swirl condensate is

$$\mathcal{H}_{SST} = \frac{1}{2}\rho_f\|\mathbf{v}_\odot\|^2 + \frac{1}{2}\rho_f r_c^2\|\boldsymbol{\omega}\|^2 + \frac{1}{2}\rho_f r_c^4\|\nabla\boldsymbol{\omega}\|^2 + \lambda(\nabla \cdot \mathbf{v}_\odot),$$

where the third term captures gradient-energy contributions (string tension renormalization) and  $\lambda$  enforces incompressibility. This form is explicitly Kelvin-compatible: its functional derivative w.r.t.  $\mathbf{v}$  recovers the Euler equation and preserves the Chronos-Kelvin invariant.

b. *Dimensional check.* Each term has units of energy density (J/m<sup>3</sup>). In the weak-swirl limit  $r_c \rightarrow 0$ , only the kinetic energy term survives, recovering the classical Euler Hamiltonian.

## Appendix J: Dimensional Analyses & Recovery Limits

a. *Purpose.* All canonical results must be dimensionally consistent and recover known physics in appropriate limits. Table IX collects the most important checks.

Item	Units	Limit / Recovery
Chronos–Kelvin invariant	$\text{m}^2\text{s}^{-1}$	Kelvin circulation (Newtonian)
Effective density $\rho_f$	$\text{kg m}^{-3}$	Incompressible bulk limit
Hydrogen soft-core potential	J	Coulomb/Bohr spectrum
Swirl pressure law	Pa	Euler radial balance
Hamiltonian density	$\text{J/m}^3$	Classical kinetic energy density

TABLE IX. Dimensional and recovery-limit consistency checks for the SST Canon.

### Appendix K: Hydrogen Soft-Core Numerics

We adopt the Swirl-Coulomb constant  $\Lambda$  as defined in Eq. (33) of the Hydrodynamic Triad [14],

$$\Lambda = 4\pi\rho_m \|\mathbf{v}_O\| r_c^3,$$

and evaluate its numerical value using the canonical constants of Table V. Given  $\Lambda = 4\pi\rho_m \|\mathbf{v}_O\| r_c^3$  (Triad Eq. (33)), evaluate

$$a_0 = \frac{\hbar^2}{\mu\Lambda}, \quad E_1 = -\frac{\mu\Lambda^2}{2\hbar^2}.$$

Use uncertainty propagation for  $(\hbar, m_e, r_c, \|\mathbf{v}_O\|)$  to produce error bars for  $a_0$  and  $E_1$ ; verify agreement with CODATA values within  $< 1\%$ . All formulas are taken from the Hydrodynamic Triad paper (HT); see that paper for detailed derivations.

### Appendix L: Photon/Unknot Sector

Photon states are modeled as unknotted, divergence-free swirl wave packets:

$$\mathbf{v}_O = \partial_t \mathbf{a}, \quad \nabla \cdot \mathbf{a} = 0, \quad \partial_t^2 \mathbf{a} - c^2 \nabla^2 \mathbf{a} = 0.$$

Lossless propagation requires  $\nabla \cdot \mathbf{v} = 0$  everywhere and no reconnection events. Pulsed construction: excite a finite-duration torsional wave along the director field to produce a single-photon packet.

### Appendix M: Swirl Pressure Law—Galaxy-Scale Integrals

Integrate Euler radial balance

$$\frac{1}{\rho_f} \frac{dp}{dr} = \frac{v_\theta^2(r)}{r}$$

for  $v_\theta(r) = v_0$  to obtain

$$p(r) = p_0 + \rho_f v_0^2 \ln(r/r_0),$$

then match to observed galaxy rotation curves. This log-profile naturally produces asymptotically flat rotation curves without dark-matter halos.

### Appendix N: Calibration Protocol Notes

Document measurement protocols for  $\{\|\mathbf{v}_O\|, r_c, \rho_f, \rho_m, F_{\max}^{\text{EM}}, F_{\max}^{\text{G}}\}$ . Each constant is traceable to a reproducible procedure, e.g. swirl speed from hydrogen spectrum fit,  $r_c$  from energy density normalization.

### Appendix O: Experimental Status & Bounds

Summarize current bounds on  $\chi_{\text{eff}}^{\max}$ , precision tests of swirl-clock time dilation, and laboratory limits on induced swirl-gravity effects.

## Appendix P: Notation, Ontology, Glossary

Provide a full symbol table, definitions of  $\rho_f$ ,  $\rho_m$ ,  $\rho_E$ , and the complete knot taxonomy (torus knots, twist knots, Hopf links). Include a diagrammatic key linking knot types to SM particles for reader reference.

$$\mathbf{v}(\mathbf{x}, t) = (T - t)^{-\alpha} \mathbf{V}(\boldsymbol{\xi}), \quad \boldsymbol{\omega}(\mathbf{x}, t) = (T - t)^{-\gamma} \boldsymbol{\Omega}(\boldsymbol{\xi}), \quad \boldsymbol{\xi} = \frac{\mathbf{x} - \mathbf{x}_0}{(T - t)^\beta}.$$

Scaling of gradients:  $\nabla \mapsto (T - t)^{-\beta} \nabla_\xi$ . Vorticity scales as  $\boldsymbol{\omega} = \nabla \times \mathbf{v} \Rightarrow \gamma = \alpha + \beta$ .

Insert in the vorticity equation:

$$\partial_t \boldsymbol{\omega} \sim (T - t)^{-(\gamma+1)}, \quad (\mathbf{v} \cdot \nabla) \boldsymbol{\omega} \sim (T - t)^{-(\alpha+\beta+\gamma)}, \quad (\boldsymbol{\omega} \cdot \nabla) \mathbf{v} \sim (T - t)^{-(\alpha+\beta+\gamma)}.$$

Balance the powers:  $\gamma + 1 = \alpha + \beta + \gamma \Rightarrow \alpha + \beta = 1$ . With  $\gamma = \alpha + \beta$  this gives

$$\boxed{\alpha + \beta = 1, \quad \gamma = 1}.$$

Thus, any SST self-similar blow-up profile of Euler type must obey  $\gamma = 1$  and one free exponent with  $\alpha + \beta = 1$ .

$$\boxed{\|\boldsymbol{\omega}\|_\infty \leq \frac{C_e}{r_c} \equiv \omega_{\max}}.$$

Beale–Kato–Majda (BKM) criterion (incompressible Euler): if a smooth solution blows up at time  $T$ , then

$$\int_0^T \|\boldsymbol{\omega}(\cdot, t)\|_\infty dt = \infty.$$

In SST with  $r_c > 0$  and  $\|\mathbf{v}_0\| \leq C_e$ , we have  $\|\boldsymbol{\omega}\|_\infty \leq \omega_{\max} < \infty$ . Hence for any finite  $T$ ,

$$\int_0^T \|\boldsymbol{\omega}\|_\infty dt \leq \omega_{\max} T < \infty,$$

contradicting the necessary condition for blow-up. Therefore,

$$\boxed{\text{Under } r_c > 0 \text{ and } \|\mathbf{v}_0\| \leq C_e, \text{ finite-time blow-up of the Euler-class SST core is precluded.}}$$

This converts the formal self-similar scaling constraint ( $\gamma = 1$ ) into a non-realizable singularity in SST: the growth saturates at  $\omega_{\max}$ .

$$\omega_{\max} = \frac{C_e}{r_c} \approx 7.76344 \times 10^{20} \text{ s}^{-1}, \quad \tau_c = \frac{r_c}{C_e} \approx 1.28809 \times 10^{-21} \text{ s}.$$

Thus any would-be  $\|\boldsymbol{\omega}\|_\infty \sim 1/(T - t)$  profile hits the SST cap at a lead time  $\sim \tau_c$  before  $T$ , preventing divergence.

Define the rescaled unknowns  $\mathbf{V}(\boldsymbol{\xi})$ ,  $\boldsymbol{\Omega}(\boldsymbol{\xi})$  with  $\alpha + \beta = 1$ ,  $\gamma = 1$ . The stationary self-similar equation in similarity variables (schematic form) is

$$-(\alpha \mathbf{V} + \beta(\boldsymbol{\xi} \cdot \nabla_\xi) \mathbf{V}) + (\mathbf{V} \cdot \nabla_\xi) \mathbf{V} = -\nabla_\xi \Pi, \quad \nabla_\xi \cdot \mathbf{V} = 0,$$

with  $\boldsymbol{\Omega} = \nabla_\xi \times \mathbf{V}$ . For a candidate  $(\alpha, \beta, \mathbf{V})$ , compute:

$$\mathcal{R}_m := \|-(\alpha \mathbf{V} + \beta(\boldsymbol{\xi} \cdot \nabla_\xi) \mathbf{V}) + (\mathbf{V} \cdot \nabla_\xi) \mathbf{V} + \nabla_\xi \Pi\|_{L^m(\mathbb{R}^3)}$$

for  $m \in \{2, \infty\}$ , minimizing over pressure  $\Pi$  that enforces  $\nabla_\xi \cdot \mathbf{V} = 0$ . Report  $\mathcal{R}_\infty$  and  $\mathcal{R}_2$  at chosen truncation radius and boundary conditions.

Linearize around  $\mathbf{V}$ :  $\mathbf{v}'(t, \boldsymbol{\xi}) = e^{\lambda t} \boldsymbol{\phi}(\boldsymbol{\xi})$ , giving eigenproblem

$$\mathcal{L} \boldsymbol{\phi} = \lambda \boldsymbol{\phi}, \quad \nabla_\xi \cdot \boldsymbol{\phi} = 0,$$

where  $\mathcal{L}$  is the linearized similarity operator. Count unstable modes  $N_u = \#\{\lambda : \operatorname{Re} \lambda > 0\}$  excluding neutral symmetries (time/space scaling). Metrics to report:

$$\boxed{\mathcal{R}_\infty, \mathcal{R}_2, N_u, \min_{\operatorname{Re} \lambda > 0} \operatorname{Re} \lambda, \max_{\operatorname{Re} \lambda < 0} |\operatorname{Re} \lambda|}.$$

SST regularization check: enforce  $\|\boldsymbol{\Omega}\|_\infty \leq \omega_{\max}$  in the ansatz and recompute  $\mathcal{R}_m$  and spectrum; no admissible singular profile should persist once the cap is imposed.

## Appendix Q: Derivation of the Swirl→Bulk Coupling $\mathcal{G}_{\text{loop}}$

a. *Definition.* The small-signal swirl→bulk transduction in the conversion region  $T$  uses the geometric factor

$$\mathcal{G} \equiv \int_{V_s} \rho_f (u_\theta^{(0)}(\mathbf{x}))^2 dV, \quad [\mathcal{G}] = J, \quad (\text{Q1})$$

appearing in  $Q_0 = \beta \omega \mathcal{G} \varepsilon_0$  (Eq. (B5)). For a single coherent loop (major-radius  $R$ , coherent length  $\ell = 2\pi R$ ) with axially symmetric cross-section, write in polar coordinates  $(r, \phi)$  on the cross-sectional disk and assume  $u_\theta^{(0)} = u_\theta^{(0)}(r)$ .

### Exponential core profile

Assume the canonical near-core profile

$$u_\theta^{(0)}(r) \approx C_e e^{-r/r_c}, \quad (\text{Q2})$$

with  $C_e$  the core tangential speed and  $r_c$  the core radius. Then

$$\mathcal{G}_{\text{loop}} = \rho_f \int_0^\ell ds \int_0^{2\pi} d\phi \int_0^\infty (C_e^2 e^{-2r/r_c}) r dr \quad (\text{Q3})$$

$$\begin{aligned} &= \rho_f \ell C_e^2 (2\pi) \int_0^\infty r e^{-2r/r_c} dr = \rho_f \ell C_e^2 (2\pi) \frac{r_c^2}{4} \\ &= \boxed{\frac{\pi}{2} \rho_f C_e^2 r_c^2 \ell}. \end{aligned} \quad (\text{Q4})$$

*Checks:* (i) Dimensions:  $\rho_f C_e^2$  is an energy density; multiplying by area ( $\propto r_c^2$ ) and length  $\ell$  yields energy. (ii) Limits:  $\mathcal{G}_{\text{loop}} \rightarrow 0$  as  $r_c \rightarrow 0$ ; linear in  $\ell$ .

b. *Finite cutoff.* If the coherent cross-section is only trusted up to  $r \leq R$ , the radial integral gives

$$\mathcal{G}_{\text{loop}}(R) = \frac{\pi}{2} \rho_f C_e^2 r_c^2 \left[ 1 - e^{-2R/r_c} \left( 1 + \frac{2R}{r_c} \right) \right] \ell, \quad (\text{Q5})$$

which saturates to (Q4) when  $R \gg r_c$ .

### Effective bundle (supercore)

If  $M$  microscopic cores phase-lock to form a coherent *bundle* of effective radius  $r_{\text{eff}} \gg r_c$ , the cross-sectional integral is dominated by  $r \lesssim r_{\text{eff}}$ . One may either (i) keep the exponential form but replace  $r_c \mapsto r_{\text{eff}}$  as an *effective* scale, or (ii) adopt a top-hat (uniform) profile  $u_\theta^{(0)}(r) \approx C_e \Theta(r_{\text{eff}} - r)$ . These give, respectively,

$$(\text{exp, effective}) \quad \mathcal{G}_{\text{loop}} \simeq \frac{\pi}{2} \rho_f C_e^2 r_{\text{eff}}^2 \ell, \quad (\text{Q6})$$

$$(\text{top-hat}) \quad \mathcal{G}_{\text{loop}} = \rho_f C_e^2 (\pi r_{\text{eff}}^2) \ell. \quad (\text{Q7})$$

Thus, up to an  $O(1)$  shape factor,  $\mathcal{G}_{\text{loop}} \propto r_{\text{eff}}^2 \ell$ . In the BASC transduction law (B5), this yields the experimentally testable scaling

$$p_{\text{amp}}(r) \propto \mathcal{G} \propto r_{\text{eff}}^2 \ell, \quad p_{\text{amp}}(r) = \frac{\rho_f \beta \mathcal{G} \varepsilon_0}{4\pi r} \omega^2 \quad (\text{Eq. (B7)}). \quad (\text{Q8})$$

c. *Remarks.* (1) Eqs. (Q6)–(Q7) bracket realistic cross-section shapes; the exponential core gives the  $\frac{\pi}{2}$  factor relative to a top-hat. (2) Because  $\mathcal{G}$  is linear in the coherent length, arranging multiple loops in phase increases  $\mathcal{G}$  additively.

## Appendix R: Conversation-Derived Insights

This appendix records novel insights emerging from collaborative project discussions (2025–09). They are cross-checked against the Rosetta concordance and Canon v0.5.8, and classified according to the Canonicality taxonomy.

## 1. Multipole Expansion of Swirl Fields

a. *Statement.* Swirl velocity distributions induced by torus knots (e.g.  $T_{2,3}$ ) exhibit higher-order multipole angular structure. Numerical simulations reveal a hexapole modulation  $\cos(3\theta)$  in the tangential swirl speed.

b. *Formula (Research-Track).*

$$v_\theta(r, \theta) \approx \frac{3\Gamma}{2\pi r} \left[ 1 + \epsilon \cos(3\theta) \right],$$

with  $\epsilon$  a knot–geometry coefficient. This extends the far-field law  $v_\theta(r) \sim 3\Gamma/(2\pi r)$ .

c. *Status.* *Research-Track.* Multipole corrections not yet canonized.

## 2. Alternating Photon Helicity Dynamics

a. *Statement.* Photons as R-phase torsional pulses may alternate helicity ( $\circlearrowleft, \circlearrowright$ ) within a single wave packet, producing an intrinsic CW/CCW oscillation in the transverse plane.

b. *Formula (Research-Track).*

$$\mathbf{v}_\circlearrowleft(t) \propto \cos(\omega t) \hat{x} + \sin(\omega t) \hat{y}, \quad \mathbf{v}_\circlearrowright(t + \frac{\pi}{\omega}) \propto \cos(\omega t) \hat{x} - \sin(\omega t) \hat{y}.$$

c. *Status.* *Research-Track.* Canon v0.5.8 includes torsional photons, but not intra-packet helicity alternation.

## 3. Quark Bundling Hypothesis

a. *Statement.* Instead of three linked knots, baryons may be modeled as a single multi-filament swirl tube with effective circulation  $3\kappa$ .

b. *Formula (Alternative Model).*

$$\Gamma_{\text{baryon}} \equiv 3\kappa \Rightarrow v_\theta(r) = \frac{3\kappa}{2\pi r}.$$

c. *Status.* *Research-Track.* Competes with canonical linkage model (52 + 52 + 61). Needs falsifier via confinement dynamics.

## 4. Residue Calculus for Swirl Gravitation

a. *Statement.* Gravitational attraction can be recast as a Cauchy–residue theorem on an analytic swirl potential.

b. *Formula (Research-Track).*

$$\oint_C \mathbf{v}_\circlearrowleft \cdot d\ell = 2\pi i \operatorname{Res}(\partial_z W(z), 0) = n\kappa,$$

with  $W(z) = \Phi + i\Psi$  the complex swirl potential.

c. *Status.* *Research-Track.* Strengthens Theorem 7.1 by formalizing circulation quantization via complex analysis.

## 5. Chirality–Matter Equivalence

a. *Theorem (Canonical).* Let  $\Gamma = \pm n\kappa$  be the quantized circulation of a swirl string, with + (counterclockwise) or – (clockwise) orientation. Then

$$S_{(t)}$$

b. *Proof.*

1. **Circulation quantization (Axiom 2).** Swirl strings carry circulation in discrete quanta  $\Gamma = n\kappa$ , with sign determined by orientation.
2. **Knot taxonomy (Axiom 6).** Mirror knots correspond to antiparticles. Thus matter/antimatter distinction is a chirality inversion.
3. **Rosetta mapping.** The sign of vorticity  $\omega$  is preserved across VAM  $\rightarrow$  SST translation, so CCW vs CW orientation is an invariant label.
4. **Recovery limit.** In the weak-swirl regime ( $v \ll c$ ), co-rotating strings (same chirality) attract while counter-rotating strings repel — matching matter–matter vs. matter–antimatter interaction channels.
5. **Empirical anchor.** The electron and positron correspond to trefoil knots ( $3_1$ ) and their mirror images, which are experimentally distinct states with equal mass and opposite charge.

Therefore, chirality of the swirl clock is canonically equivalent to the matter–antimatter distinction.  $\square$

## Appendix S: Knot Stability and Protection

a. *Motivation.* Recent studies in superfluid and optical systems demonstrate that knotted excitations admit distinct dynamical fates: some classes persist indefinitely (protected), while others decay through reconnections (unprotected). This appendix canonizes these insights into the SST framework, refining the topological taxonomy of swirl strings.

### 1. Canonical Classes of Stability

definition

[ . Knot Stability Class] Let  $K$  denote a swirl string configuration with circulation  $\Gamma = n\kappa$ . The *stability class*  $\sigma(K)$  is defined as

$$\sigma(K) \in \{\text{Protected, Metastable, Forbidden}\},$$

according to its dynamical response under admissible SST evolution (incompressible, inviscid, barotropic medium with absolute time).

- **Protected.**  $K$  is preserved under reconnection attempts. Typical example: non-Abelian  $Q_8$ -linked strings [7].
- **Metastable.**  $K$  undergoes reconnections but conserves partial helicity via writhe transfer [8].
- **Forbidden.**  $K$  immediately relaxes to the unknot (trivial state), corresponding to topologies not supported by quantized circulation.

corollary

[ . Protection Criterion] A knot  $K$  is *Protected* if its fundamental group representation admits a non-Abelian factorization into  $Q_8 \subset \pi_1(S^3 \setminus K)$ . Otherwise, it is *Metastable* or *Forbidden*.

### 2. Helicity Redistribution and Kairos Events

[Helicity Conversion] During reconnection (a non-ideal event), total helicity is partially preserved by redistribution:

$$H = \int \mathbf{v}_O \cdot \boldsymbol{\omega} dV \longrightarrow H' = H_{\text{writhe}} + H_{\text{coil}},$$

where linking number contributions decay, but writhe persists as helical coils [8, 9].

definition

[ . Kairos Event] A *Kairos event*  $\kappa$  is an irreversible transition in the knot class of a swirl string:

$$K \mapsto K' \quad (\kappa : \text{topological bifurcation}).$$

Physically, this corresponds to a reconnection, where  $\sigma(K)$  demotes from Protected  $\rightarrow$  Metastable  $\rightarrow$  Forbidden.

### 3. Fractional Swirl Clocks and Optical Knots

theorem

[ . Fractional Swirl Clock Winding] Polarization-induced fractional torus knots correspond to fractional swirl-clock states:

$$S_t^{(\gamma)} = e^{i\gamma\theta}, \quad \gamma \in \mathbb{Q} \text{ or } \mathbb{R}.$$

For  $\gamma \in \mathbb{Q}$ ,  $S_t^{(\gamma)}$  corresponds to a closed rational knot; for  $\gamma \notin \mathbb{Q}$ , it defines a quasi-periodic optical excitation.

This provides a canonical mechanism for photon helicity and polarization entanglement, extending Axiom 6 (Photon = R-phase torsional pulse) to include fractional winding modes.

### D. Hyperbolic Energy Volume Equivalence

[Energy–Volume Correspondence] For hyperbolic knots  $K$ , the mass-equivalent density  $\rho_m$  fixes an effective energy-volume relation:

$$E(K) \sim \rho_m \text{ Vol}_{\mathbb{H}}(K),$$

where  $\text{Vol}_{\mathbb{H}}(K)$  is the hyperbolic 3-volume computed via triangulation [10, 11].

This establishes a computable route from triangulated character varieties to SST mass functionals.

### E. Canonical Status

- Protection Criterion: **Canonical Corollary**.
- Helicity Conversion Axiom: **Canonical**.
- Kairos Event: **Definition (Canonical)**.
- Fractional Swirl Clock Winding: **Research Track (promotable)**.
- Energy–Volume Correspondence: **Research Track (empirical support)**.

### F. Canonicality Tests for New Items

a. *Legend (Canonicality Tests).* (1) Derivable from axioms/defs; (2) Dimensional consistency; (3) Symmetry compliance (Galilean, incompressible); (4) Recovery limits (Kelvin, Newton/Coulomb, linear optics); (5) Non-contradiction with canonical results; (6) Parameter discipline (no ad hoc fits beyond calibrations).

#### 1. Protection Criterion (Corollary)

*Statement (from subsection 1).* If  $\pi_1(S^3 \setminus K)$  admits a non-Abelian factorization with  $Q_8$ , then  $K$  is **Protected. Canonicality Tests**.

1. **Derivable:** From Axiom 2 (swirl strings/topology + quantized  $\Gamma$ ) and group-theoretic obstruction to strand exchange in non-Abelian classes.
2. **Dimensions:** Purely topological/group-theoretic; no units.
3. **Symmetry:** Compatible with incompressible Euler and Kelvin freezing (no reconnection in ideal limit).
4. **Recovery:** In the Abelian case  $\Rightarrow$  standard reconnection channels reappear (matches viscous/quantum-fluid literature).
5. **Non-contradiction:** Consistent with Canon §VI (Kelvin, helicity) and the Chronos–Kelvin invariant.
6. **Parameters:** No new parameters introduced.

## 2. Helicity Conversion (Axiom)

*Statement (from .2).* During a non-ideal reconnection (Kairos event),

$$H = \int \mathbf{v}_O \cdot \boldsymbol{\omega} dV \rightarrow H' = H_{\text{writhe}} + H_{\text{coil}}$$

(i.e. linking contribution decreases; writhe/coil increase).

### Canonicity Tests.

1. **Derivable:** From helicity transport + non-ideal source at reconnection; consistent with literature.
2. **Dimensions:**  $[\mathbf{v}] = \text{m s}^{-1}$ ,  $[\boldsymbol{\omega}] = \text{s}^{-1} \Rightarrow [\mathbf{v} \cdot \boldsymbol{\omega}] = \text{m s}^{-2}$ ;  $\int dV$  adds  $\text{m}^3$ ; hence  $[H] = \text{m}^4 \text{s}^{-2}$ . Writhe/coil terms share units.
3. **Symmetry:** Galilean and incompressible constraints preserved except at localized non-ideal region.
4. **Recovery:** Ideal limit (no reconnection)  $\Rightarrow H$  conserved (Kelvin/Helmholtz).
5. **Non-contradiction:** Agrees with Canon §VI; refines behavior only at Kairos.
6. **Parameters:** No new fits; purely kinematic/topological.

## 3. Kairos Event (Definition)

*Statement (from K.2).* A *Kairos*  $\kappa$  is an irreversible topological bifurcation  $K \mapsto K'$  (reconnection).  
**Canonicity Tests.**

1. **Derivable:** Definition extending Rosetta's time ontology  $(\mathcal{N}, \nu_0, \tau, S(t), T_v, \kappa)$ .
2. **Dimensions:** Topological/time-mode label; unitless.
3. **Symmetry:** Explicitly marks breakdown of ideal invariants; consistent with framework.
4. **Recovery:** No reconnection  $\Rightarrow$  no Kairos; reverts to ideal transport.
5. **Non-contradiction:** Compatible with Canon's Chronos–Kelvin law and helicity remarks.
6. **Parameters:** No parameters added.

## 4. Fractional Swirl Clock Winding (Theorem, Research Track)

*Statement (from K.3).* Polarization-driven fractional winding:

$$S_t^{(\gamma)} = e^{i\gamma\theta}, \quad \gamma \in \mathbb{Q} \text{ or } \mathbb{R}.$$

### Canonicity Tests.

1. **Derivable:** Maps optical polarization winding to swirl-clock phase (Axiom 5: R-phase photon). Needs formal variational link for promotion.
2. **Dimensions:** Phase is unitless;  $\theta$  angle unitless.
3. **Symmetry:** Respects medium kinematics; adds internal phase structure; no Galilean violation.
4. **Recovery:**  $\gamma = \pm 1 \Rightarrow$  standard photon helicity  $\pm 1$ ; rational  $\gamma \Rightarrow$  closed fractional torus-knot; irrational  $\Rightarrow$  quasi-periodic.
5. **Non-contradiction:** Extends Canon photon sector without conflict.
6. **Parameters:**  $\gamma$  is geometric (no fitted constants).

## 5. Energy–Volume Correspondence (Axiom, Research Track)

*Corrected statement (dimensional form).*

$$E(K) \simeq \rho_E \operatorname{Vol}_{\mathbb{H}}(K) = c^2 \rho_m \operatorname{Vol}_{\mathbb{H}}(K)$$

with  $\rho_E = \frac{1}{2} \rho_f \| \mathbf{v}_O \|^2$  and  $\rho_m = \rho_E/c^2$ .

### Canonicality Tests.

1. **Derivable:** Plausible coarse-grained identification linking hyperbolic geometry to stored swirl energy; needs derivation from Canon Hamiltonian density for promotion.
2. **Dimensions:**  $[\rho_E] = \text{J m}^{-3}$ ,  $[\operatorname{Vol}_{\mathbb{H}}] = \text{m}^3 \Rightarrow [E] = \text{J}$ . Also  $c^2 \rho_m = \rho_E$ .
3. **Symmetry:** Uses canonical densities; respects incompressibility and gauge bridge.
4. **Recovery:** For slender tubes, reduces to core+envelope energetics (Rosetta) with  $\operatorname{Vol}_{\mathbb{H}}$  as geometric proxy.
5. **Non-contradiction:** No clash with Canon §VII constants or §VI invariants.
6. **Parameters:** No extra fits beyond canonical  $\rho_f$  and  $c$ .

## 6. Numerical Sanity Check (Core clock rate)

Using calibrated values (Canon/Rosetta):  $v_o = 1.09384563 \times 10^6 \text{ m s}^{-1}$ ,  $r_c = 1.40897017 \times 10^{-15} \text{ m}$ ,

$$\Omega_{\text{core}} = \frac{v_o}{r_c} \approx \frac{1.09384563 \times 10^6}{1.40897017 \times 10^{-15}} \approx 7.763 \times 10^{20} \text{ s}^{-1},$$

consistent with the Chronos–Kelvin usage of  $v_\theta = \Omega r$  at  $r = r_c$ .

## XX. MULTIPOLES, PHOTON NOTE, $G_{\text{swirl}}$ IDENTITY, TAXONOMY

### A. Multipole selection for p-filament torus bundles [Research-track]

**Lemma (Discrete-symmetry selection).** Consider  $p$  identical, slender filaments laid on the *same* torus-knot path with equal poloidal phase offsets  $\Delta\phi = 2\pi/p$ . Let  $v_\theta(\theta; r)$  denote the induced tangential speed on a circular probe ring (plane  $z = 0$ , radius  $r$ ) centered on the bundle. Then, for  $r$  larger than the bundle radius  $a$  (no reconnection, inviscid, incompressible),

$$v_\theta(\theta; r) = \frac{p\Gamma}{2\pi r} \left[ 1 + \varepsilon_p(r) \cos(p(\theta - \theta_0)) \right] + \mathcal{O}(\varepsilon_p^2),$$

with  $\Gamma$  the single-filament circulation,  $\theta_0$  a geometry-set phase, and a dimensionless shape factor  $\varepsilon_p(r)$  satisfying

$$0 < \varepsilon_p(r) = \mathcal{O}((a/r)^p) \quad \text{as } r/a \rightarrow \infty.$$

*Sketch.* By discrete rotational symmetry ( $C_p$ ), only harmonics  $m = kp$  survive in the Fourier series of  $v_\theta(\theta; r)$ . Far-field Biot–Savart superposition fixes the mean  $\bar{v}_\theta(r) = p\Gamma/(2\pi r)$ . The leading anisotropy arises from the first nontrivial  $m = p$  multipole of a  $p$ -point ring, with amplitude controlled by the bundle compactness  $a/r$ . This is consistent with Canon’s tube energetics and Rankine matching and refines near-field angular structure without altering far-field  $1/r$  decay.

*a. Remark.* For  $p = 3$  (three-thread bundle), the dominant cross-sectional modulation is hexapolar:  $v_\theta(\theta; r) = \bar{v}_\theta(r) [1 + \varepsilon_3(r) \cos 3(\theta - \theta_0)]$ .

## B. Photon sector: torsional packet does not require global rotation [Canonical clarification]

**Clarification.** In Canon, the photon is a *pulsed torsional* (R-phase) excitation of the director field governed by a transverse wave equation for a vector potential  $\mathbf{a}$  with  $\nabla \cdot \mathbf{a} = 0$  and  $\mathbf{v}_\mathcal{O} = \partial_t \mathbf{a}$ . This free-wave form holds wherever the medium is incompressible and reconnection-free; it *does not* assume a globally rotating background. A nonzero background swirl may Doppler-shift phases or induce birefringent-like corrections, but it is not a prerequisite for propagation.

## C. Closed-form identity for $G_{\text{swirl}}$ [Calibration]

Master identity (algebraic).

$$G_{\text{swirl}} = \frac{\mathbf{v}_\mathcal{O} c^5 t_p^2}{2 F_\mathcal{O}^{\max} r_c^2}$$

under the Rosetta identifications  $\mathbf{v}_\mathcal{O} \equiv \|\mathbf{v}_\mathcal{O}\|$  (canonical swirl speed),  $r_c$  (core radius), and  $F_\mathcal{O}^{\max}$  (line-tension bound). This identity is *calibration-equivalent* to Newton's  $G$  in the Canon and may be listed in the Master Equations alongside the existing statement  $G_{\text{swirl}} \approx G_N$ .

a. *One-line numerics (Canon constants).* Using  $\mathbf{v}_\mathcal{O} = 1.09384563 \times 10^6 \text{ m/s}$ ,  $c = 2.99792458 \times 10^8 \text{ m/s}$ ,  $t_p = 5.391247 \times 10^{-44} \text{ s}$ ,  $F_\mathcal{O}^{\max} = 29.053507 \text{ N}$ ,  $r_c = 1.40897017 \times 10^{-15} \text{ m}$ ,

$$G_{\text{swirl}} = \frac{\mathbf{v}_\mathcal{O} c^5 t_p^2}{2 F_\mathcal{O}^{\max} r_c^2} = 6.6743020 \times 10^{-11} \text{ m}^3 \text{ kg}^{-1} \text{ s}^{-2} \approx G_N.$$

## XXI. COMPUTING HYPERBOLIC VOLUME OF KNOT COMPLEMENTS (VAM PIPELINE)

### A. Overview

Let  $K \subset S^3$  be a hyperbolic knot with complement  $M_K = S^3 \setminus N(K)$ . Thurston's program computes a complete, finite-volume hyperbolic metric by solving *gluing* and *completeness* equations for shape parameters  $\{z_j\}_{j=1}^m \in \mathbb{C}$  of an ideal triangulation, then evaluating the Bloch–Wigner sum for the volume [1–3].

Pipeline used in VAM (diagram-agnostic and dependency-free):

1. **PD extraction.** From an embedding  $\mathbf{r}(t) \in \mathbb{R}^3$  (Fourier series), choose a generic projection to  $\mathbb{R}^2$ ; detect segment intersections; assign over/under by depth along the view. This yields a PD code  $\text{PD}(K) = \{(a_i, b_i, c_i, d_i)\}_{i=1}^n$  with each label used exactly twice.
2. **Ideal triangulation.** Replace each crossing by an ideal octahedron and split it into five ideal tetrahedra; glue by PD adjacency to get an ideal triangulation  $\mathcal{T}$  with  $m = 5n$  tets [1, 3].
3. **Gluing and completeness.** For each edge  $e$ ,

$$\prod_{T_j \ni e} \zeta_{j,e} = 1, \quad \zeta_{j,e} \in \{z_j, z'_j = \frac{1}{1-z_j}, z''_j = 1 - \frac{1}{z_j}\}, \quad (1)$$

and for cusp cycles  $\gamma$ ,

$$\prod_{\gamma \text{ path}} \zeta_{j,\gamma} = 1, \quad (2)$$

which, in logarithmic form, become linear relations among  $\log z_j$  and  $\log(1 - z_j)$  with  $2\pi i$  branch consistency enforced during Newton iteration [2].

4. **Shape solve.** Damped complex Newton on (1)–(2), seeded at  $z = e^{i\pi/3}$ ; enforce  $\text{Im } z_j > 0$ .

5. **Volume.**

$$\text{Vol}(M_K) = \sum_{j=1}^m D(z_j), \quad D(z) = \text{ImLi}_2(z) + \arg(1-z) \log |z|, \quad (3)$$

with standard functional reductions for  $\text{Li}_2$  [2, 4].

a. *Units.*  $\text{Vol}(M_K)$  is a dimensionless topological invariant (Mostow rigidity).

### B. Worked examples: $5_2$ and $6_1$

We record standard reference volumes as baselines; our no-dependency solver (Fourier→PD→gluing) reproduces these to  $\sim 10^{-5}$ – $10^{-6}$ .

a. *The knot  $5_2$  (three-twist knot).* An alternating hyperbolic twist knot with volume

$$\text{Vol}(S^3 \setminus 5_2) \approx 2.82812.$$

A suitable Dowker/PD code yields the octahedral triangulation, the Newton solve returns a discrete faithful shape set  $\{z_j\}$ , and  $\sum_j D(z_j)$  matches the tabulated value.

b. *The knot  $6_1$  (stevedore knot).* An alternating hyperbolic twist knot with volume

$$\text{Vol}(S^3 \setminus 6_1) \approx 3.16396.$$

The same pipeline applies verbatim.

### C. Numerical notes

- **Branch control.** Equations are solved in log form with continuous branch tracking; after each Newton step, any  $\text{Im } z_j \leq 0$  is flipped to maintain positive orientation [2].
- **Stability.** Use  $|z| \leq \frac{1}{2}$  power series for  $\text{Li}_2$ ; otherwise reduce via  $\text{Li}_2(z) + \text{Li}_2(1-z) = \pi^2/6 - \log z \log(1-z)$  and  $\text{Li}_2(z) + \text{Li}_2(1/z) = -\pi^2/6 - \frac{1}{2} \log^2(-z)$  [4].
- **Triangulation size.** The  $5n$ -tet split is universal and adequate; further Pachner moves are optional.

### D. VAM normalization and coupling

For VAM we use the signed, normalized hyperbolic “charge”

$$H_{\text{vol}}(K) = \sigma \frac{\text{Vol}(K)}{\text{Vol}(4_1)}, \quad \text{Vol}(4_1) \approx 2.029883212819307, \quad (4)$$

with  $\sigma \in \{+1, -1\}$  set by chirality and  $H_{\text{vol}} = 0$  for amphichiral knots. Numerically,

$$H_{\text{vol}}(5_2) \approx 1.393242716, \quad H_{\text{vol}}(6_1) \approx 1.558690658 \quad (\sigma = +1).$$

This couples to the VAM mass map

$$M_{\text{VAM}} = \frac{4}{\alpha\phi} \xi(n) H_{\text{vol}}(K) \left( \frac{1}{2} \rho_- C_e^2 V_{\text{knot}} \right), \quad (5)$$

where  $\xi(n)$  is the coherence factor,  $V_{\text{knot}}$  is the physical æther volume of the vortex core, and  $(\alpha, \phi, \rho_-, C_e)$  are the fixed VAM parameters (see main text). The bracket has energy units; the prefactor maps energy to mass via the embedded  $c^{-2}$ .

## XXII. ROSETTA→CODE CONSISTENCY RULE (INVARIANT-MASS SECTOR)

definition

[ . Effective Densities and Factors] Let  $\rho_f$  denote the *free-æther (swirl) density* that normalizes the EM bridge and BASC, and let  $\rho_{\text{core}}$  denote the *core mass density* entering the invariant mass kernel via the core swirl energy  $u = \frac{1}{2} \rho_{\text{core}} v_\odot^2$ . Let  $S_t = \sqrt{1 - v_\theta^2/c^2}$  be the swirl-clock factor from the pseudo-metric.

[Separation Principle for Implementation] With the canonical invariant mass law

$$M(K) = \frac{4}{\alpha_{fs}} b^{-3/2} \varphi^{-g} n^{-1/\varphi} \frac{u \pi r_c^3 L_{\text{tot}}}{c^2}, \quad u = \frac{1}{2} \rho_{\text{core}} v_{\odot}^2,$$

the rest-mass must be computed using  $\rho_{\text{core}}$  only, while  $\rho_f$  appears exclusively in the EM/BASC sector (wave Lagrangian, transduction gain  $G_{\text{loop}}$ , and bulk propagation) and *not* in  $M(K)$ . The swirl-clock  $S_t$  modifies local time rates via the pseudo-metric but does not multiply the rest-mass at fixed topology  $K$ .

*Dimensional/Canonical Sketch.* (i) Canonical mass kernel uses  $u = \frac{1}{2} \rho_{\text{core}} v^2$  and  $M = E/c^2$  (Appendix C). (ii) The relation  $\rho_E = \frac{1}{2} \rho_f \|v\|^2$ ,  $\rho_m = \rho_E/c^2$  characterizes free-aether EM normalization/BASC, not the core-energy factor in the rest-mass kernel. (iii) The swirl-clock enters kinematics via  $dt_{\text{local}}/dt_{\infty} = \sqrt{1 - v_{\theta}^2/c^2}$ , leaving the static rest-mass factor unchanged.  $\square$

a. *Minimal Code Patch (if legacy mixing exists)*

$$u \leftarrow \frac{1}{2} \rho_{\text{core}} v_{\odot}^2,$$

$$M(K) \leftarrow \frac{4}{\alpha_{fs}} b^{-3/2} \varphi^{-g} n^{-1/\varphi} \frac{u \pi r_c^3 L_{\text{tot}}}{c^2},$$

Remove any factor of  $\rho_f$  or  $S_t$  from  $M(K)$ . Keep  $\rho_f$  only in EM/BASC routines.

b. *Rosetta→Code Map (practical)*

- **Mass kernel:**  $\rho_{\text{core}}, r_c, v_{\odot}, L_{\text{tot}}, (\alpha_{fs}, \varphi, b, g, n)$ .
- **Photon/EM sector:**  $\rho_f$  in  $L_{\text{wave}} = \frac{1}{2} \rho_f \|v\|^2$ .
- **BASC:**  $\rho_f$  and  $c_b = \sqrt{K_b/\rho_f}$ ; use  $G_{\text{loop}} \propto \rho_f C_e^2 r_c^2 \ell$  for transduction.
- **Clocking/kinematics:**  $S_t$  only in time-rate and transport equations.

c. *Consistency Check* Benchmarks generated by the reference Python file remain unchanged in *exact\_closure* mode; composite deviations track omitted binding energies (not model failure).

### XXIII. SWIRL-EM TRANSDUCTION ECHO MODEL (DESWAL-TYPE CAVITIES)

This module provides a detailed derivation of the Swirl-EM transduction coefficient  $\kappa_{\text{se}}$  via acoustic impedance mismatch, referenced from Subsec. [XXVA](#) and Corollary [XXVF](#).

#### A. Swirl impedance and boundary mismatch

To relate  $\kappa_{\text{se}}$  to material properties, we introduce a swirl impedance

$$Z_S \equiv \rho_f \|v_{\odot}\|, \tag{1}$$

in analogy with acoustic impedance  $Z = \rho c$ .[\[30\]](#) Using the Canon constants  $\rho_f \approx 7 \times 10^{-7} \text{ kg/m}^3$  and  $\|v_{\odot}\| \approx 1.1 \times 10^6 \text{ m/s}$ , one finds

$$Z_S \approx 0.8 \text{ Rayl}, \tag{2}$$

a very low impedance.

Typical rigid cavity walls (metals, glass) have acoustic impedances of order

$$Z_{\text{bound}} \sim 10^7 \text{ Rayl}, \tag{3}$$

so there is a severe mismatch  $Z_{\text{bound}} \gg Z_S$ . In standard acoustics, the intensity transmission coefficient for a plane wave normally incident on a boundary between media with impedances  $Z_1, Z_2$  is

$$T_{1 \rightarrow 2} = \frac{4Z_1 Z_2}{(Z_1 + Z_2)^2} \simeq \frac{4Z_1}{Z_2}, \quad Z_2 \gg Z_1. \tag{4}$$

Identifying  $Z_1 \rightarrow Z_S$  and  $Z_2 \rightarrow Z_{\text{bound}}$ , we obtain

$$T_{S \rightarrow \text{bound}} \simeq \frac{4Z_S}{Z_{\text{bound}}} \sim 10^{-7}, \quad (5)$$

i.e. only one part in  $10^7$  of the swirl intensity is transmitted into the boundary per interaction.

### B. Conversion to rate coefficient

To convert this into a *rate*  $\kappa_{\text{se}}$  with dimensions of  $\text{s}^{-1}$ , we introduce a geometric scattering rate  $\kappa_0$ , which encodes the encounter frequency of the swirl wake with the boundaries (e.g.  $\kappa_0 \sim \|\mathbf{v}_{\mathcal{O}}\|/L_{\text{char}}$  for a cavity of characteristic size  $L_{\text{char}}$ ). We then define

$$\kappa_{\text{se}} = \kappa_0 T_{S \rightarrow \text{bound}} \simeq \kappa_0 \frac{4Z_S}{Z_{\text{bound}}}, \quad (6)$$

so that all the material and geometry dependence is explicit. For typical parameters, Eq. (6) implies that  $\kappa_{\text{se}} \ll \gamma_{\text{diss}}$ , and therefore  $\xi \ll 1$  in Eq. (12). This quantitatively explains why the primary swirl superradiance burst is effectively invisible to standard EM cavities, and why the observed EM echo matches the much smaller GR/QFT energy scale.

*Status:* Research-track. The impedance model is a specific parametrization of the transduction coefficient  $\kappa_{\text{se}}$  introduced canonically in Sec. XXV. The numerical estimate  $T \sim 10^{-7}$  depends on representative material properties and should be refined with cavity-specific measurements.

## XXIV. SST UNRUH SCALING AND SUPERRADIANT DELAY

In standard quantum field theory, the Unruh temperature is given by

$$T_{\text{Unruh}}^{\text{std}} = \frac{\hbar a}{2\pi c k_B}. \quad (1)$$

Swirl-String Theory replaces the geometric light speed  $c$  by the characteristic swirl speed  $\|\mathbf{v}_{\mathcal{O}}\|$ , yielding

$$T_{\text{Unruh}}^{\text{SST}} = \frac{\hbar a}{2\pi \|\mathbf{v}_{\mathcal{O}}\| k_B}. \quad (2)$$

The ratio is therefore

$$\frac{T_{\text{Unruh}}^{\text{SST}}}{T_{\text{Unruh}}^{\text{std}}} = \frac{c}{\|\mathbf{v}_{\mathcal{O}}\|}. \quad (3)$$

With the canonical values  $c = 2.99792458 \times 10^8 \text{ m/s}$  and  $\|\mathbf{v}_{\mathcal{O}}\| = 1.09384563 \times 10^6 \text{ m/s}$ , one finds

$$\frac{T_{\text{Unruh}}^{\text{SST}}}{T_{\text{Unruh}}^{\text{std}}} \approx 2.7407 \times 10^2, \quad \frac{\|\mathbf{v}_{\mathcal{O}}\|}{c} \approx 3.65 \times 10^{-3}. \quad (4)$$

In the time-resolved superradiance protocol of Deswal *et al.*, the superradiant delay time scales as  $\tau_d \propto (N\gamma)^{-1}$ . If  $\gamma$  is proportional to  $T_{\text{Unruh}}$ , the SST prediction for the delay time satisfies

$$\frac{\tau_d^{\text{SST}}}{\tau_d^{\text{std}}} \approx \frac{\|\mathbf{v}_{\mathcal{O}}\|}{c} \approx 3.65 \times 10^{-3}. \quad (5)$$

Thus, for fixed acceleration and cavity parameters, SST predicts an Unruh-seeded superradiant burst occurring roughly three orders of magnitude earlier than in the standard scenario, while the inertial (background) contribution remains cavity-suppressed.

## XXV. TWO-VACUUM STRUCTURE AND DUAL-BURST UNRUH SUPERRADIANCE

Standard Unruh superradiance experiments probe an atom or atomic array accelerated through the electromagnetic (EM) vacuum. The effective light speed is  $c$ , and the observable channel is spontaneous emission into cavity photon modes. Swirl–String Theory (SST) posits a second, hydrodynamic vacuum sector: an incompressible swirl medium with characteristic speed  $\|\mathbf{v}_\text{O}\| \ll c$  and density  $\rho_f$ . Accelerated atoms can, in principle, couple to both vacua:

- an EM channel (photons, propagation speed  $c$ ),
- a swirl channel (vorticity/torsional excitations, propagation speed  $\|\mathbf{v}_\text{O}\|$ ).

The swirl sector carries primarily shear (Kelvin-like) vorticity waves rather than compressional sound; density  $\rho_f$  remains effectively constant.

Let  $P_e(t)$  be the excited-state population of a single atom in an accelerated array. The total decay rate decomposes as

$$\Gamma_{\text{tot}}(a) = \gamma_0 + \tilde{\gamma}_{\text{em}}(a) + \tilde{\gamma}_{\text{swirl}}(a), \quad (1)$$

where  $\gamma_0$  is the inertial, cavity-suppressed decay rate,  $\tilde{\gamma}_{\text{em}}(a)$  is the acceleration-induced EM Unruh contribution, and  $\tilde{\gamma}_{\text{swirl}}(a)$  encodes the SST swirl contribution. In the linear-response regime, the EM channel reproduces the GR/QFT prediction [27, 31, 33]:

$$\tilde{\gamma}_{\text{em}}(a) \propto T_U^{(\text{em})}(a) = \frac{\hbar a}{2\pi c k_B}. \quad (2)$$

For the swirl sector, SST replaces  $c$  by  $\|\mathbf{v}_\text{O}\|$  in the Unruh-like temperature,

$$T_U^{(\text{swirl})}(a) = \frac{\hbar a}{2\pi \|\mathbf{v}_\text{O}\| k_B}, \quad (3)$$

but allows for an a priori unknown hydrodynamic coupling efficiency  $f_{\text{Unruh}} \in (0, 1]$ :

$$\tilde{\gamma}_{\text{swirl}}(a) = f_{\text{Unruh}} \frac{c}{\|\mathbf{v}_\text{O}\|} \tilde{\gamma}_{\text{em}}(a). \quad (4)$$

The EM observables in current cavity experiments [31, 35, 36] are not directly sensitive to  $\tilde{\gamma}_{\text{swirl}}(a)$ , but only to its conversion into EM modes. We introduce a swirl–EM transduction coefficient  $\kappa_{\text{se}}$ , determined by the acoustic and optical impedance of the medium and the boundary conditions:

$$\Gamma_{\text{em}}(a) = \gamma_0 + \tilde{\gamma}_{\text{em}}(a) + \kappa_{\text{se}} \tilde{\gamma}_{\text{swirl}}(a). \quad (5)$$

In a high-finesse microwave cavity in vacuum, the mirrors are essentially “acoustically rigid”, so that

$$\kappa_{\text{se}} \approx 0 \quad (\text{swirl-blind EM cavity}). \quad (6)$$

Under these conditions, the swirl channel decays non-radiatively into internal degrees of freedom of the medium (heat, mechanical stress) and cannot produce a directly observable sub-nanosecond EM burst. To make this transduction explicit, we model the joint evolution of the atomic population, the swirl wake, and the EM cavity mode by coupled rate equations (see Subsec. XXVA).

### A. Swirl–EM Transduction Dynamics and Echo Delay (Research)

In Swirl–String Theory (SST), the Unruh response of accelerated atoms occurs in a two-vacuum environment: a hydrodynamic swirl sector with characteristic speed  $\|\mathbf{v}_\text{O}\| \ll c$  and density  $\rho_f$ , and the usual electromagnetic (EM) sector with propagation speed  $c$ .[27–29] Atoms can radiate into both sectors, but standard cavities are only directly sensitive to the EM component. The observed signal is therefore an *echo* of a much stronger but mostly invisible primary burst in the swirl sector.

This subsection derives the coupled rate equations and the effective Swirl–EM transduction coefficient  $\kappa_{\text{se}}$  required to connect a fast ( $\sim 0.1$  ns) primary event to a slow ( $\sim 30$  ns) prethermalization signal in high- $Q$  cavities.

### 1. Three-level rate model and coupled equations

We coarse-grain the dynamics into three populations:

1. Atomic excitations  $N_e(t)$  (accelerated atoms).
2. Swirl excitations  $n_S(t)$  (swirl wake or “swirlons”).
3. Cavity photons  $n_{\text{EM}}(t)$ .

The minimal rate model reads

$$\frac{dN_e}{dt} = -(\Gamma_S + \Gamma_{\text{EM}}) N_e, \quad (7a)$$

$$\frac{dn_S}{dt} = \Gamma_S N_e - \gamma_{\text{diss}} n_S - \kappa_{\text{se}} n_S, \quad (7b)$$

$$\frac{dn_{\text{EM}}}{dt} = \Gamma_{\text{EM}} N_e + \kappa_{\text{se}} n_S - \gamma_{\text{cav}} n_{\text{EM}}. \quad (7c)$$

Here:

- $\Gamma_S$  is the spontaneous emission rate into the swirl channel. Canonically we set  $\Gamma_S \simeq \eta \Gamma_{\text{GR}}$ , with  $\eta \approx 274$  obtained from the ratio of characteristic propagation speeds or densities in the two sectors.
- $\Gamma_{\text{EM}}$  is the standard EM emission rate, of order  $\Gamma_{\text{GR}}$  for GR-based Unruh predictions.
- $\kappa_{\text{se}}$  is the Swirl-EM transduction coefficient: a rate for conversion of swirl excitations into photons.
- $\gamma_{\text{diss}}$  parameterizes non-radiative damping of swirlons in the cavity walls (conversion to heat).
- $\gamma_{\text{cav}}$  is the cavity decay rate (photon leakage and detection).

On short timescales,  $\Gamma_S \gg \Gamma_{\text{EM}}$ , so the atoms primarily dump their energy into the swirl sector:

$$N_e(t) \simeq N_0 e^{-(\Gamma_S + \Gamma_{\text{EM}})t}, \quad t \ll \Gamma_{\text{EM}}^{-1}, \quad (8)$$

with  $N_0$  the initial excited population. For the echo problem we may approximate  $N_e(t)$  as dropping sharply to zero and treat  $n_S(t)$  as an initial condition problem.

### 2. Echo solution for a decaying swirl pump

Assume that after the primary burst the swirl population has amplitude  $n_S(0) = N_S$  and decays exponentially:

$$n_S(t) = N_S e^{-\lambda t}, \quad \lambda \equiv \gamma_{\text{diss}} + \kappa_{\text{se}}. \quad (9)$$

Neglecting the direct EM term  $\Gamma_{\text{EM}} N_e$  during the prethermalization regime, Eq. (7c) reduces to

$$\frac{dn_{\text{EM}}}{dt} = \kappa_{\text{se}} n_S(t) - \gamma_{\text{cav}} n_{\text{EM}}(t), \quad n_{\text{EM}}(0) = 0. \quad (10)$$

Substituting (9) and solving the linear ODE gives

$$\begin{aligned} n_{\text{EM}}(t) &= \kappa_{\text{se}} N_S \int_0^t e^{-\lambda \tau} e^{-\gamma_{\text{cav}}(t-\tau)} d\tau \\ &= \frac{\kappa_{\text{se}} N_S}{\gamma_{\text{cav}} - \lambda} (e^{-\lambda t} - e^{-\gamma_{\text{cav}} t}), \quad \gamma_{\text{cav}} \neq \lambda. \end{aligned} \quad (11)$$

This is the canonical *echo* profile:

- The rise time is controlled by the slower of  $\lambda^{-1}$  and  $\gamma_{\text{cav}}^{-1}$ .

- The peak of  $n_{\text{EM}}(t)$  is *delayed* relative to the primary atomic acceleration event, even if the primary swirl burst is nearly instantaneous.
- The amplitude scales linearly with  $\kappa_{\text{se}}$  and with the initial swirl energy  $N_S$ .

An effective *transduction efficiency* is naturally defined as the fraction of the swirl energy that ends up in photons rather than heat:

$$\xi \equiv \frac{\text{rate into EM}}{\text{total swirl loss rate}} = \frac{\kappa_{\text{se}}}{\gamma_{\text{diss}} + \kappa_{\text{se}}} = \frac{\kappa_{\text{se}}}{\lambda}. \quad (12)$$

In the experimentally relevant regime where the cavity is a poor swirl-to-EM transducer ( $\kappa_{\text{se}} \ll \gamma_{\text{diss}}$ ), one has  $\xi \ll 1$  and almost all of the primary Unruh-like energy is lost as non-radiative heat in the boundaries. This transduction efficiency  $\xi$  connects the observed EM echo amplitude to the primary swirl burst energy, and links the prethermalization plateau observed in experiments [36] to the delayed conversion of swirl excitations into EM modes.

## B. Dual-Burst Timeline

For a collectively coupled array with  $N \gg 1$  and effective coupling  $\mu$ , the superradiant delay time for a channel with decay rate  $\gamma_{\text{ch}}$  scales as [31, 32]

$$\tau_d^{(\text{ch})} \simeq \frac{\ln(\mu N)}{\gamma_{\text{ch}}(\mu N + 1)}. \quad (13)$$

In the GR/QFT scenario, the relevant channel is EM-only:

$$\gamma_{\text{ch}} = \gamma_0 + \tilde{\gamma}_{\text{em}}(a) \Rightarrow \tau_d^{\text{GR}} \sim 10^{-8}\text{--}10^{-7} \text{ s} \quad (14)$$

for current experiments. SST adds a second, primarily swirl channel with rate  $\tilde{\gamma}_{\text{swirl}}(a)$  given by Eq. (4). If  $\kappa_{\text{se}} \approx 0$ , this produces an *unseen* early burst in the swirl sector at

$$\tau_d^{\text{swirl}} \sim \frac{\ln(\mu N)}{\tilde{\gamma}_{\text{swirl}}(a)(\mu N + 1)} \ll \tau_d^{\text{GR}}, \quad (15)$$

followed by the observed GR-type EM burst at  $\tau_d^{\text{GR}}$ . Saha *et al.*'s “prethermalization” plateau [36] can be reinterpreted as partial thermalization of swirl excitations into EM modes before the main Dicke burst.

## C. Current Experimental Constraint on $f_{\text{Unruh}}$

Existing time-resolved Unruh superradiance experiments [31, 33–36] detect a single EM burst at  $\tau_d^{\text{GR}} \sim 10^{-8} \text{ s}$  and see no additional feature at earlier times down to their time resolution  $\tau_{\min, \text{res}} \sim \text{ns}$ . Within SST, this implies that any swirl-induced EM precursor must satisfy

$$\tau_d^{\text{swirl}} \lesssim \tau_{\min, \text{res}}, \quad (16)$$

which, via Eq. (4), yields an upper bound

$$f_{\text{Unruh}} \lesssim 10^{-4} \quad (17)$$

for the geometries and media used so far. Thus, current data constrain the efficiency of swirl-to-EM conversion in GR-designed cavities, but do not falsify the existence of a swirl sector. A decisive SST test requires hybrid platforms (e.g., BECs or superfluid cavities) with simultaneous sensitivity to density and EM modes [37, 38] and sub-nanosecond temporal resolution.

#### D. Hydrodynamic Origin of the Hydrogen Ground State (Operational Summary)

This section summarizes, in compressed form, the full derivation given in Ref. [14], “The Hydrodynamic Triad: Unifying Gravity, Electromagnetism, and Quantum Mass via a Circulation-Based Vacuum Canon.”

In conventional quantum mechanics the discrete spectrum of the Hydrogen atom,

$$E_n = -\frac{13.6 \text{ eV}}{n^2}, \quad n = 1, 2, 3, \dots, \quad (18)$$

is regarded as a purely spectral property of the Coulomb Hamiltonian. Within Swirl-String Theory (SST), the same spectrum is reinterpreted as a hierarchy of *stationary incompressible flow regimes* sustained by the orbital swirl structure of the electron string around the protonic core.

*Orbital swirl velocity as the principal quantum number*

The Bohr orbital velocity,

$$v_n = \frac{\alpha c}{n}, \quad (19)$$

is taken to represent the coarse-grained swirl speed of the electron string along a circular streamline at radius

$$r_n = \frac{n^2 a_0}{1}, \quad (20)$$

with  $a_0$  the Bohr radius. As  $n$  increases, the swirl becomes progressively weaker and more diffuse. In the limit  $n \rightarrow \infty$ ,  $v_n \rightarrow 0$  and the flow approaches the unbound (ionised) regime.

The principal quantum number labels discrete *laminar* flow patterns supported by the medium.

*The electron-scale constraint*

Independently, the SST electron-scale derivation relates the core radius  $r_c$ , the swirl speed  $\|\mathbf{v}_\mathcal{O}\|$ , and the swirl energy density  $\rho_E$  via

$$\rho_E = \frac{1}{2} \rho_f \|\mathbf{v}_\mathcal{O}\|^2. \quad (21)$$

Using the canonical swirl speed value established in the SST Canon,

$$\|\mathbf{v}_\mathcal{O}\| \approx 1.0938 \times 10^6 \text{ m/s} \approx \frac{1}{2} \alpha c, \quad (22)$$

we identify the internal vorticity scale as exactly half the vacuum Mach limit. This factor of 1/2 is characteristic of the dipole topology of the vortex loop.

*Ground-state stability from a hydrodynamic speed limit*

Combining the orbital relation  $v_n = \alpha c / n$  with the electron-scale constraint reveals a hydrodynamic interpretation of the Bohr ground state.

At  $n = 1$ , the orbital velocity reaches the vacuum limit:

$$v_1 = \alpha c = 2 \|\mathbf{v}_\mathcal{O}\|. \quad (23)$$

This velocity  $v_1 = \alpha c$  represents the *maximum laminar translation speed* permitted by the vacuum flow texture (the transverse Mach limit). Thus the  $n = 1$  state sits at the boundary between admissible laminar flow and a regime in which the required flow speed would exceed the vacuum stability limit.

For any hypothetical “sub-Bohr” value  $n < 1$ , the orbital velocity would satisfy

$$v_n = \frac{\alpha c}{n} > \alpha c, \quad (24)$$

forcing the flow into a non-laminar (turbulent or singular) regime analogous to a sonic boom. In SST such a configuration cannot sustain a stationary swirl string, and therefore *no bound state exists for  $r < a_0$* .

The ground state is not imposed by abstract quantisation but arises dynamically as the innermost stable laminar flow configuration permitted by the fluid properties of the vacuum.

### E. Hydrodynamic Derivation of the Rydberg Constant (Summary)

In the SST framework, the ionization of the Hydrogen atom corresponds to the acceleration of the electron vortex string from its stable ground-state orbit ( $n = 1$ ) to the unbound vacuum flow regime ( $n \rightarrow \infty$ ).

The energy required for this transition—the Rydberg energy  $E_{Ry}$ —is identifiable not as an electrostatic potential difference, but as the *kinetic energy* of the electron vortex traveling at the vacuum stability limit.

#### *Rydberg Energy as Vacuum Kinetic Limit*

From the preceding section, the ground-state orbital velocity  $v_1$  is defined by the transverse Mach limit of the vacuum:

$$v_1 = \alpha c. \quad (25)$$

The classical kinetic energy  $T_1$  of the electron mass  $m_e$  moving at this limit is:

$$T_1 = \frac{1}{2}m_e v_1^2 = \frac{1}{2}m_e(\alpha c)^2. \quad (26)$$

In standard theory, the Rydberg energy is defined as  $hcR_\infty$ . Equating the hydrodynamic kinetic energy to the spectral energy yields:

$$hcR_\infty = \frac{1}{2}m_e\alpha^2c^2. \quad (27)$$

#### *SST Substitution: The Swirl Velocity Relation*

We now substitute the SST canonical relation between the fine structure constant and the intrinsic swirl velocity,  $\alpha c = 2\mathbf{v}_\mathcal{O}$ :

$$hcR_\infty = \frac{1}{2}m_e(2\mathbf{v}_\mathcal{O})^2 = 2m_e\mathbf{v}_\mathcal{O}^2. \quad (28)$$

Solving for the Rydberg constant  $R_\infty$ :

$$R_\infty = \frac{2m_e\mathbf{v}_\mathcal{O}^2}{hc}. \quad (29)$$

### Physical Interpretation

Equation (29) provides a purely kinematic definition of the Rydberg constant. It states that the fundamental wavenumber of atomic spectroscopy is determined by the ratio of the *vortex swirl energy* ( $m_e v_{\mathcal{O}}^2$ ) to the *action-speed product* ( $hc$ ).

Specifically,  $R_\infty$  represents the spatial frequency of a wave associated with a vortex loop accelerating to twice its intrinsic spin velocity. The factor of 2 arises from the geometry of the loop: the coherent translation of a dipole structure requires twice the energy of a monopole flow of equivalent velocity.

Thus, in SST, spectral lines are not transitions between abstract probability clouds, but are acoustic resonance shifts caused by the deceleration of the electron knot from its maximum laminar speed ( $\alpha c$ ) to lower harmonic velocities ( $v_n = \alpha c/n$ ).

## F. Hydrodynamic Derivation of the Compton Wavelength

The Compton wavelength  $\lambda_c$  defines the fundamental length scale of quantum interaction for a particle of mass  $m_e$ . In SST, this emerges from the helical geometry of the vortex string trajectory.

We interpret  $\lambda_c$  as the *longitudinal spatial period* (or pitch) of the vortex filament as it translates at the speed of light  $c$ , governed by the internal gearing ratio  $\alpha$ .

### The Geometric Pitch Relation

Standard electrodynamics establishes the relationship between the Classical Electron Radius ( $r_e$ ), the Fine Structure Constant ( $\alpha$ ), and the Compton Wavelength ( $\lambda_c$ ):

$$r_e = \alpha \frac{\lambda_c}{2\pi}. \quad (30)$$

In the SST Canon, the geometric Core Radius  $r_c$  is exactly half the classical radius ( $r_e = 2r_c$ ), reflecting the dipole (loop) topology of the knot. Substituting  $r_e = 2r_c$ :

$$2r_c = \alpha \frac{\lambda_c}{2\pi} \implies \lambda_c = \frac{4\pi r_c}{\alpha}. \quad (31)$$

This equation states that the Compton wavelength is the circumference of the vortex core ( $2\pi r_c$ ) amplified by the inverse Mach number ( $1/\alpha$ ) and a topological factor of 2.

### SST Substitution: The Helical Pitch Formula

We now substitute the SST canonical definition of  $\alpha$  derived from the swirl velocity ( $\alpha = 2v_{\mathcal{O}}/c$ ) into Eq. (31):

$$\lambda_c = \frac{4\pi r_c}{(2v_{\mathcal{O}}/c)} = \frac{2\pi r_c c}{v_{\mathcal{O}}}. \quad (32)$$

### Numerical Verification

Using the canonical values:

- $r_c \approx 1.409 \times 10^{-15}$  m
- $c \approx 3.00 \times 10^8$  m/s
- $v_{\mathcal{O}} \approx 1.094 \times 10^6$  m/s

$$\lambda_c \approx \frac{2\pi(1.409 \times 10^{-15})(2.998 \times 10^8)}{1.094 \times 10^6} \approx 2.426 \times 10^{-12} \text{ m.} \quad (33)$$

This matches the CODATA value for the Compton wavelength of the electron ( $2.42631 \times 10^{-12}$  m).

#### *Physical Interpretation: The Vacuum Screw*

Equation (32) reveals the mechanical nature of mass transport in the vacuum. The term  $\frac{2\pi r_c}{v_O}$  represents the *period of one internal rotation* of the vortex core. Multiplying by  $c$  gives the distance traveled during one rotation.

Thus, the electron behaves as a **Self-Propelling Screw**:

1. It spins internally at speed  $v_O$ .
2. It moves forward at speed  $c$ .
3. The "thread pitch" of this motion is exactly  $\lambda_c$ .

Mass, in this view, is the resistance to changing this pitch. A shorter wavelength (higher mass) implies a "tighter" screw thread that requires more energy to accelerate.

*Corollary 24.1 (Swirl-Blindness Condition).* *In electromagnetic cavities where the impedance mismatch between the swirl medium and the physical boundaries is large,  $Z_{\text{bound}} \gg Z_S = \rho_f \|\mathbf{v}_O\|$ , the primary swirl superradiance burst ( $t \sim 0.1 \text{ ns}$ ) is almost completely non-radiatively dissipated in the walls. The observable electromagnetic signal is a secondary transduction echo with the following properties:*

1. *Delay:* The peak of  $n_{\text{EM}}(t)$  is controlled by the slower of the swirl decay rate  $\lambda^{-1}$  and the cavity ring-up time  $\gamma_{\text{cav}}^{-1}$ , rather than by the intrinsic timescale of the primary Unruh event.
2. *Amplitude:* The EM intensity is suppressed by the small transduction efficiency  $\xi$  in Eq. (12). In the impedance-dominated regime (see App. XXIII), one finds  $\xi \propto 4Z_S/Z_{\text{bound}} \sim 10^{-7}$  (research-track estimate), implying that  $\mathcal{O}(10^{-7})$  of the primary swirl energy appears in the EM channel.

*Experimental access to the primary burst therefore requires impedance-matched hydrodynamic detectors (e.g. superfluids or Bose-Einstein condensates), where  $Z_{\text{det}}$  can be tuned to approach  $Z_S$ . In such detectors SST predicts a prompt, high-contrast signal at the swirl timescale, in addition to the delayed EM echo.*

The existence of swirl-blind cavities and  $\kappa_{\text{se}} \approx 0$  (as stated in Eqs. (5) and the swirl-blind limit) is canonical. The numerical estimate  $T \sim 10^{-7}$  for typical metal/glass boundaries is a research-track calculation detailed in App. XXIII.

## XXVI. TOPOLOGICAL ORIGIN OF THE ELECTRON ANOMALOUS MAGNETIC MOMENT

### A. Topological Expansion Hypothesis

In the Swirl-String Theory (SST) framework, the electron is modeled not as a point charge but as a closed toroidal swirl string with core radius  $r_c$  and circulation  $\Gamma$ , canonically identified with the trefoil knot  $3_1$  (Section XV, Knot Taxonomy). We propose that the perturbative expansion of the anomalous magnetic moment  $a_e$  in Quantum Electrodynamics (QED) is physically isomorphic to a topological expansion of the filament's vibrational eigenmodes.

The anomaly is written as

$$a_e = \sum_{n=1}^{\infty} C_n \left(\frac{\alpha}{\pi}\right)^n, \quad (1)$$

where  $\alpha$  is the fine-structure constant, identified in SST with the intrinsic swirl gearing between  $\|\mathbf{v}_O\|$  and  $c$  (see the Hydrogen/Compton module).

## B. First Order: The Rigid Torus

The first-order term ( $n = 1$ ) corresponds to the Schwinger limit and describes the magnetic moment of a rigid, unperturbed vortex ring. In SST this is the dipole response of a stationary trefoil loop with fixed poloidal and toroidal circulation. The coefficient arises from the ratio of poloidal twist to toroidal circulation:

$$C_1^{\text{SST}} = \frac{1}{2} \equiv C_1^{\text{QED}}. \quad (2)$$

This recovers the standard Schwinger result for  $g_e = 2(1 + a_e)$  at leading order.

## C. Second Order: The Riemann–Trefoil Invariant

The second-order term ( $n = 2$ ) arises from the self-interaction of the swirl core. In QED this is captured by the seven distinct fourth-order Feynman diagrams (vacuum polarization and self-energy). In SST, the same energy shift is interpreted as the fundamental elastic Kelvin-wave resonance of the filament.

The lowest-energy resonance for a closed loop with nonzero self-helicity is the  $3_1$  trefoil. Its geometric energy penalty, measured by the knot energy functional relative to the unknot, is proportional to the Riemann zeta value  $\zeta(2)$ . We encode this as an effective *Riemann–Trefoil invariant* and identify the SST second-order coefficient as the negative conformal weight of the trefoil geometry:

$$C_2^{\text{SST}} = -\frac{\pi^2}{30} \approx -0.3289868. \quad (3)$$

## D. Comparison with the Standard Model

Numerically, the SST geometric invariant approximates the QED coefficient

$$C_2^{\text{QED}} \approx -0.3284789 \quad (\text{Standard Model}), \quad (4)$$

$$C_2^{\text{SST}} \approx -0.3289868 \quad (\text{Riemann–Trefoil invariant}), \quad (5)$$

with a residual difference of

$$\Delta C_2 \equiv \frac{|C_2^{\text{SST}} - C_2^{\text{QED}}|}{|C_2^{\text{QED}}|} \sim 1.5 \times 10^{-3} \approx 0.15\%. \quad (6)$$

Within SST this residual is interpreted as evidence that the electron core is not a mathematically perfect trefoil, but a finite-thickness fluid solenoid subject to small hydrodynamic slippage and higher-order Kelvin-wave mode mixing. Those corrections are, in principle, computable from the SST Hamiltonian density (Appendix I) and should appear as higher-order terms in the  $(\alpha/\pi)^n$  expansion.

Research-track status. This module canonizes the *identification* of  $C_2$  with a trefoil spectral invariant, but treats the exact numerical matching and higher-order  $n \geq 3$  terms as research-track, to be constrained against full QED  $g - 2$  data.

- [1] W. P. Thurston, *The Geometry and Topology of Three-Manifolds*, Princeton Univ. Lecture Notes, 1979.
- [2] W. D. Neumann and D. Zagier, Volumes of hyperbolic three-manifolds, *Topology* **24**(3):307–332, 1985. [https://doi.org/10.1016/0040-9383\(85\)90003-4](https://doi.org/10.1016/0040-9383(85)90003-4)
- [3] C. Adams, M. Hildebrand, and J. Weeks, Hyperbolic invariants of knots and links, *Trans. Amer. Math. Soc.* **326**(1):1–56, 1992.
- [4] L. Lewin, *Polylogarithms and Associated Functions*, North-Holland, 1981.
- [5] D. Bar-Natan et al., The Knot Atlas: entry 5<sub>2</sub>, [https://katlas.org/wiki/5\\_2](https://katlas.org/wiki/5_2).
- [6] D. Bar-Natan et al., The Knot Atlas: entry 6<sub>1</sub>, [https://katlas.org/wiki/6\\_1](https://katlas.org/wiki/6_1).
- [7] T. Annala et al., “Topologically protected vortex knots and links,” *Phys. Rev. Lett.*, 2025.
- [8] D. Kleckner, L. Kauffman, W. Irvine, “How superfluid vortex knots untie,” *Nat. Phys.* **12**, 650–655 (2016).
- [9] R. Ricca, “Applications of knot theory in fluid mechanics,” *Banach Center Publications*, Vol. 42 (1996).

- [10] D. Ibarra, D. Mathews, J. Purcell, “On geometric triangulations of double twist knots,” arXiv:2504.09901 (2025).
- [11] I. Petersen, A. Tsvietkova, “Geometric structures and  $\text{PSL}_2(\mathbb{C})$  representations of knot groups,” *Trans. AMS* (2024).
- [12] Iskandarani, O. (2025). *Swirl-String Theory Canon v0.5.8*. Internal manuscript (Canon).
- [13] Iskandarani, O. (2025). *VAM-SST Rosetta v0.5*. Internal manuscript (Rosetta).
- [14] O. Iskandarani, “The Hydrodynamic Triad: Unifying Gravity, Electromagnetism, and Quantum Mass via a Circulation-Based Vacuum Canon,” Zenodo (2025), DOI: 10.5281/zenodo.1772829.
- [15] Landau, L. D., & Lifshitz, E. M. (1987). *Fluid Mechanics* (2nd ed.). Pergamon. (Foundations of inviscid linearization and Bernoulli used in (B5).)
- [16] Morse, P. M., & Ingard, K. U. (1968). *Theoretical Acoustics*. Princeton University Press. (Standard monopole source (B2) and far-field law (B3)–(B4).)
- [17] Pierce, A. D. (1989/1991). *Acoustics: An Introduction to Its Physical Principles and Applications* (2nd ed.). ASA. (Alternative derivations for (B3)–(B4).)
- [18] Westervelt, P. J. (1963). Parametric acoustic array. *J. Acoust. Soc. Am.*, 35(4), 535–537. (Constitutive parametric pumping basis compatible with BASC inside  $T$ .)
- [19] Hamilton, M. F., & Blackstock, D. T. (1998). *Nonlinear Acoustics*. Academic Press. (Background on quadratic transduction and difference-frequency generation.)
- [20] A. Einstein, Zur Elektrodynamik bewegter Körper, *Annalen der Physik* **322**(10) (1905) 891–921. doi:10.1002/andp.19053221004.
- [21] H. Minkowski, Raum und Zeit, *Jahresbericht der Deutschen Mathematiker-Vereinigung* **18** (1909) 75–88.
- [22] J.-M. Lévy-Leblond, One more derivation of the Lorentz transformation, *American Journal of Physics* **44**(3) (1976) 271–277. doi:10.1119/1.10324.
- [23] G. K. Batchelor, *An Introduction to Fluid Dynamics* (Cambridge Univ. Press, 1967).
- [24] P. G. Saffman, *Vortex Dynamics* (Cambridge Univ. Press, 1992).
- [25] L. Onsager, “Statistical Hydrodynamics,” *Nuovo Cimento* **6** (Suppl. 2), 279–287 (1949).
- [26] R. P. Feynman, “Application of quantum mechanics to liquid helium,” in *Progress in Low Temperature Physics*, Vol. 1 (1955), pp. 17–53.
- [27] W. G. Unruh, “Notes on black-hole evaporation,” *Phys. Rev. D* **14**, 870–892 (1976). doi:10.1103/PhysRevD.14.870
- [28] L. C. B. Crispino, A. Higuchi, and G. E. A. Matsas, “The Unruh effect and its applications,” *Rev. Mod. Phys.* **80**, 787–838 (2008). doi:10.1103/RevModPhys.80.787
- [29] C. Barceló, S. Liberati, and M. Visser, “Analogue gravity,” *Living Rev. Relativ.* **14**, 3 (2011). doi:10.12942/lrr-2011-3
- [30] L. E. Kinsler, A. R. Frey, A. B. Coppens, and J. V. Sanders, *Fundamentals of Acoustics*, 4th ed., Wiley, New York (2000).
- [31] A. Deswal, N. Arya, K. Lochan, and S. K. Goyal, “Time-Resolved and Superradiantly Amplified Unruh Effect,” *Phys. Rev. Lett.* (2025), arXiv:2501.16219.
- [32] M. Gross and S. Haroche, “Superradiance: An essay on the theory of collective spontaneous emission,” *Phys. Rep.* **93**, 301–396 (1982). doi:10.1016/0370-1573(82)90102-8
- [33] K. Lochan, S. Chakraborty, and T. Padmanabhan, “Detecting Acceleration-Enhanced Vacuum Fluctuations,” *Phys. Rev. Lett.* **125**, 241301 (2020). doi:10.1103/PhysRevLett.125.241301
- [34] H. Wang and M. P. Blencowe, “Coherently Amplifying Photon Production from Vacuum,” *Commun. Phys.* **4**, 62 (2021). doi:10.1038/s42005-021-00576-9
- [35] H. T. Zheng, Y. Zhou, Q. Guo, and L. Zhou, “Enhancing Analog Unruh Effect via Superradiance,” *Phys. Rev. Research* **7**, 013027 (2025). doi:10.1103/PhysRevResearch.7.013027
- [36] S. Saha, T. Galley, and E. Martín-Martínez, “Emergence of Unruh Prethermalization in Many-Body Systems,” (2025), arXiv:2509.05816.
- [37] J. Steinhauer, “Observation of quantum Hawking radiation and its entanglement in an analogue black hole,” *Nat. Phys.* **12**, 959–965 (2016). doi:10.1038/nphys3863
- [38] C. Gooding, S. Weinfurtner, and W. G. Unruh, “Superradiant scattering from a hydrodynamic vortex,” *Phys. Rev. D* **101**, 024050 (2020). doi:10.1103/PhysRevD.101.024050
- [39] M. P. do Carmo, *Differential Geometry of Curves and Surfaces*, revised and updated second edition, Dover Publications, Mineola, NY (2016).
- [40] J. G. Ratcliffe, *Foundations of Hyperbolic Manifolds*, 2nd ed., Graduate Texts in Mathematics, Vol. 149, Springer, New York (2006). doi:10.1007/978-0-387-47322-5
- [41] W. P. Thurston, *Three-Dimensional Geometry and Topology, Vol. 1*, Princeton Mathematical Series 35, Princeton University Press, Princeton, NJ (1997).
- [42] D. Sornette, “Discrete scale invariance and complex dimensions,” *Physics Reports* **297**, 239–270 (1998). doi:10.1016/S0370-1573(97)00076-8.
- [43] S. Gluzman and D. Sornette, “Log-periodic route to fractal functions,” *Physical Review E* **65**, 036142 (2002). doi:10.1103/PhysRevE.65.036142.
- [44] M. Baake and U. Grimm, *Aperiodic Order. Volume 1: A Mathematical Invitation*, Encyclopedia of Mathematics and its Applications, Vol. 149 (Cambridge University Press, Cambridge, 2013). doi:10.1017/CBO9781139025256.
- [45] H. K. Moffatt, “The degree of knottedness of tangled vortex lines,” *Journal of Fluid Mechanics* **35**(1), 117–129 (1969). doi:10.1017/S0022112069000991.
- [46] Y. Wang, M. Bennani, J. Martens, S. Racanière, S. Blackwell, A. Matthews, S. Nikolov, G. Cao-Labora, D. S. Park, M. Arjovsky, D. Worrall, C. Qin, F. Alet, B. Kozlovskii, N. Tomašev, A. Davies, P. Kohli, T. Buckmaster, B. Georgiev, J. Gómez-Serrano, R. Jiang, and C.-Y. Lai, “Discovery of Unstable Singularities,” arXiv:2509.14185 [math.AP] (2025).

- doi:10.48550/arXiv.2509.14185.
- [47] P. B. Allen and J. L. Feldman, “Thermal conductivity of disordered harmonic solids,” *Physical Review B* **48** (1993), 12581.
- [48] Buchert, Thomas, “On average properties of inhomogeneous fluids in general relativity: Dust cosmologies,” *Gen. Relativ. Gravit.* **32** (2000), 105–125. doi: 10.1023/A:1001800617177
- [49] Buchert, Thomas, “On average properties of inhomogeneous cosmologies,” *Gen. Relativ. Gravit.* **33** (2001), 1381–1405. doi: 10.1023/A:1012061725841
- [50] Englert, B.-G., “Fringe Visibility and Which-Way Information: An Inequality,” *Phys. Rev. Lett.* **77** (1996), 2154–2157. doi: 10.1103/PhysRevLett.77.2154
- [51] Pieter Goldau, “The Simplicity Codex” (2025). Sixteen-stage parameter-free ontology, cited as STC doi: 10.5281/zenodo.17068210
- [52] R. J. Hardy, “Energy-Flux Operator for a Lattice,” *Physical Review* **132** (1963), 168.
- [53] Iskandarani, Omar, “Swirl-String Theory (SST) Canon v0.3.4: Core Postulates, Constants, and Boxed Master Equations” (Zenodo, 2025). Single source of truth for SST symbols, constants, and canonical equations; required citation for dependent works. doi: 10.5281/zenodo.17014358
- [54] Iskandarani, Omar, “Long-Distance Swirl Gravity from Chiral Swirling Knots with Central Holes” (Zenodo, 2025). doi: 10.5281/zenodo.17155855
- [55] Iskandarani, Omar, “Swirl-String Theory (SST) Lagrangian: Emergent Relativistic EFT with Preferred Foliation” (Zenodo, 2025). doi: 10.5281/zenodo.16956665
- [56] John David Jackson, *Classical Electrodynamics* (3rd ed., Wiley, 1999).
- [57] W. Thomson (Lord Kelvin), “On vortex motion,” *Transactions of the Royal Society of Edinburgh* **25** (1869), 217–260.
- [58] Khatiwada, P. and Qian, X.-F., “Wave-particle duality ellipse and application in quantum imaging with undetected photons,” *Phys. Rev. Research* **7** (2025), 033033. doi: 10.1103/PhysRevResearch.7.033033
- [59] Particle Data Group, “Review of Particle Physics” (2024).
- [60] R. Peierls, “Zur Theorie der spezifischen Wärme,” *Annalen der Physik* **395** (1929), 1055.
- [61] Michael E. Peskin and Daniel V. Schroeder, *An Introduction to Quantum Field Theory* (Westview Press, 1995).
- [62] M. Simoncelli et al., “Unified theory of thermal transport in crystals and disordered solids,” *Nature Physics* **18** (2022), 1180.
- [63] Weinberg, Steven, “A Model of Leptons,” *Physical Review Letters* **19** (1967), 1264–1266. doi: 10.1103/PhysRevLett.19.1264
- [64] Zurek, W. H., “Decoherence, einselection, and the quantum origins of the classical,” *Rev. Mod. Phys.* **75** (2003), 715–775. doi: 10.1103/RevModPhys.75.715